# DNA Sequence

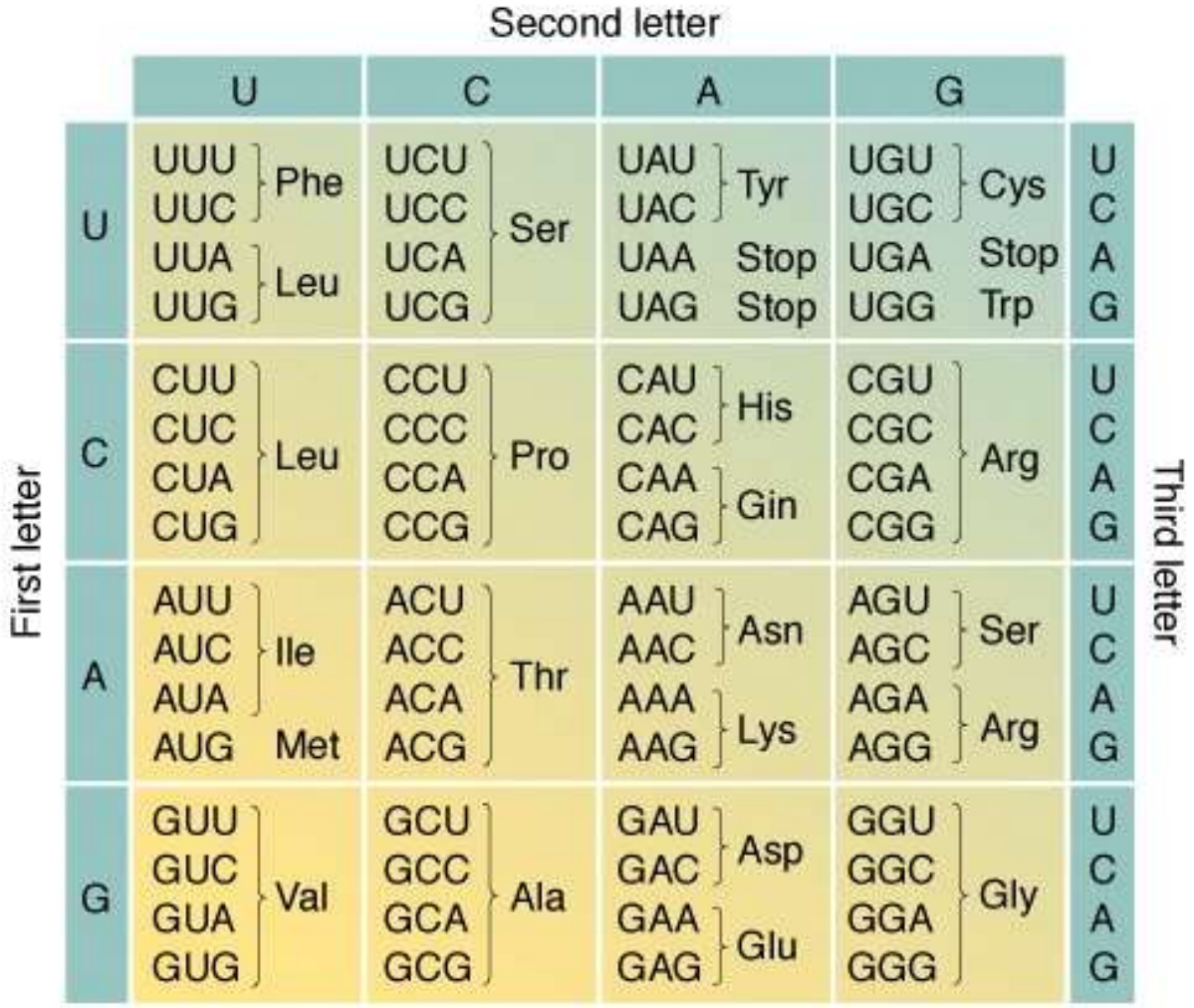

# PCR : Polymerase Chain Reaction

30 - 40 cycles of 3 steps :

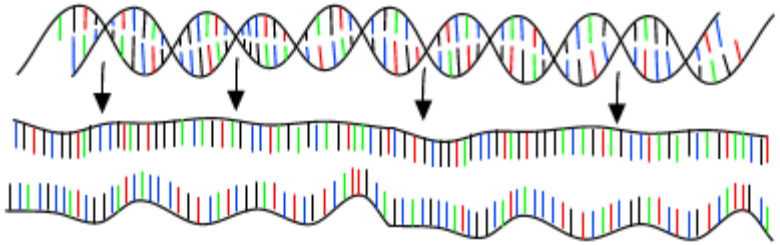

**Step 1 : denaturation**

1 minut 94 °C

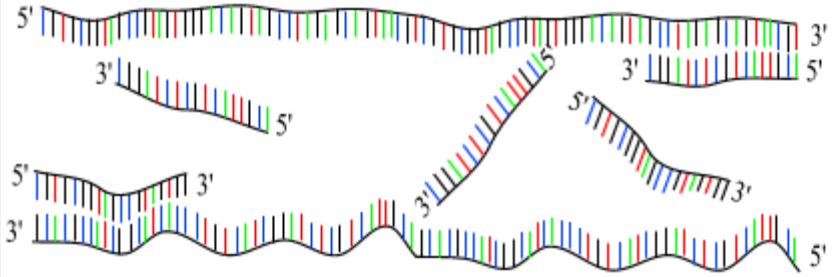


**Step 2 : annealing**

45 seconds 54 °C

forward and reverse primers !!!

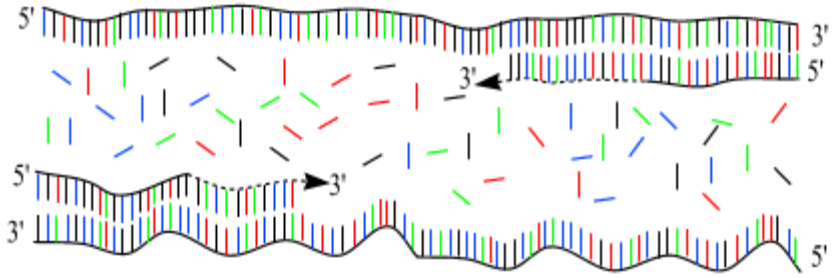


**Step 3 : extension**

2 minutes 72 °C

only dNTP's

(Andy Vierstraete 1999)

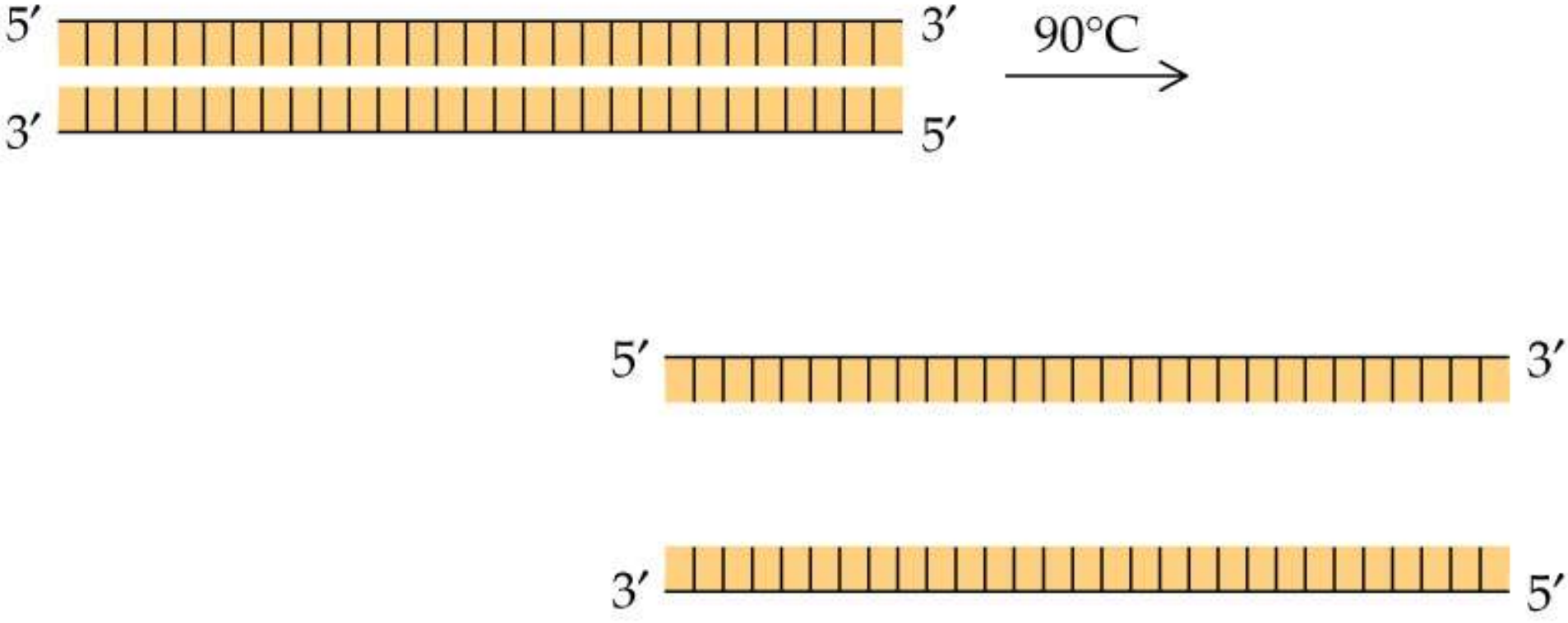
5′
3′
90°C
3′
5′
5′
3′
3′
5′

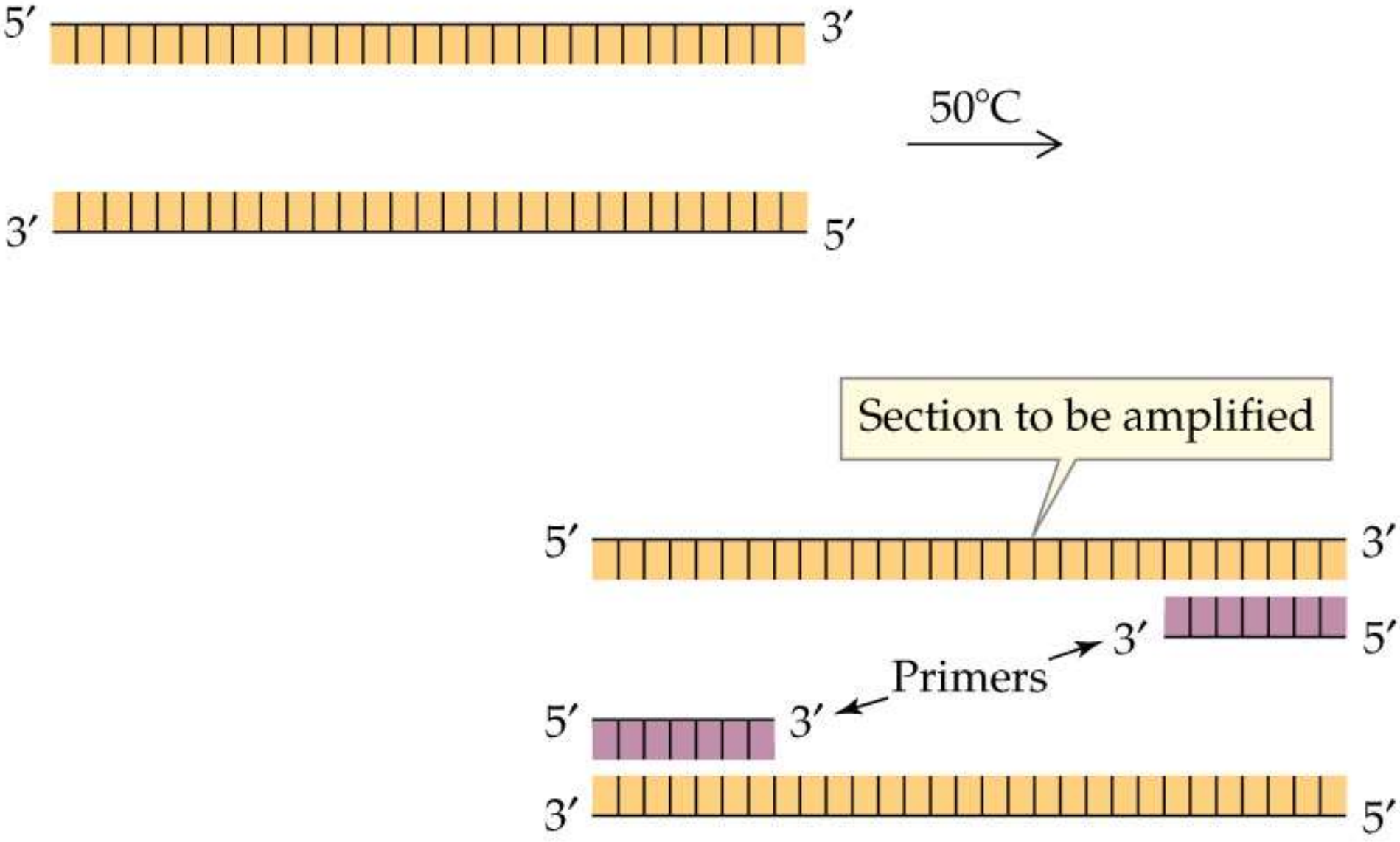
5′
3′
50°C
3′
5′
Section to be amplified
5′
3′
3′
5′
Primers
5′
3′
3′
5′

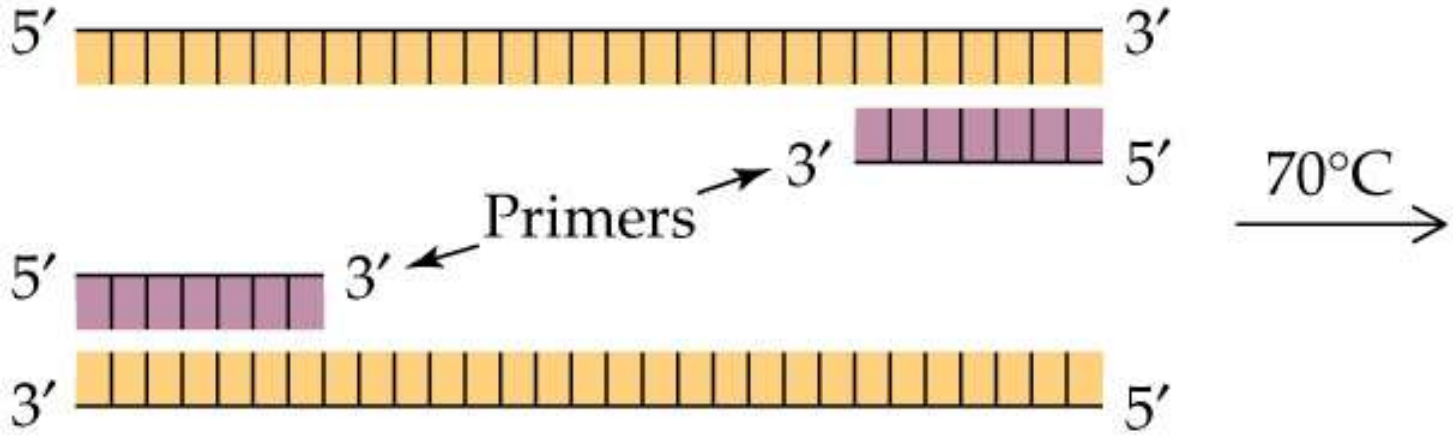
5′
3′
3′
5′
Primers
5′
3′
3′
5′
70°C

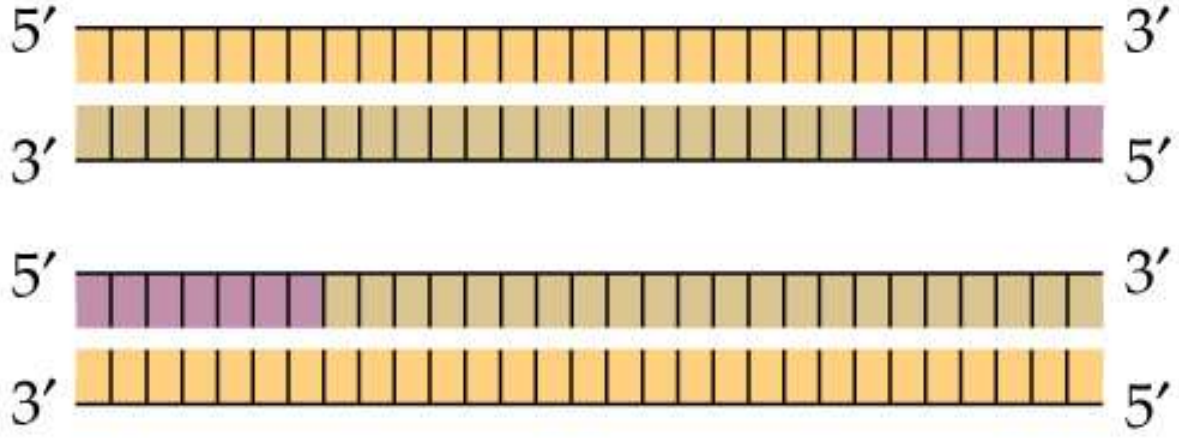
5′
3′
3′
5′
5′
3′
3′
5′

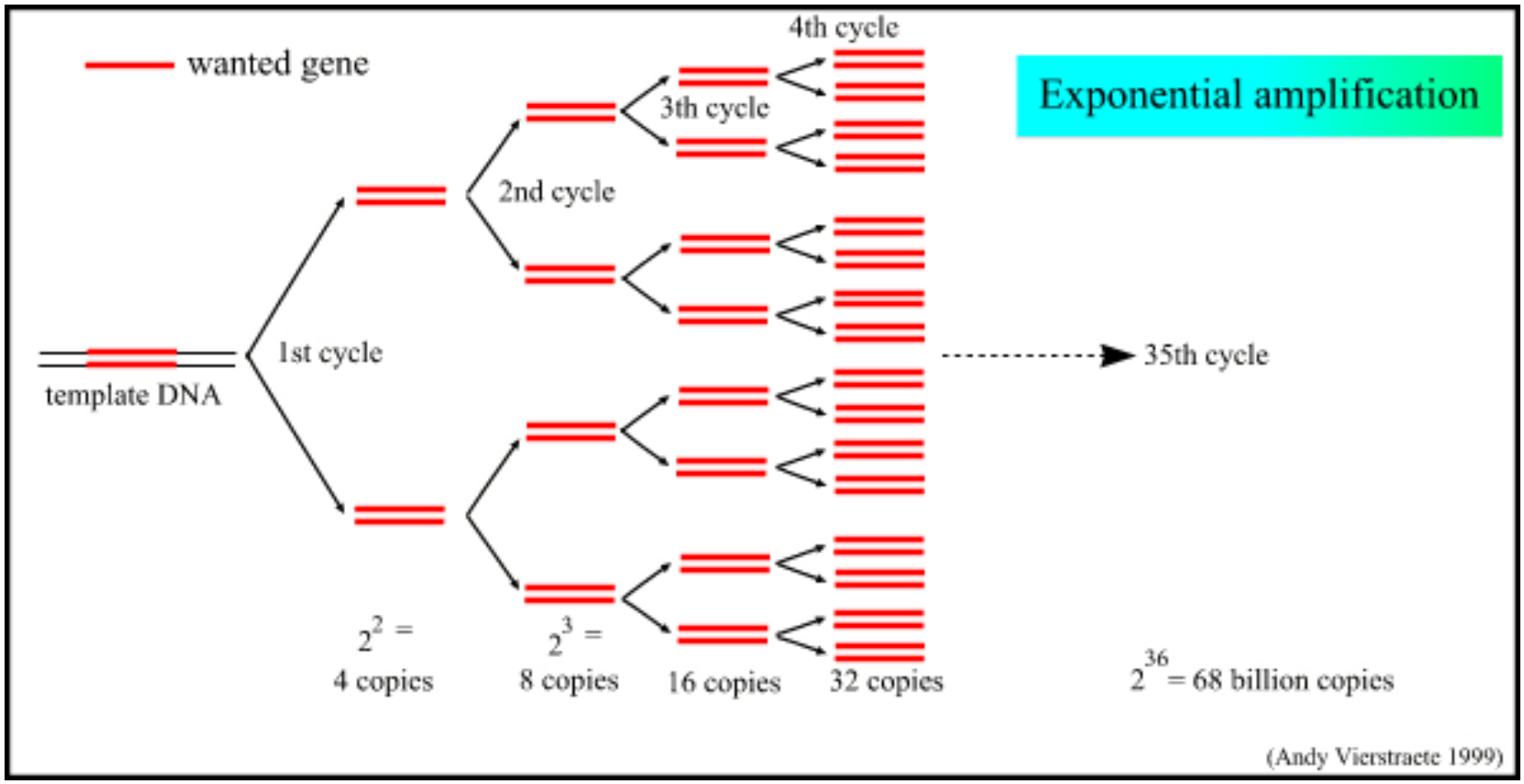
wanted gene
Exponential amplification
4th cycle
3th cycle
2nd cycle
1st cycle
template DNA
35th cycle
$2^2$ =
4 copies
$2^3$ =
8 copies
16 copies
32 copies
$2^{36}$ = 68 billion copies
(Andy Vierstraete 1999)

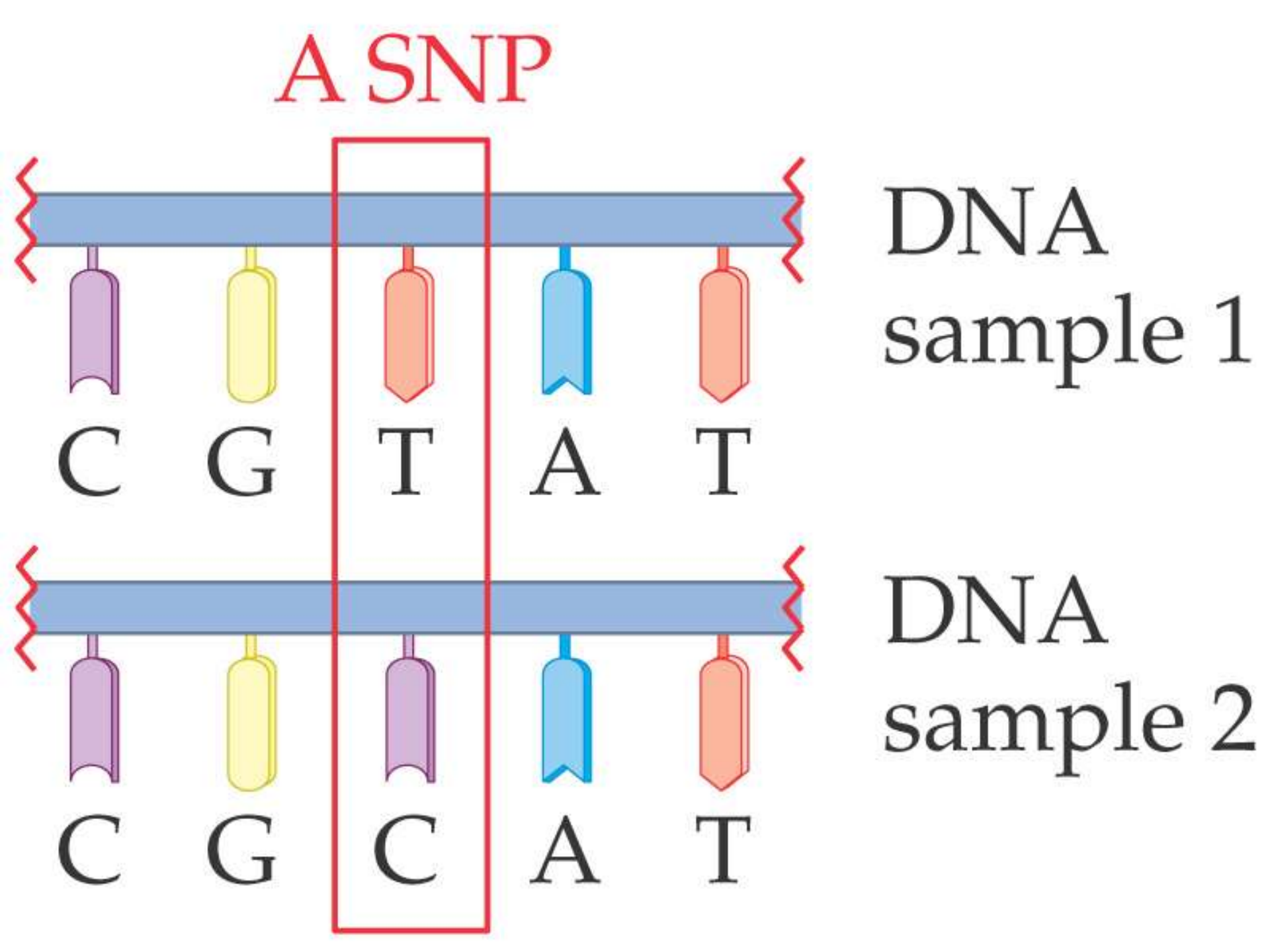
A SNP
DNA sample 1
C G T A T
DNA sample 2
C G C A T

# Recombinant DNA

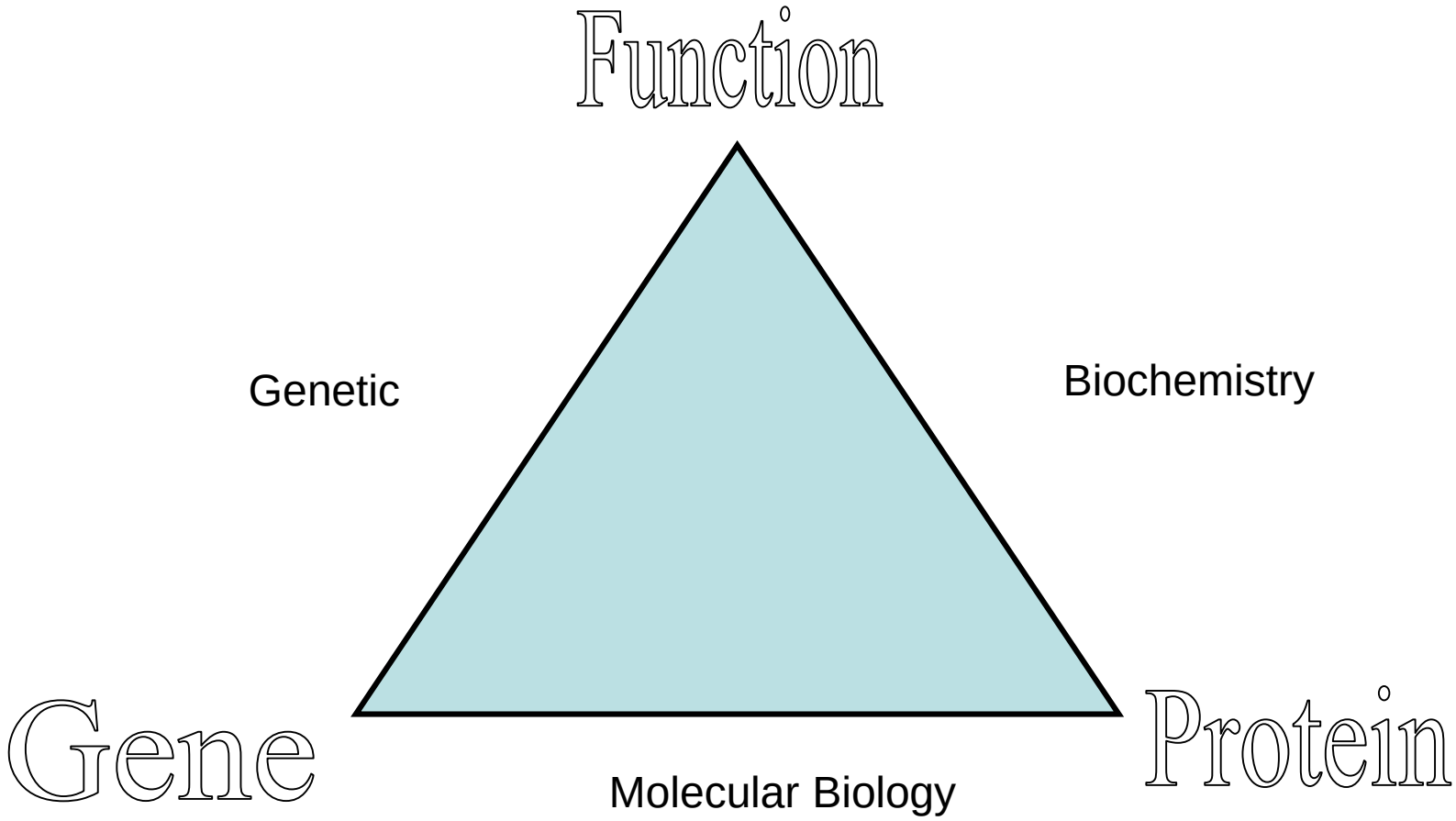

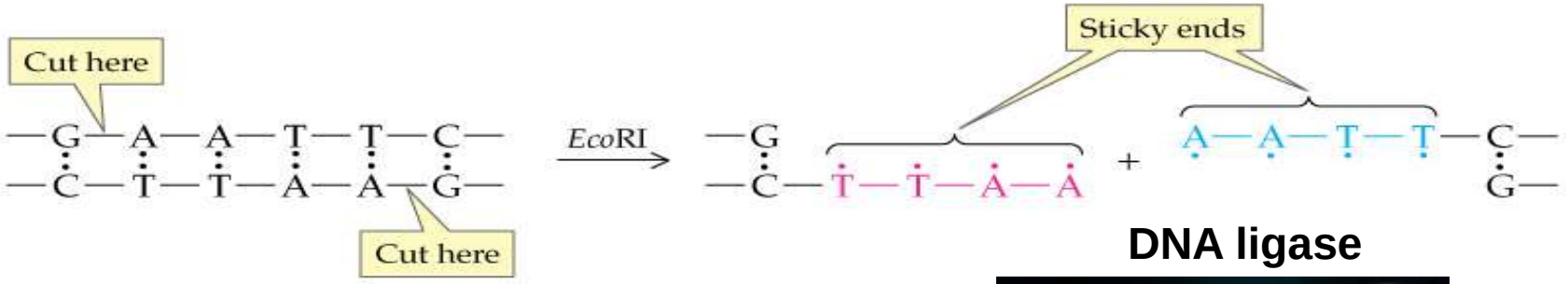


## Restriction Enzyme

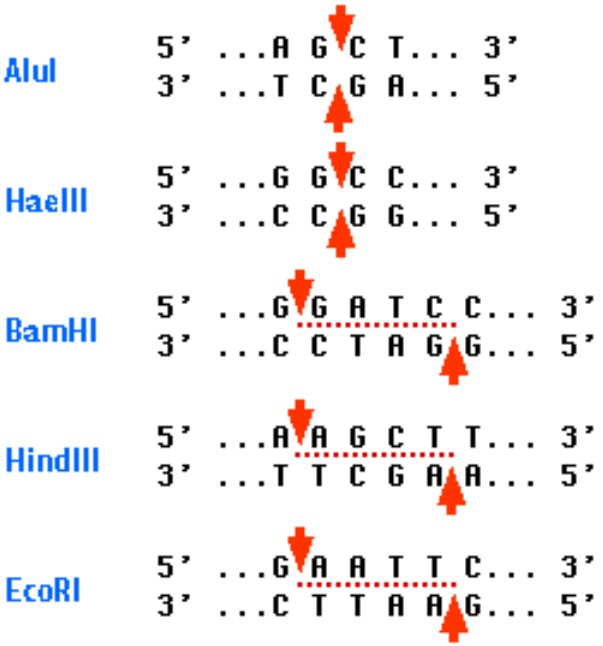


**AluI** and **HaeIII** produce blunt ends

**BamHI** **HindIII** and **EcoRI** produce "sticky" ends

## DNA ligase

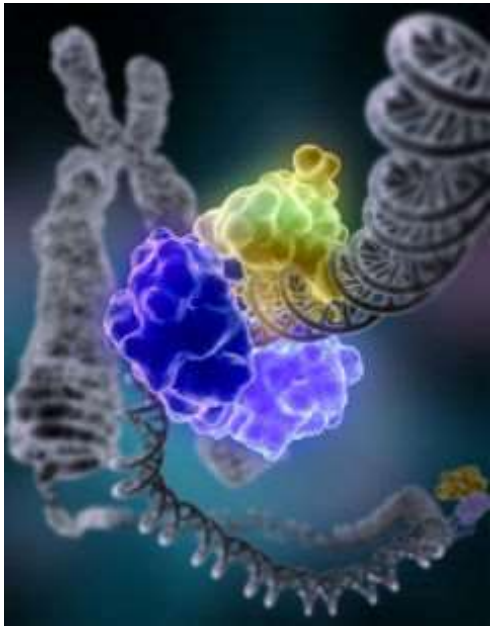

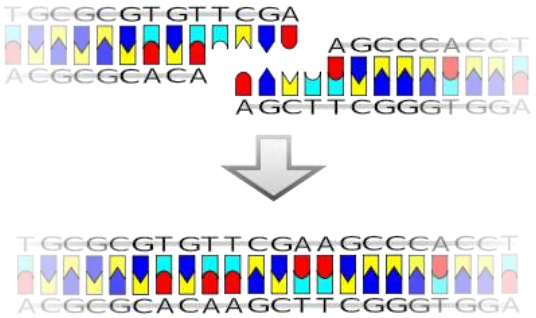

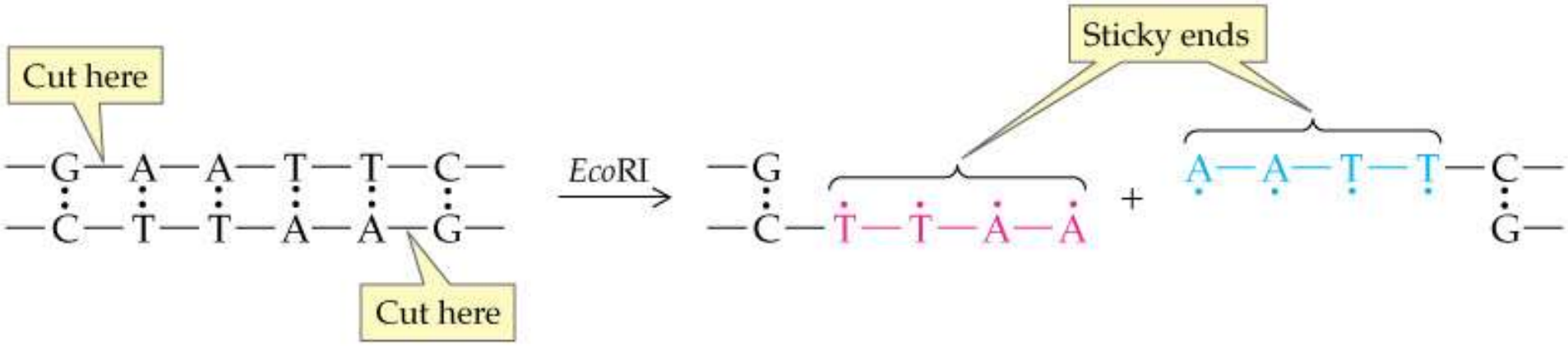
Cut here
G A A T T C
C T T A A G
Cut here
EcoRI
Sticky ends
G
C T T A A
+
A A T T C
G

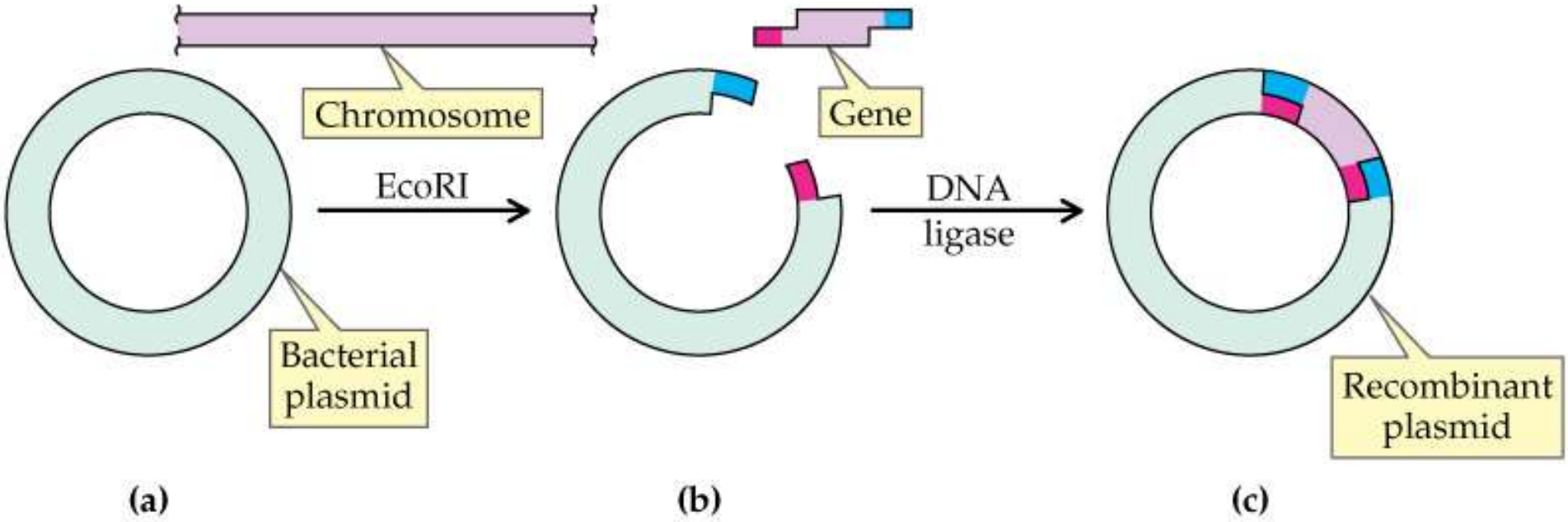
Chromosome
Bacterial plasmid
EcoRI
Gene
DNA ligase
Recombinant plasmid
(a)
(b)
(c)

# β-Galactosidase

The enzyme that splits lactose into glucose and galactose. Coded by a gene (lacZ) in the lac operon of Escherichia coli.

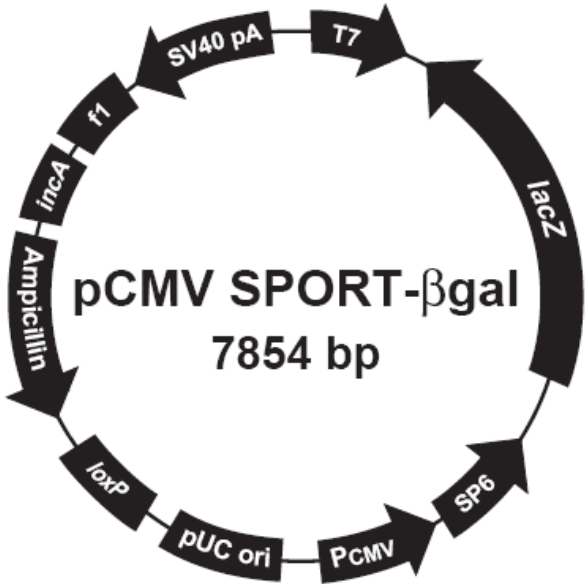


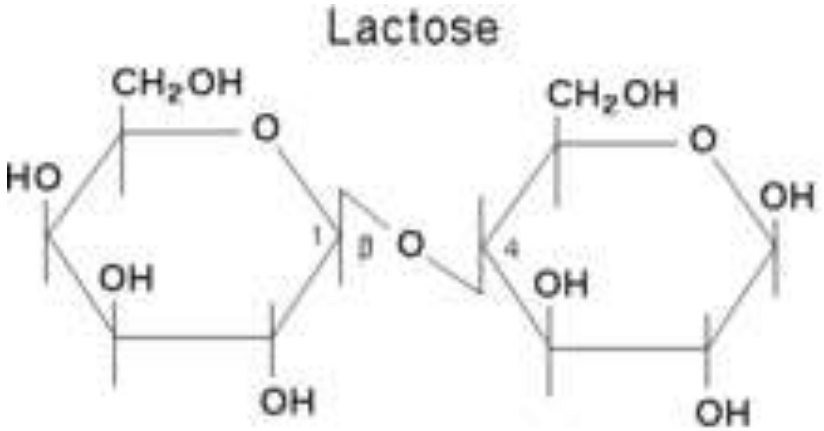


PUC is a family of plasmids that have an ampicillin resistance gene and more importantly a *lacZ* gene. A functional lacZ gene will produce the protein β - galactosidase. Bacterial colonies in which β - galactosidase is produced, will form blue colonies in the presence of the substrate 5 - bromo - 4 - chloro - 3 - indolyl - b - D - galactoside or as it is more commonly referred to, X-gal.

# DNA Sequencing

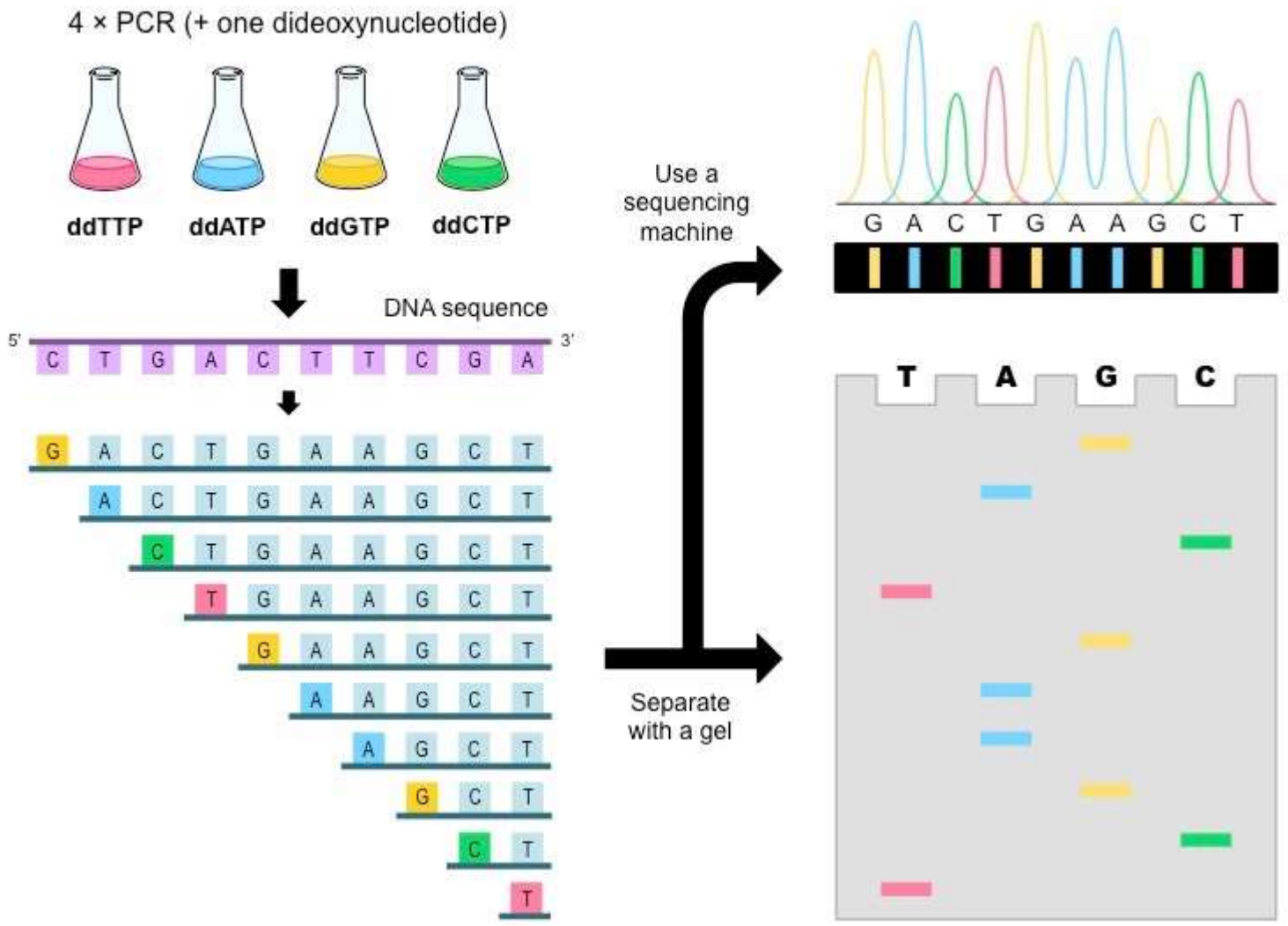

# DNA Sequencing

https://www.youtube.com/watch?v=vK-HlMaitnE

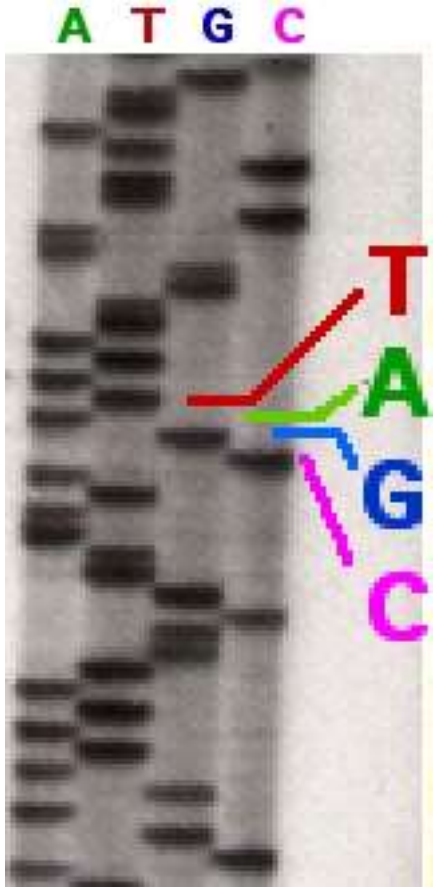


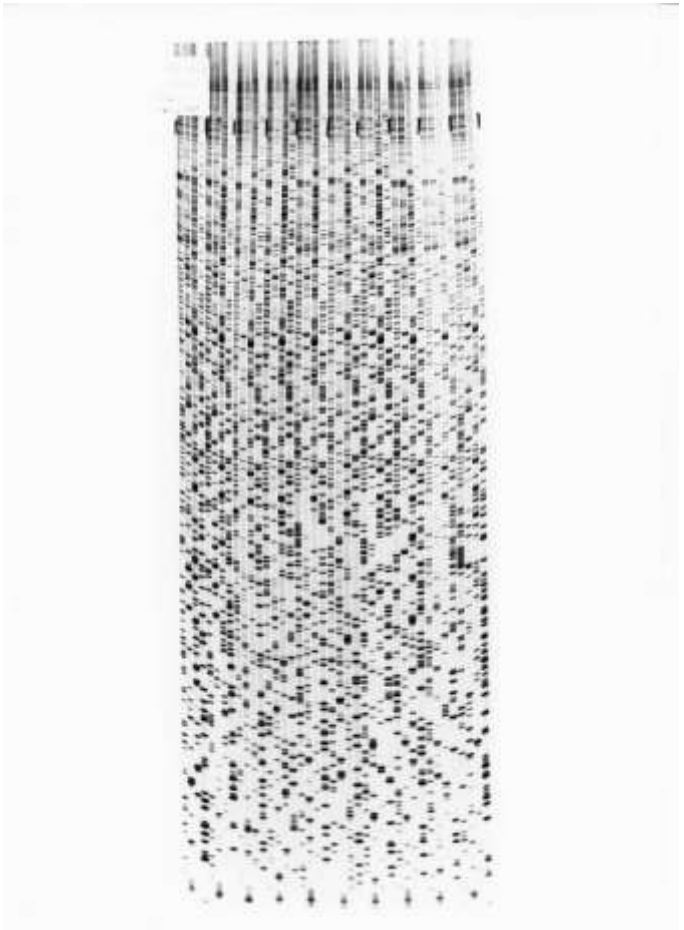

# Dye Terminations

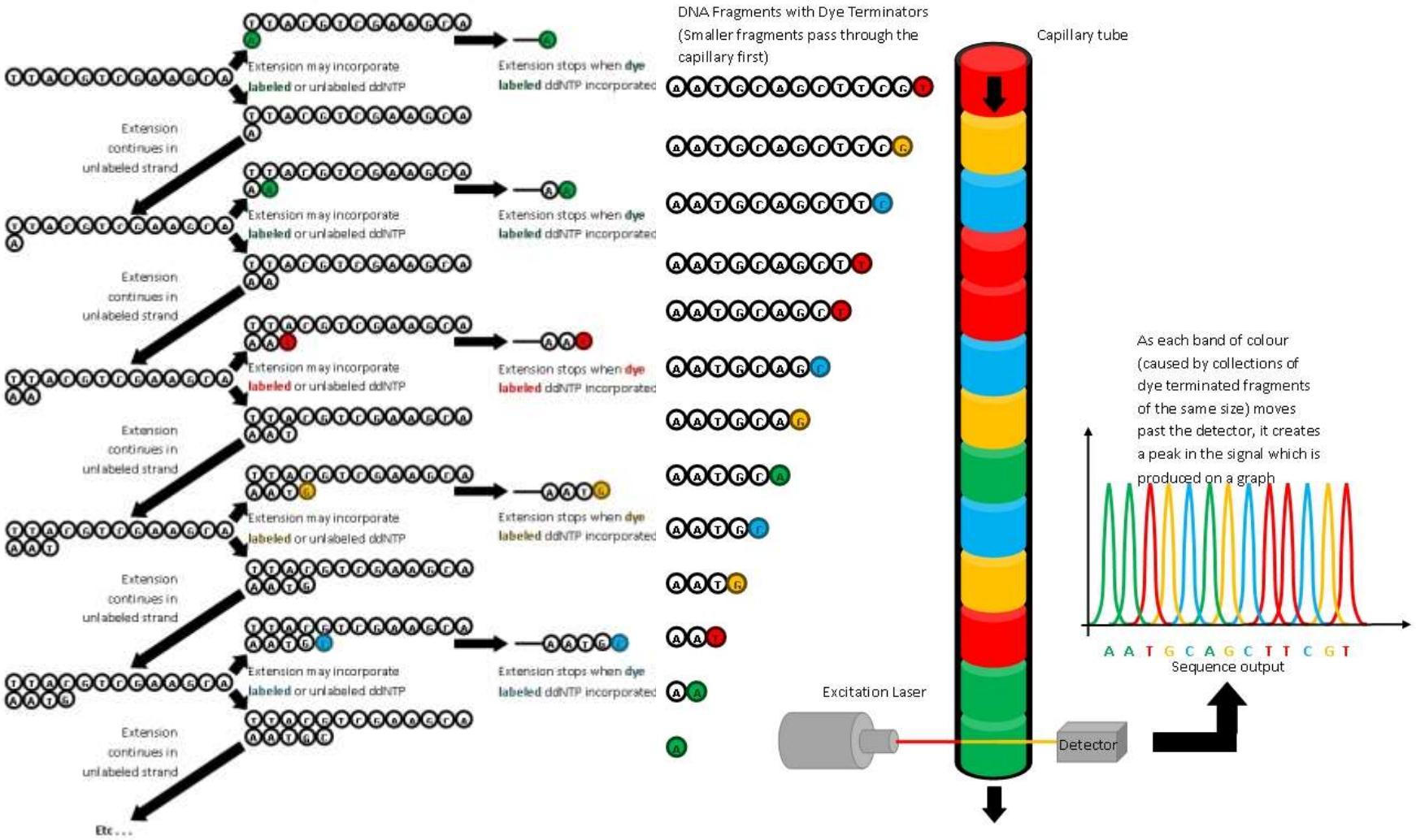

# GeneChip

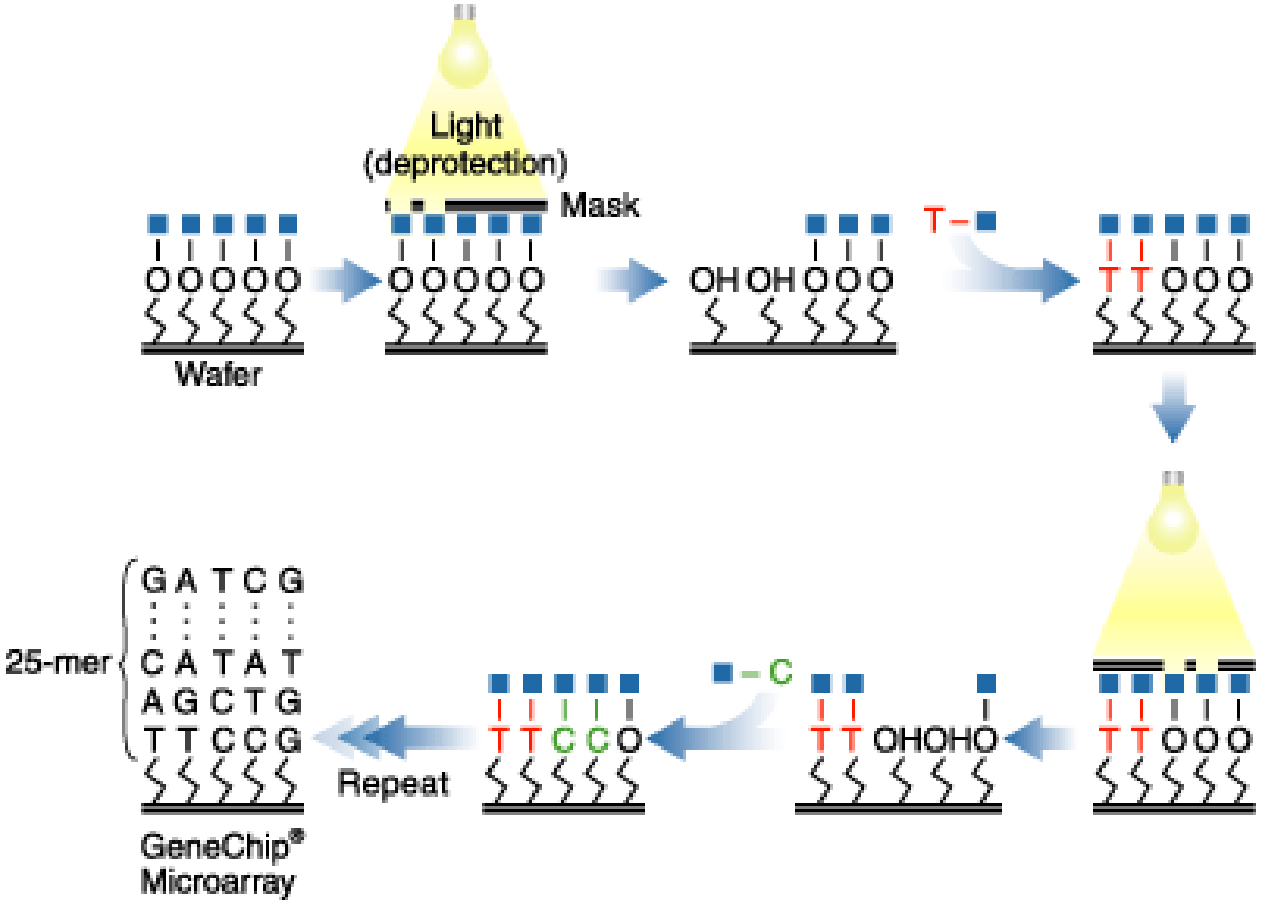
Light
(deprotection)
Mask
Wafer
T –
– C
Repeat
25-mer
G A T C G
C A T A T
A G C T G
T T C C G
GeneChip®
Microarray

# Scheme

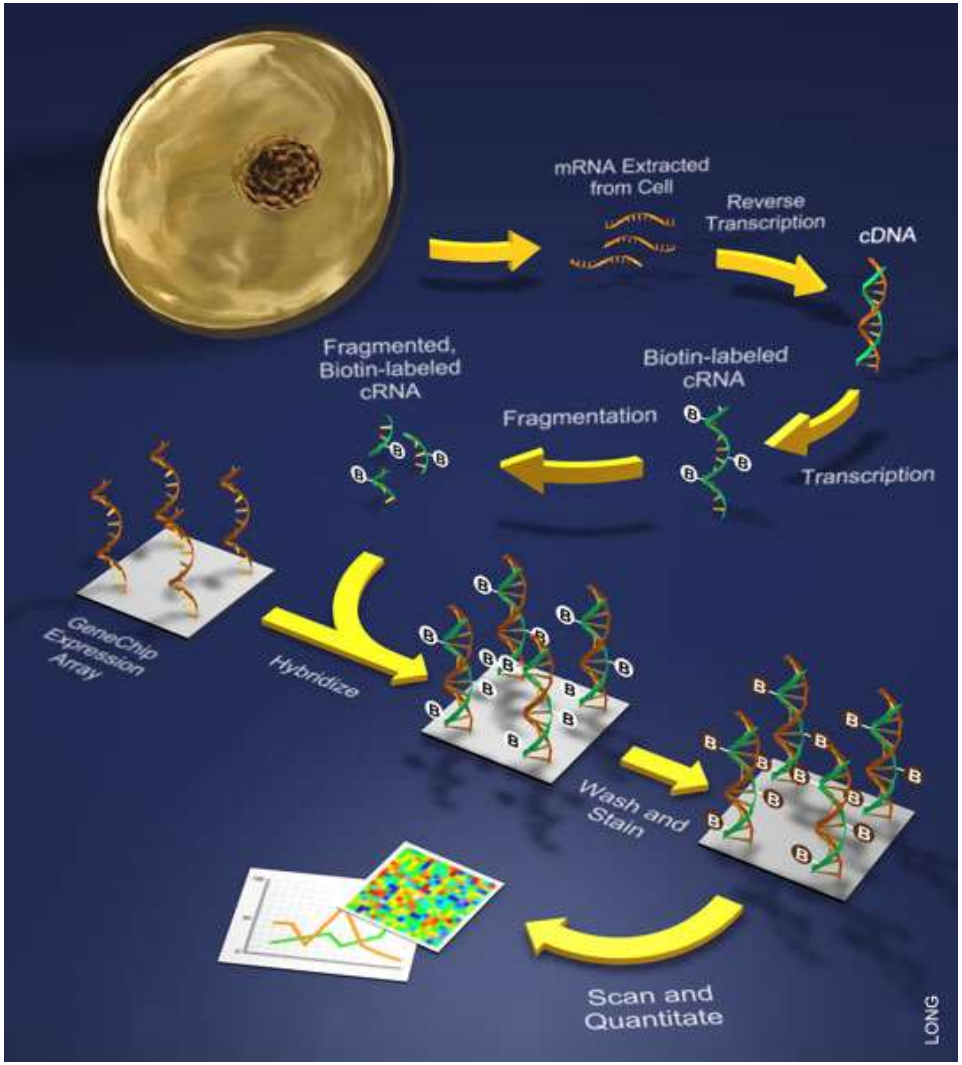
mRNA Extracted from Cell
Reverse Transcription
cDNA
Fragmented, Biotin-labeled cRNA
Biotin-labeled cRNA
Fragmentation
Transcription
GeneChip Expression Array
Hybridize
Wash and Stain
Scan and Quantitate
LONG

# cDNA Microarray

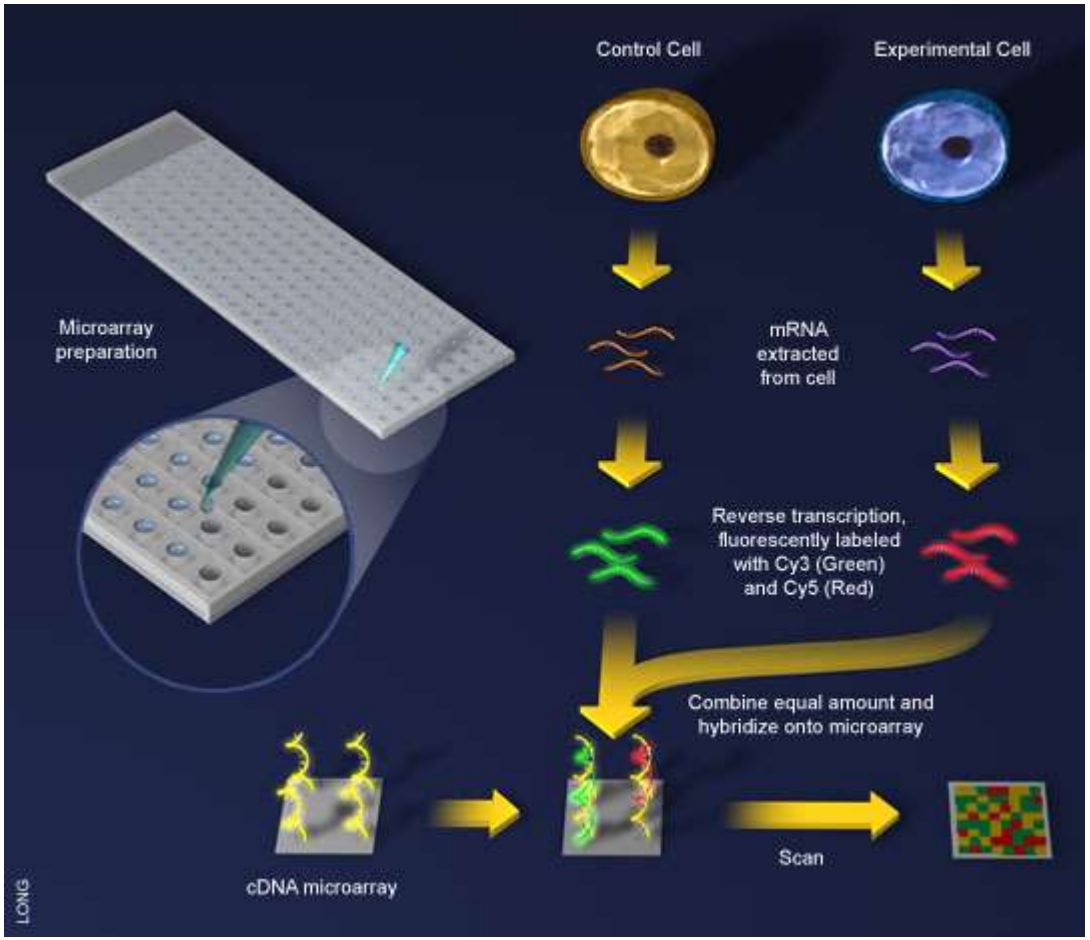

# NGS Illumina

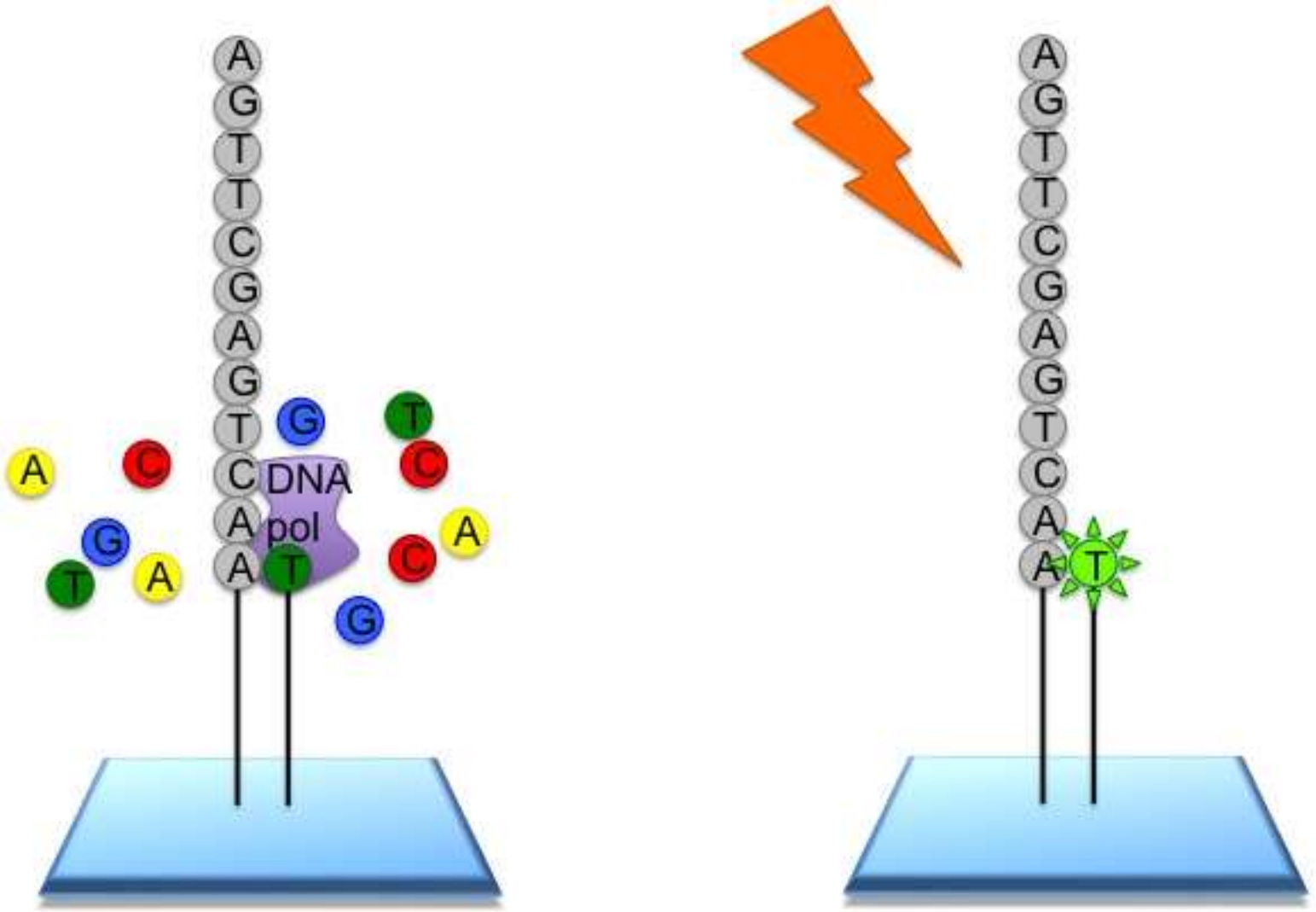


100-150 bp

# NGS Illumina

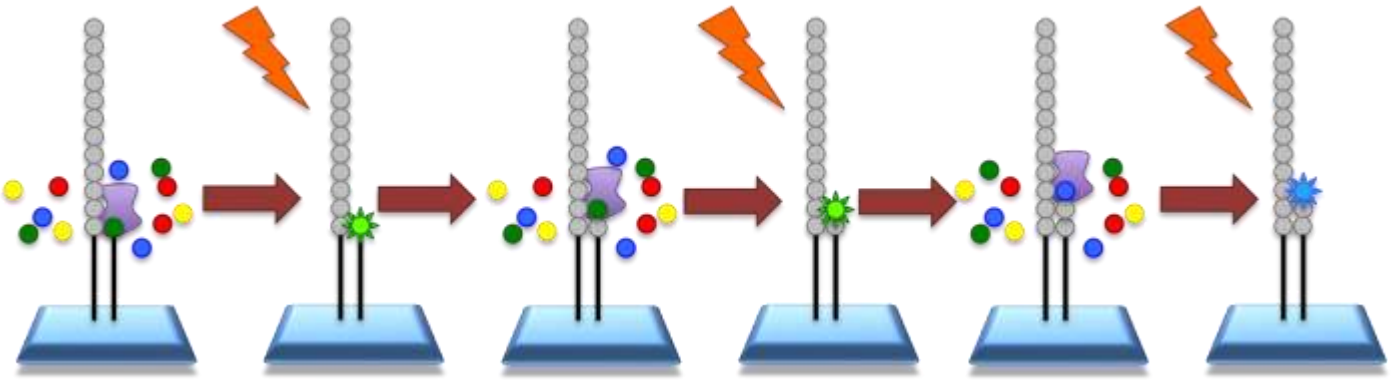

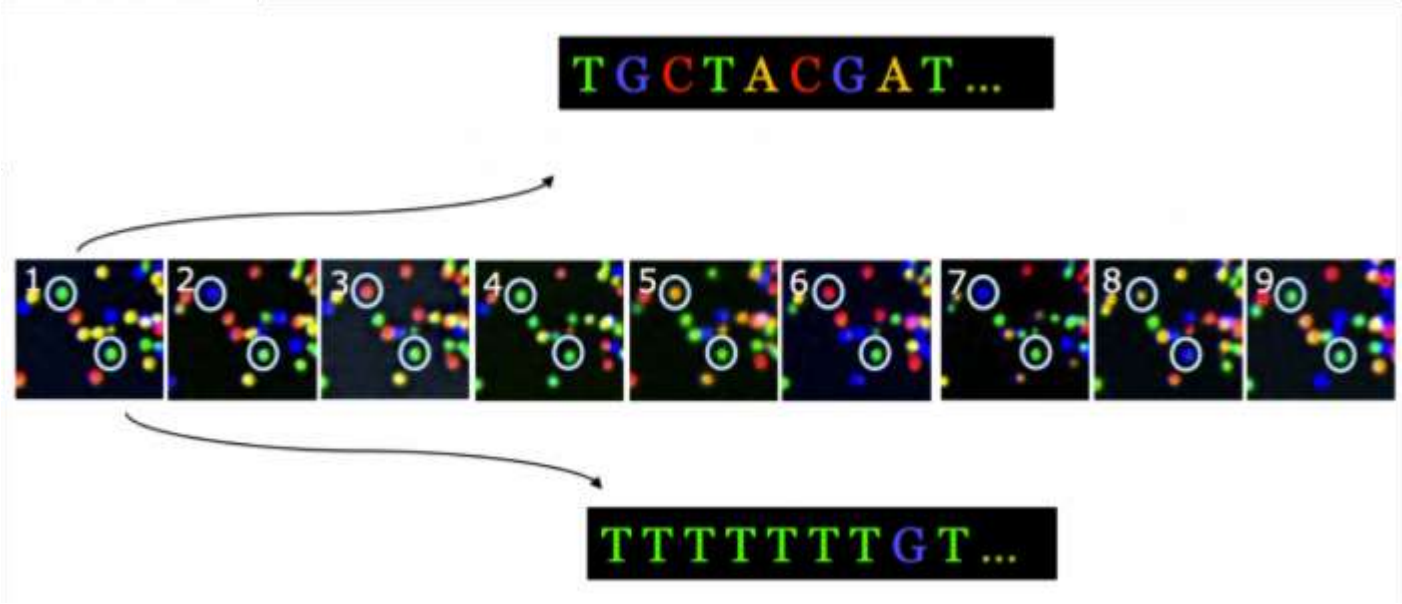

# Roche 454 sequencing

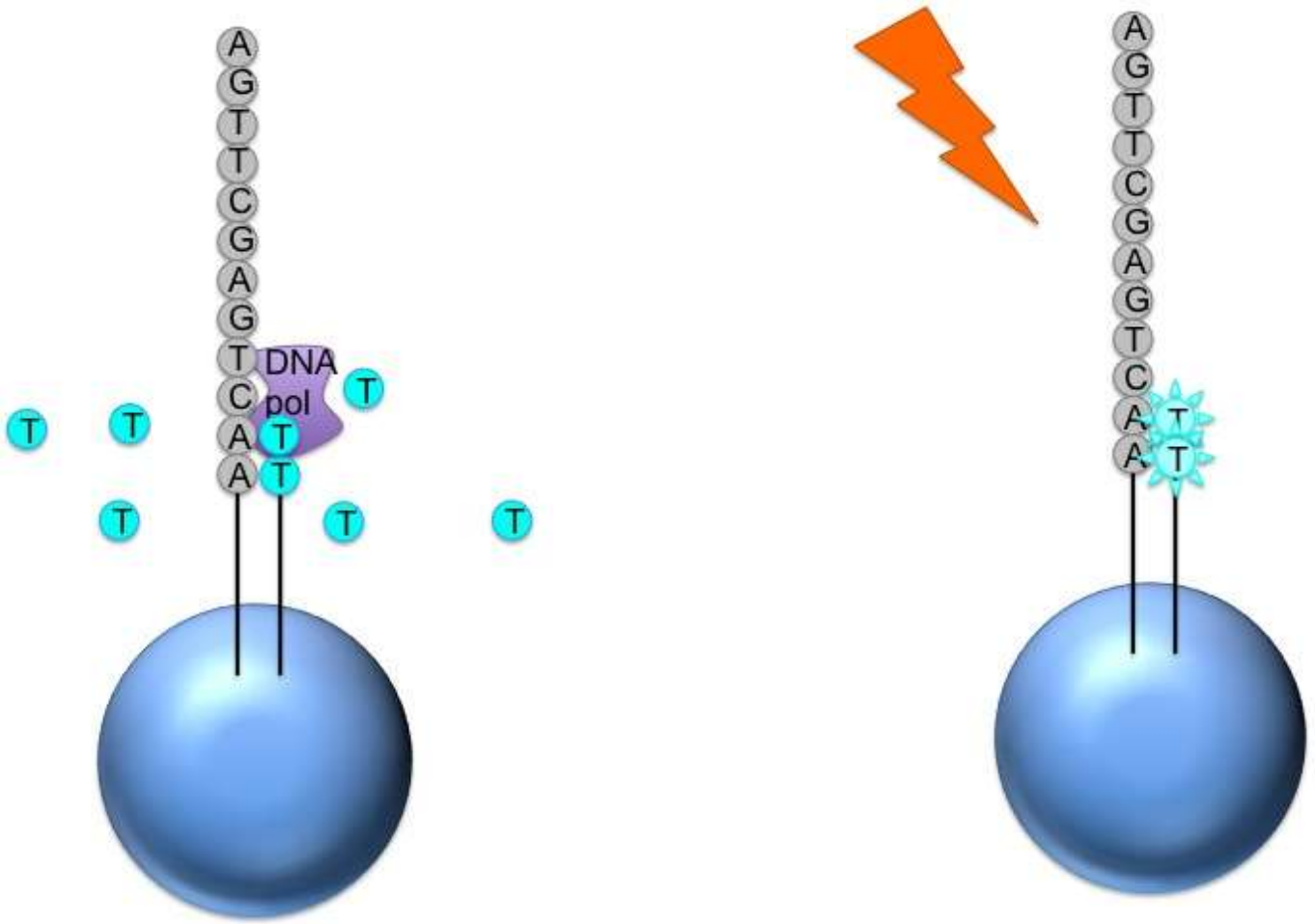


1000 bp

# Roche 454 sequencing

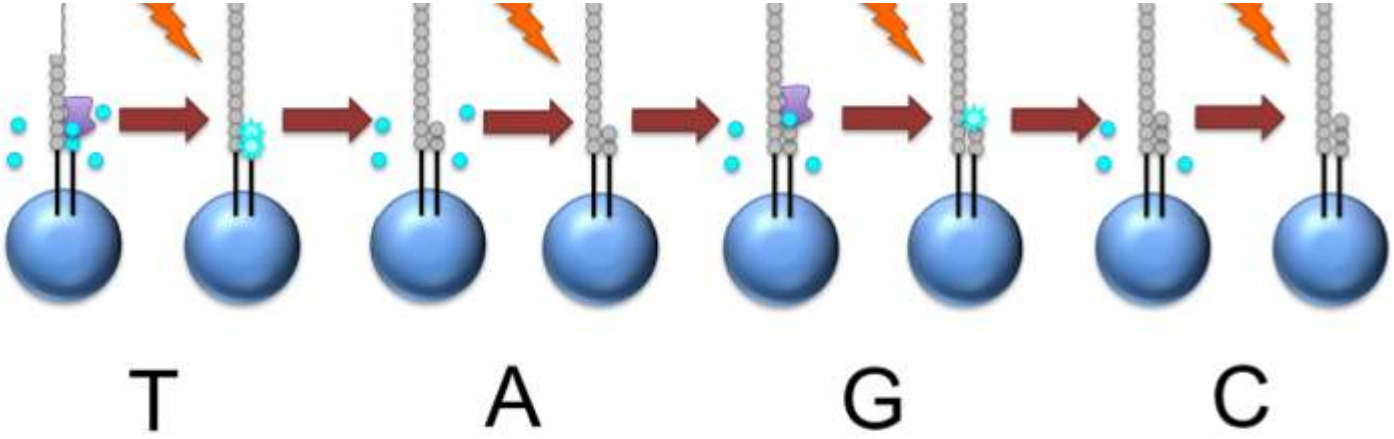


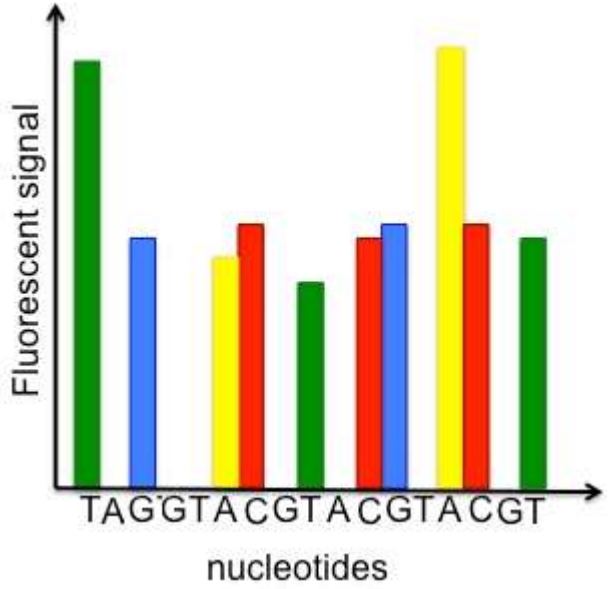

The four main advantages of NGS over classical Sanger sequencing are:

**speed**
**cost**
**sample size**
**accuracy**

NGS is significantly cheaper, quicker, needs significantly less DNA and is more accurate and reliable than Sanger sequencing.

NGS is quicker than Sanger sequencing in two ways. Firstly, the chemical reaction may be combined with the signal detection in some versions of NGS, whereas in Sanger sequencing these are two separate processes. Secondly and more significantly, only one read (maximum ~1kb) can be taken at a time in Sanger sequencing, whereas NGS is massively parallel, allowing 300Gb of DNA to be read on a single run on a single chip.
The first human genome sequence cost in the region of £300M. Using modern Sanger sequencing methods, aided by data from the known sequence, a full human genome would still cost £6M. Sequencing a human genome with Illumina today would cost only £6,000.

# Third Generation Sequencing

PacBio SMRT seq

DNA passes thru polymerase in an illuminated volume

Raw output is fluorescent signal of the nucleotide incorporation, specific to each nucleotide

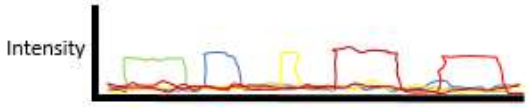


A,C,T,G have known pulse durations, which are used to infer methylated nucleotides

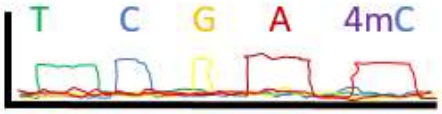


Oxford Nanopore

DNA passes thru nanopore

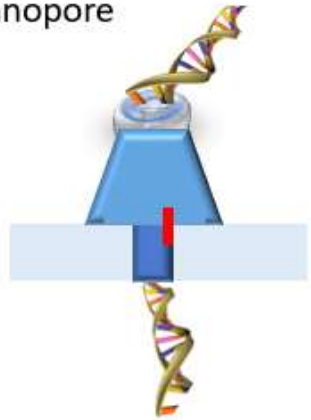

Raw output is electrical signal caused by nucleotide blocking ion flow in nanopore

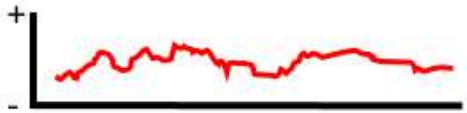


Each nucleotide has a specific electric "signature"

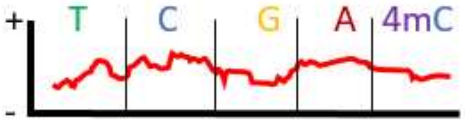

# Digital PCR


## Droplet digital PCR

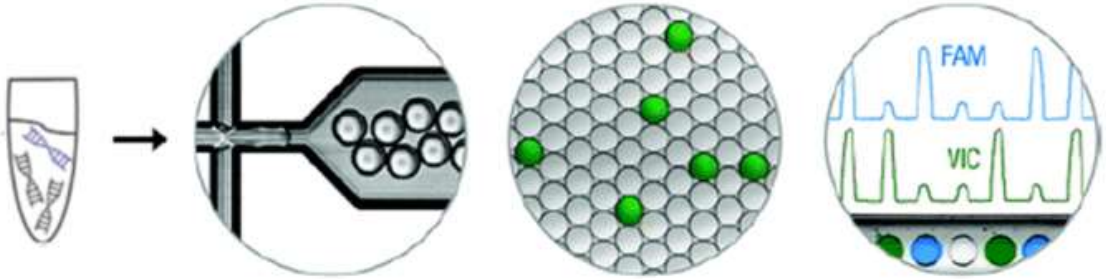


Bio-Rad QX100

| 1. MAKE | 2. CYCLE | 3. READ | |
|---|---|---|---|
| Sample is partitioned into 20,000 droplets | Run PCR cycles in all droplets simultaneously | Measure fluorescence intensity in each droplet | Calculate concentration from number of positive droplets |

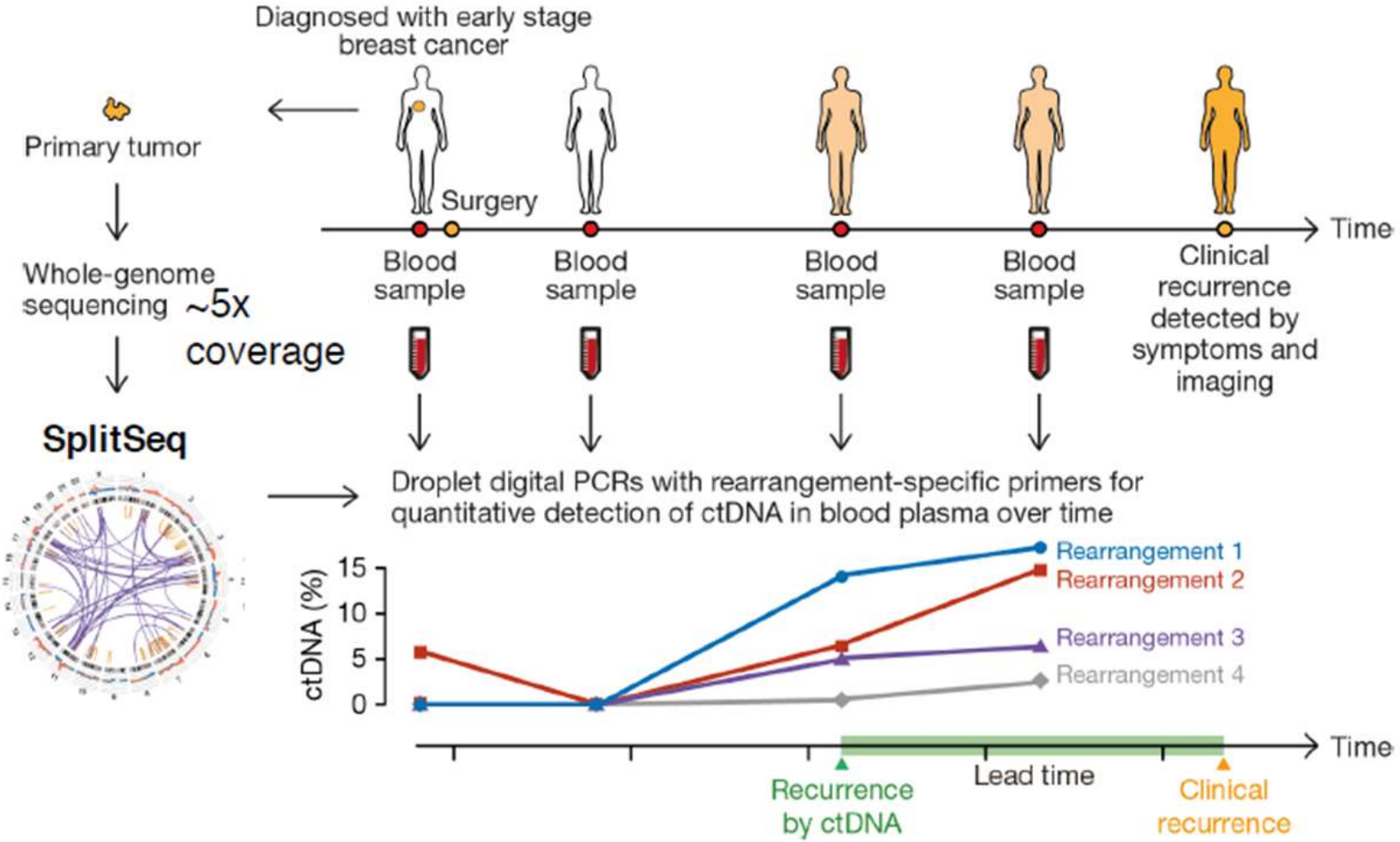
Diagnosed with early stage breast cancer
Primary tumor
Surgery
Time
Whole-genome sequencing
~5x coverage
Blood sample
Blood sample
Blood sample
Blood sample
Clinical recurrence detected by symptoms and imaging
SplitSeq
Droplet digital PCRs with rearrangement-specific primers for quantitative detection of ctDNA in blood plasma over time
ctDNA (%)
15
10
5
0
Rearrangement 1
Rearrangement 2
Rearrangement 3
Rearrangement 4
Time
Lead time
Recurrence by ctDNA
Clinical recurrence

# Microarray

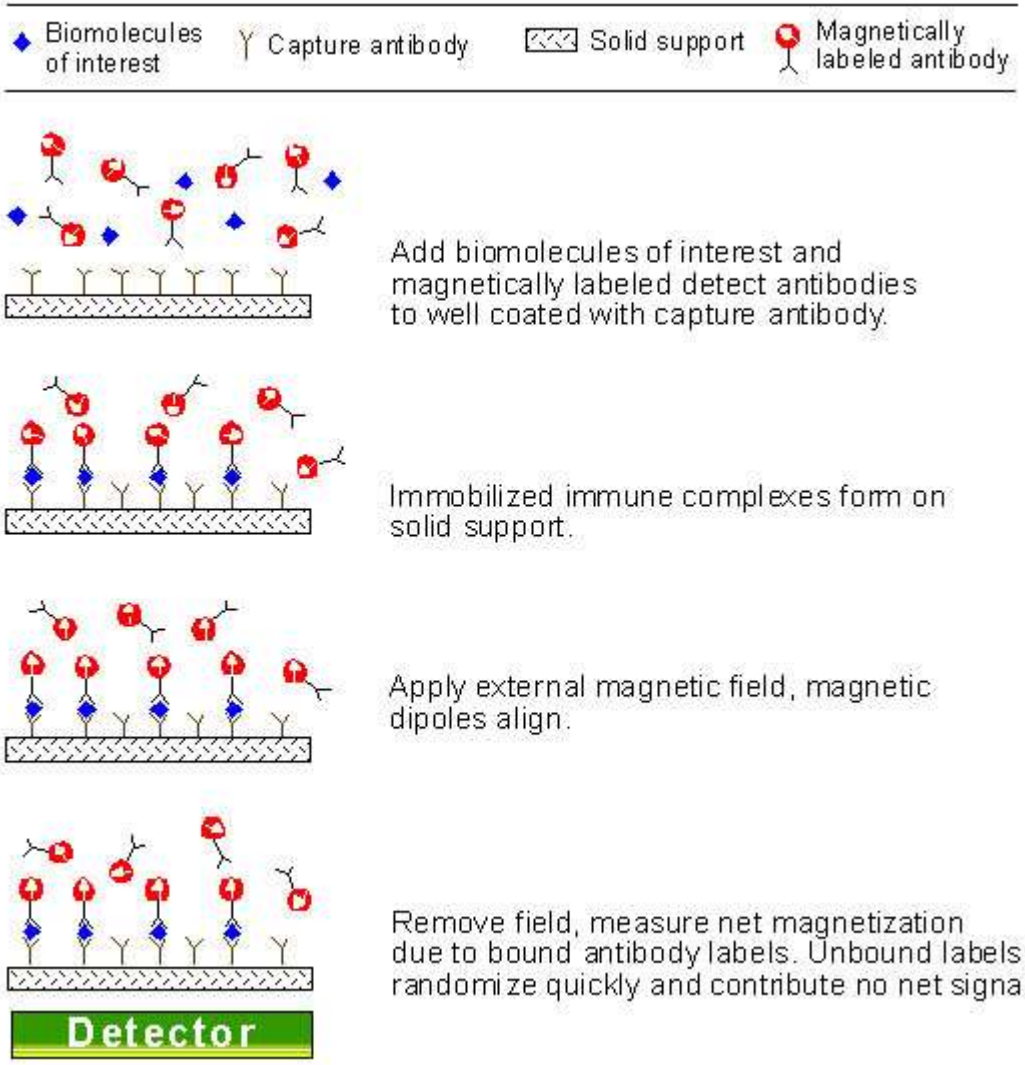
Biomolecules of interest
Capture antibody
Solid support
Magnetically labeled antibody
Add biomolecules of interest and magnetically labeled detect antibodies to well coated with capture antibody.
Immobilized immune complexes form on solid support.
Apply external magnetic field, magnetic dipoles align.
Remove field, measure net magnetization due to bound antibody labels. Unbound labels randomize quickly and contribute no net signal.
Detector

# Microarray

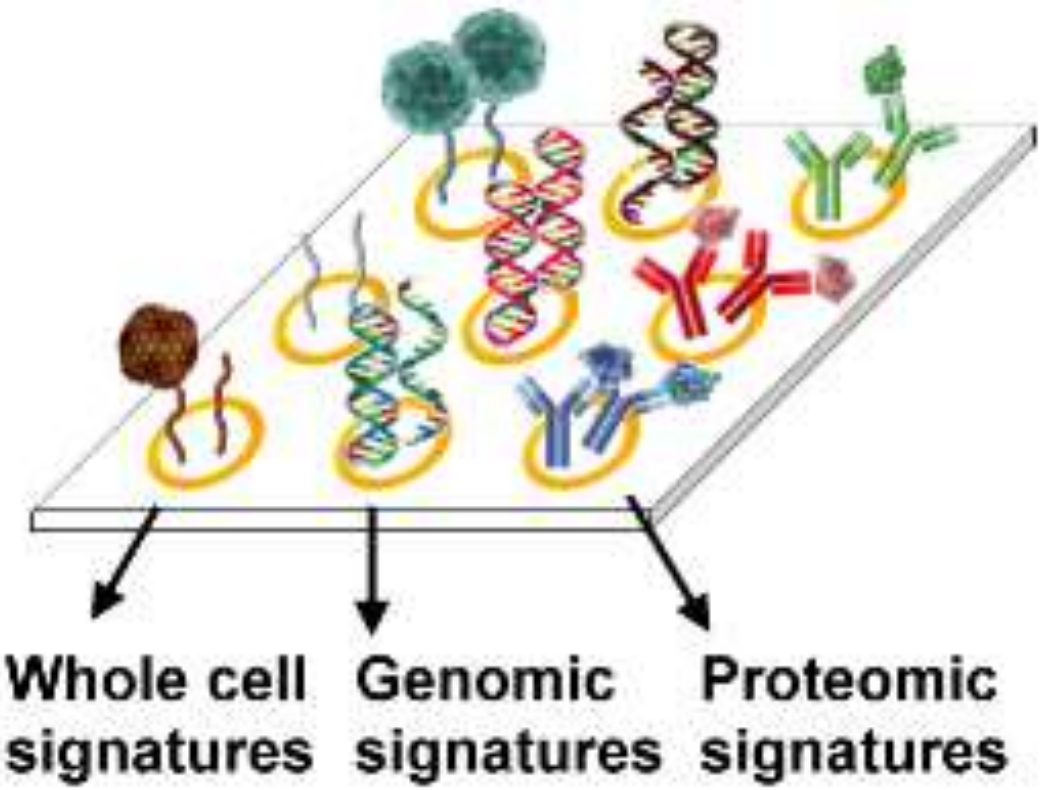
Whole cell signatures
Genomic signatures
Proteomic signatures

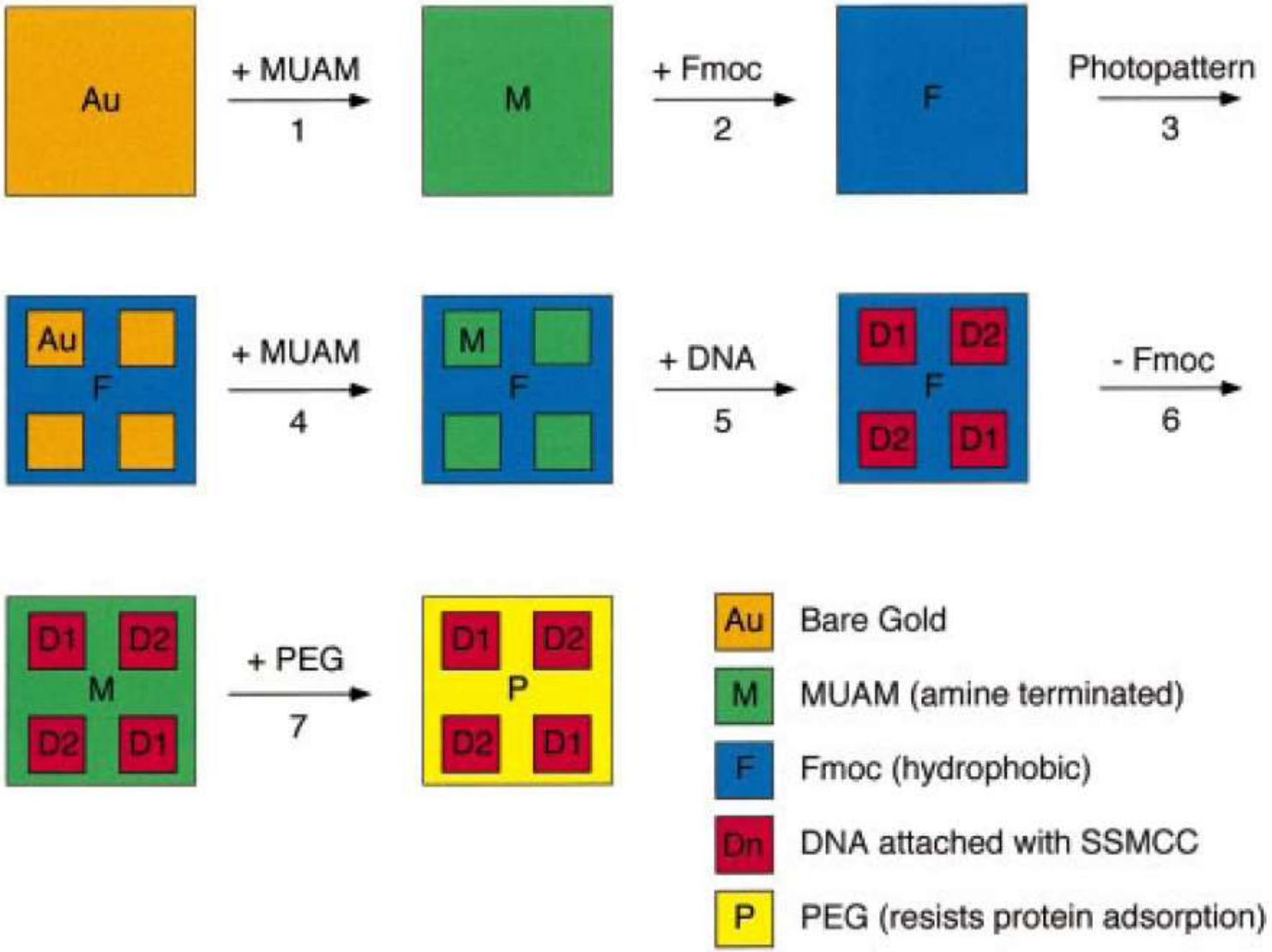


**Figure 1.** Fabrication scheme for the construction of multi-element DNA arrays. A clean gold surface is reacted with the amine-terminated alkanethiol MUAM, and subsequently reacted with Fmoc-NHS to create a hydrophobic surface. This surface is then exposed to UV radiation through a quartz mask and rinsed with solvent to remove the MUAM+Fmoc from specific areas of the surface, leaving bare gold pads. These bare gold areas on the sample surface are filled in with MUAM, resulting in an array of MUAM pads surrounded by a hydrophobic Fmoc background. Solutions of DNA are then delivered by pipet onto the specific array locations and are covalently bound to the surface via the bifunctional linker SSMCC. In the final two steps, the Fmoc-terminal groups on the array background are removed and replaced by PEG groups which prohibit the nonspecific binding of analyte proteins to the background.

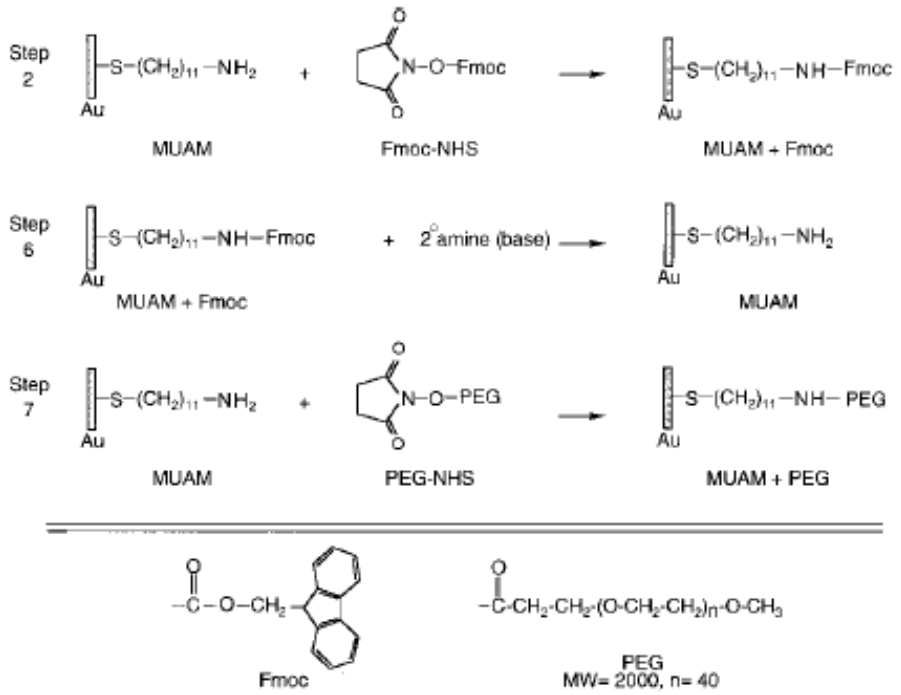


**Figure 2.** Surface reaction scheme showing the steps involved in the reversible modification of the array background. (Step 2) The starting amine-terminated alkanethiol surface (MUAM) is reacted with the Fmoc-NHS protecting group to form a carbamate linkage thus creating a hydrophobic Fmoc-terminated surface. (Step 6) After DNA immobilization (see Figure 3), the hydrophobic Fmoc group is removed from the surface with a basic secondary amine, resulting in the return of the original MUAM surface. (Step 7) In the final array fabrication step, the deprotected MUAM is reacted with PEG-NHS to form an amide bond that covalently attaches PEG to the array surface.

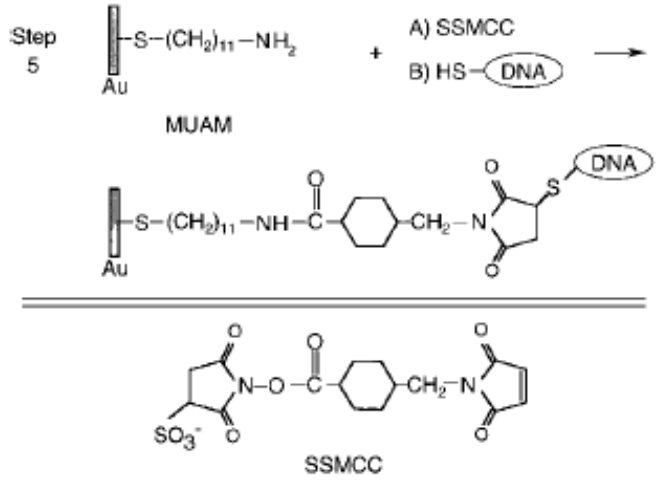


**Figure 3.** Surface reaction scheme showing the immobilization of thiol-terminated DNA to the array surface. In Step 5 of the DNA array fabrication, the heterobifunctional linker SSMCC is used to attach 5′-thiol modified oligonucleotide sequences to reactive pads of MUAM. This linker contains an NHSS ester functionality (reactive toward amines) and a maleimide functionality (reactive toward thiols). The surface is first exposed to a solution of the linker, whereby the NHSS ester end of the molecule reacts with the MUAM surface. Excess linker is rinsed away and the array surface is then spotted with 5′-thiol-modified DNA that reacts with the maleimide groups forming a covalent bond to the surface monolayer.

# Glass Surface Modification

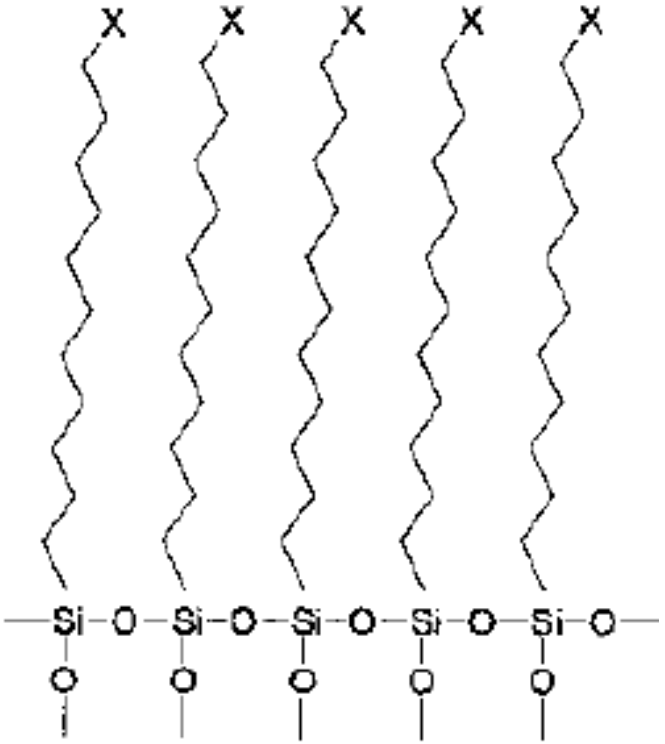


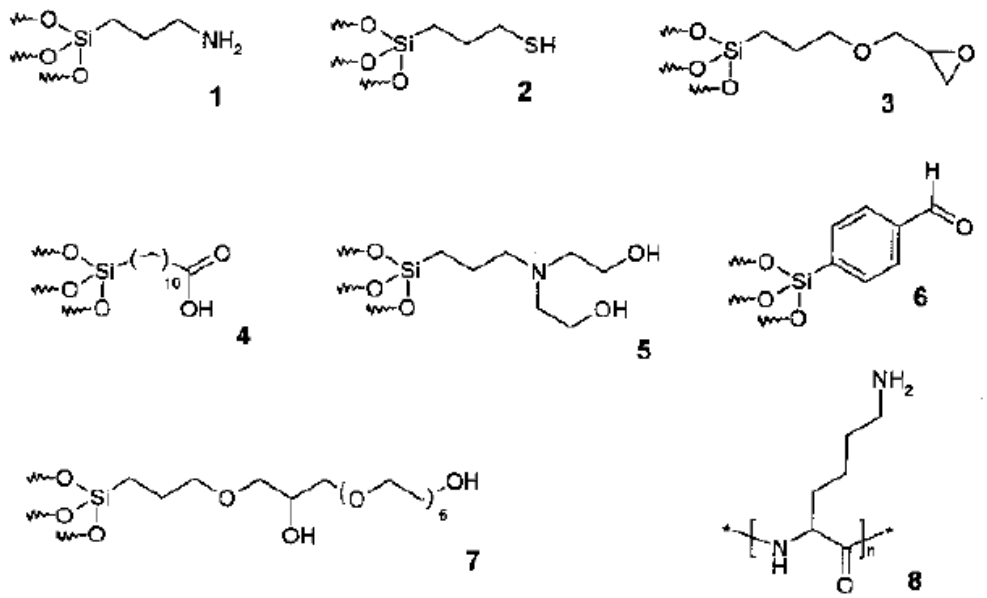


**Scheme 2.2** Reagents for derivatization of glass surfaces. 1 APTES = aminopropyltriethoxysilane; **2** MPTS = 3-mercaptopropyltrimethoxysilane; **3** GPTS = glycidoxypropyltrimethoxysilane; **4** TETU = triethoxysilane undecanoic acid; **5** HE-APTS = bis(hydroxyethyl)aminopropyltriethoxysilane); **6** 4-trimethoxysilylbenzaldehyde; **7** GPTS/HEG = glycidoxypropyltrimethoxysilane-hexaethylene glycol; **8** poly(lysine).

**Scheme 2.1** 2D schematic description of a polysiloxane monolayer on a glass surface (X = terminal functional

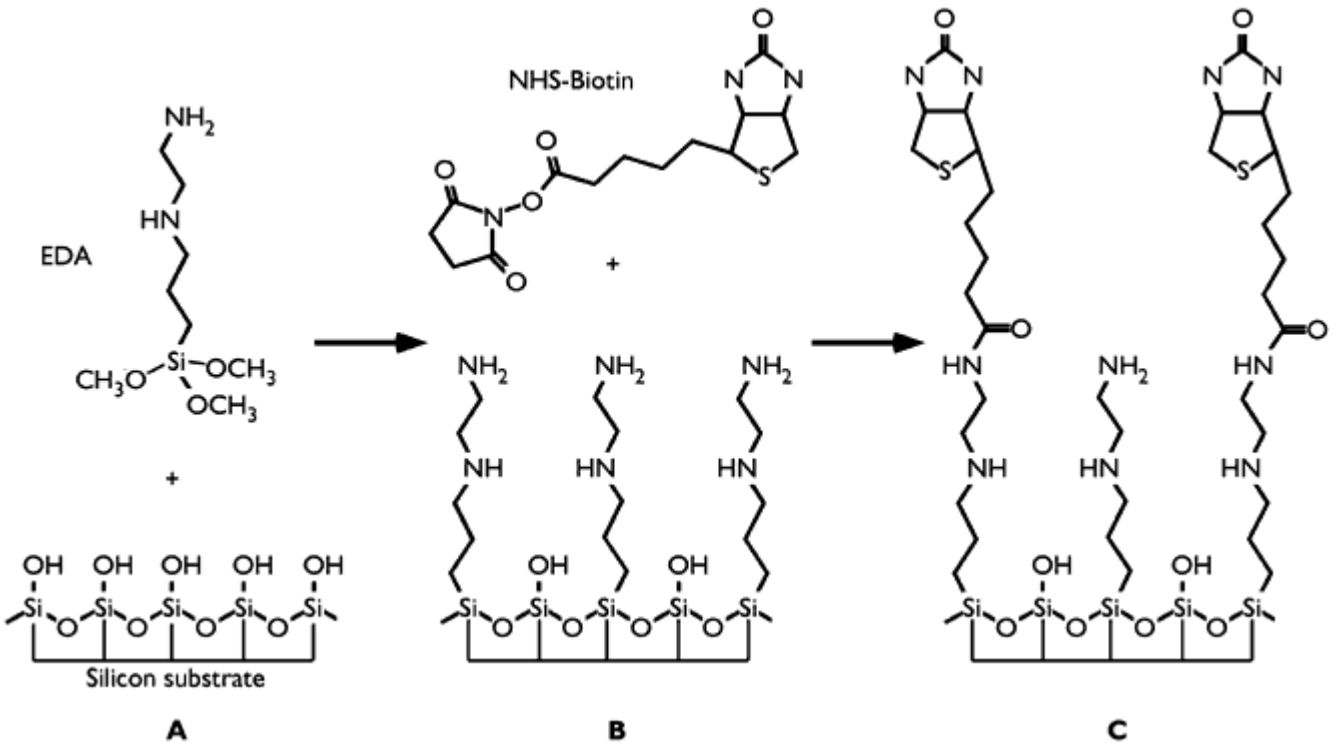
NHS-Biotin
EDA
Silicon substrate
A
B
C

# Biotin-Streptavidin

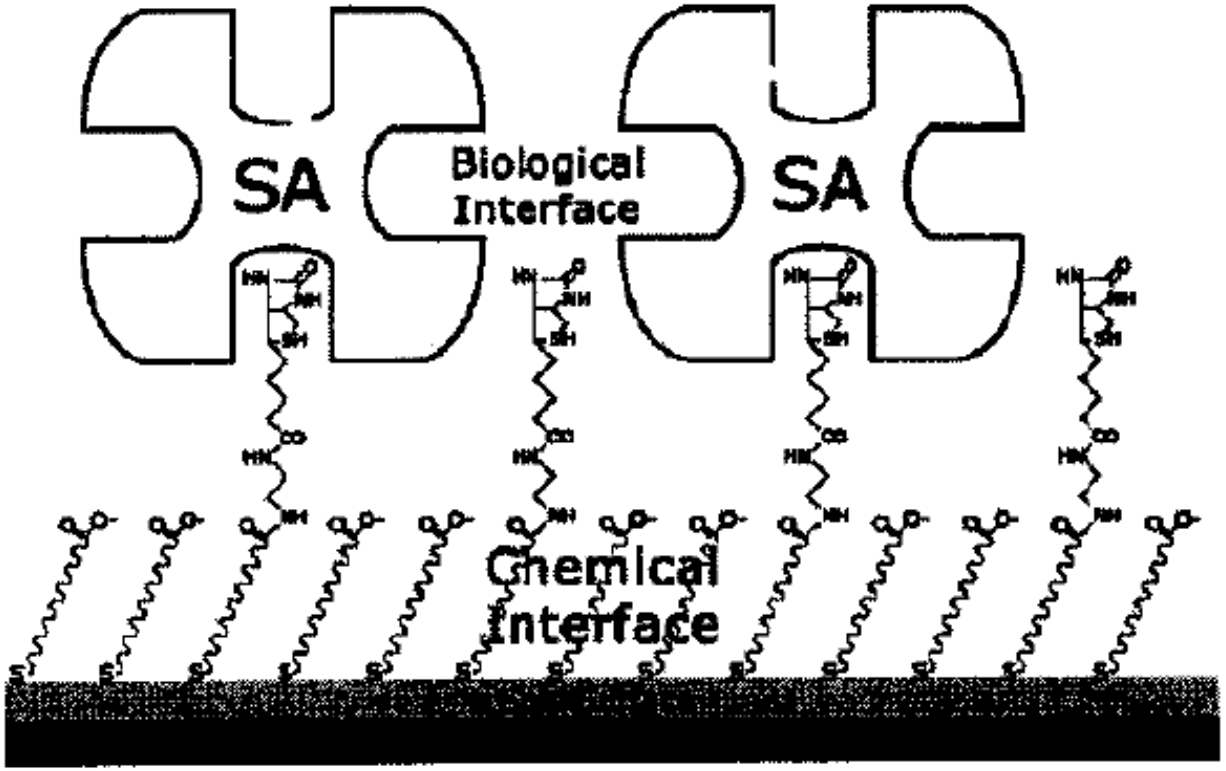


**Figure 2.3** Schematic respresentation of a steptavidin sensor surface assembled on a reaction-controlled biotinylated SAM [28].

# Protein Array

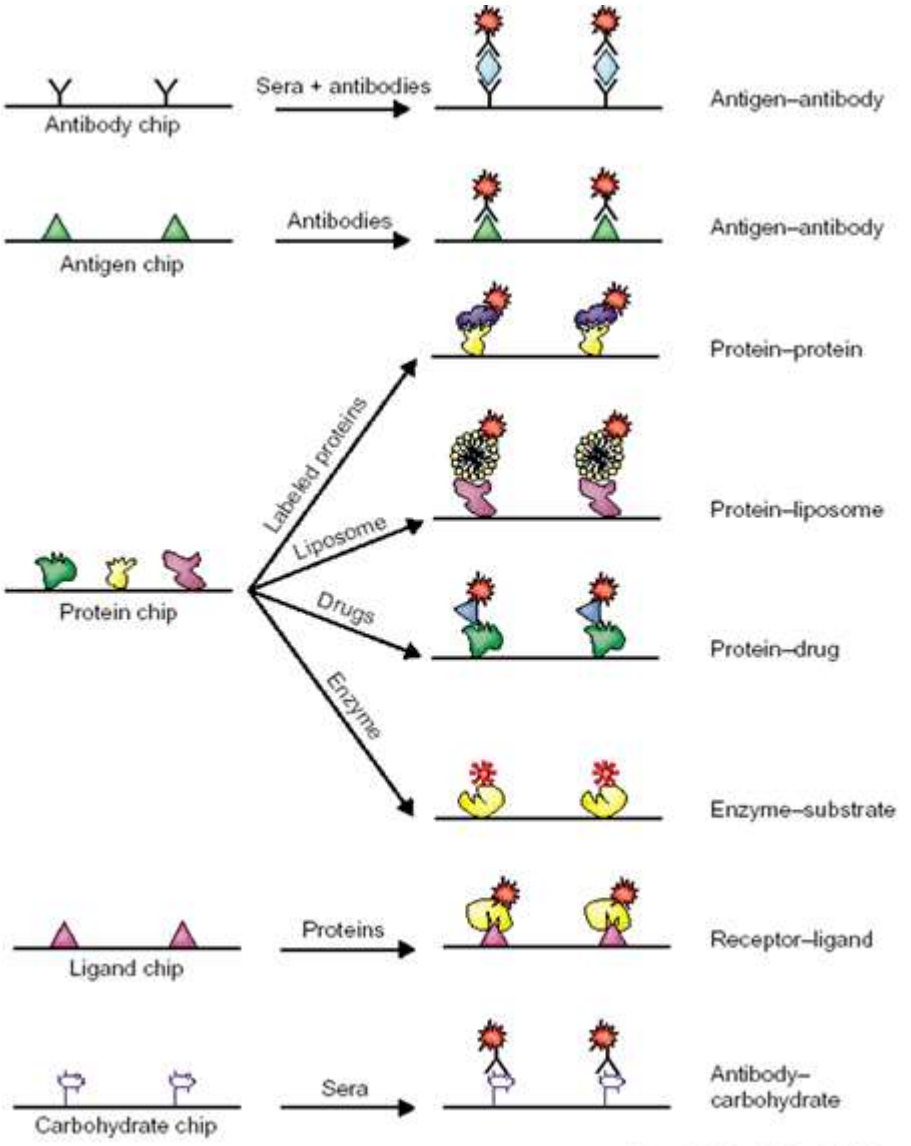

# BSA Blocking

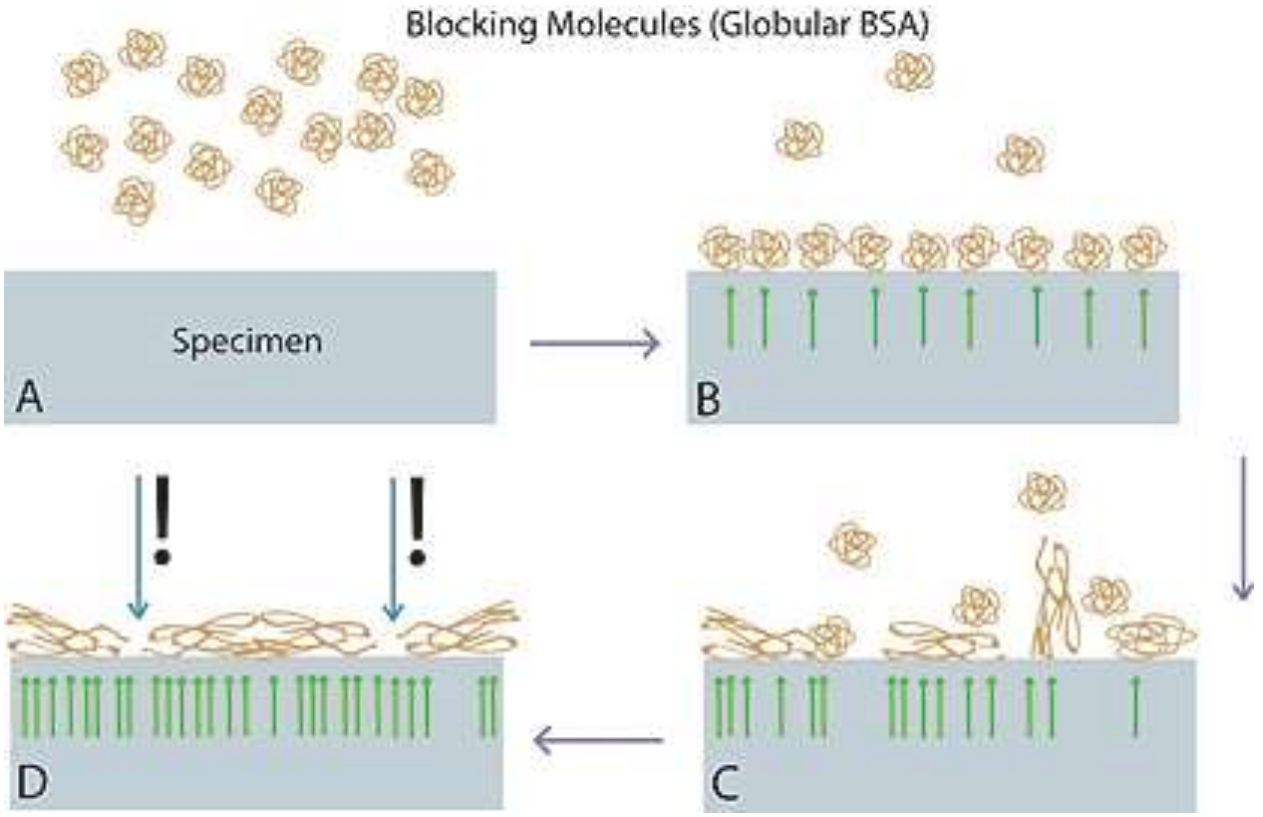

# Cell Array

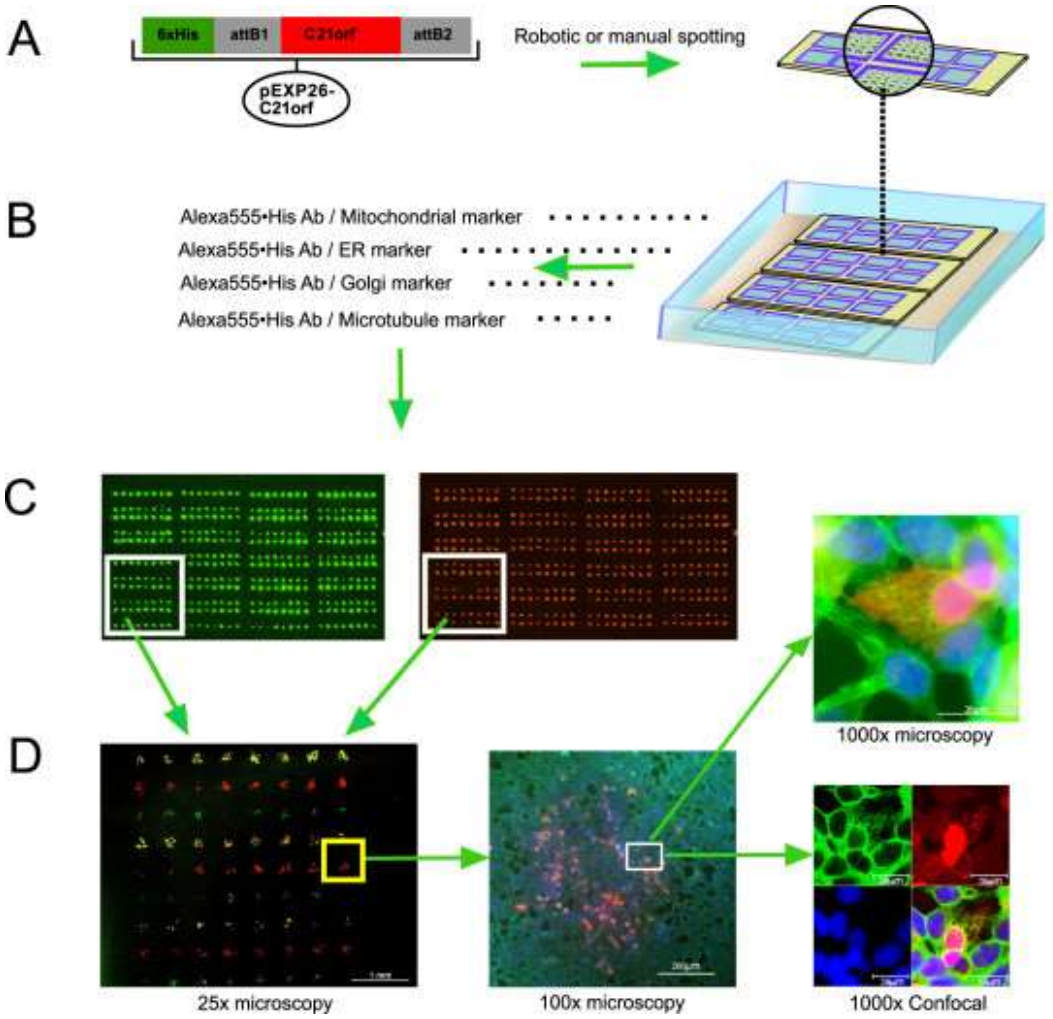
A
6xHis
attB1
C21orf
attB2
pEXP26-C21orf
Robotic or manual spotting
B
Alexa555•His Ab / Mitochondrial marker
Alexa555•His Ab / ER marker
Alexa555•His Ab / Golgi marker
Alexa555•His Ab / Microtubule marker
C
D
25x microscopy
100x microscopy
1000x microscopy
1000x Confocal

# hCG immunoassay


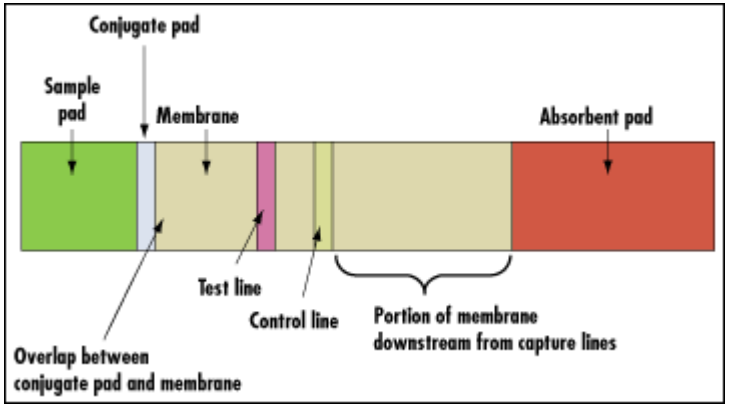


human chorionic gonadotropin (hCG)

# Nucleotide Sensor

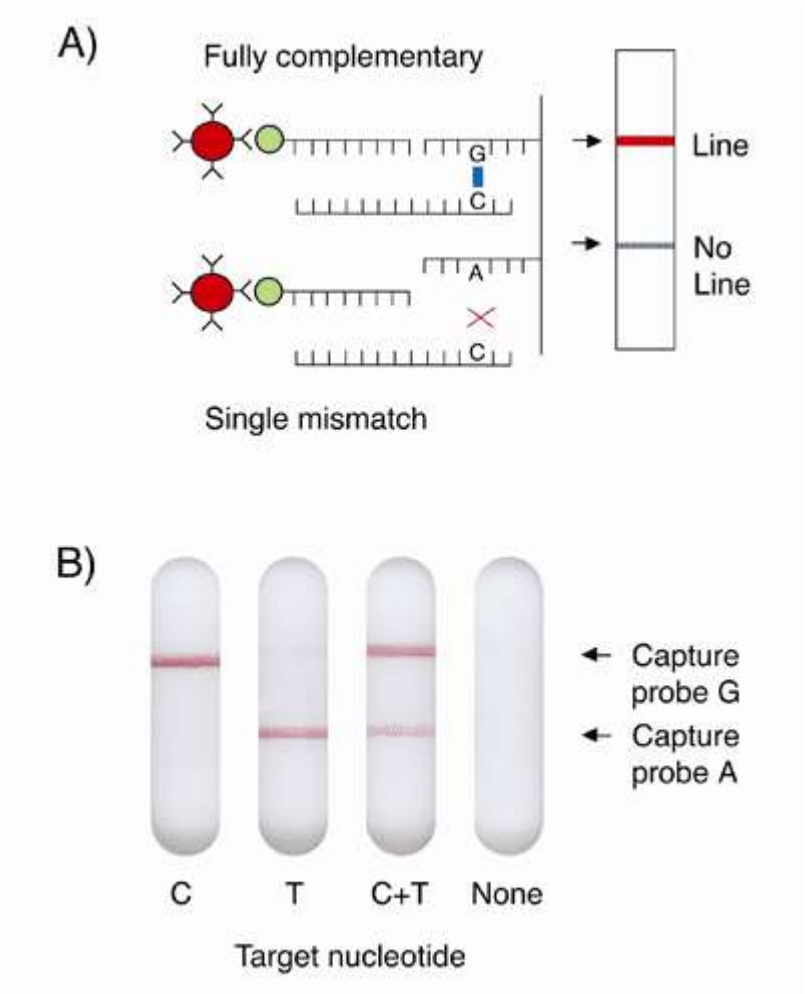

# Bio-Bar-Code-Based DNA Detection with PCR-like Sensitivity

Jwa-Min Nam, Savka I. Stoeva, and Chad A. Mirkin*

J. AM. CHEM. SOC. 2004, *126*, 5932−5933

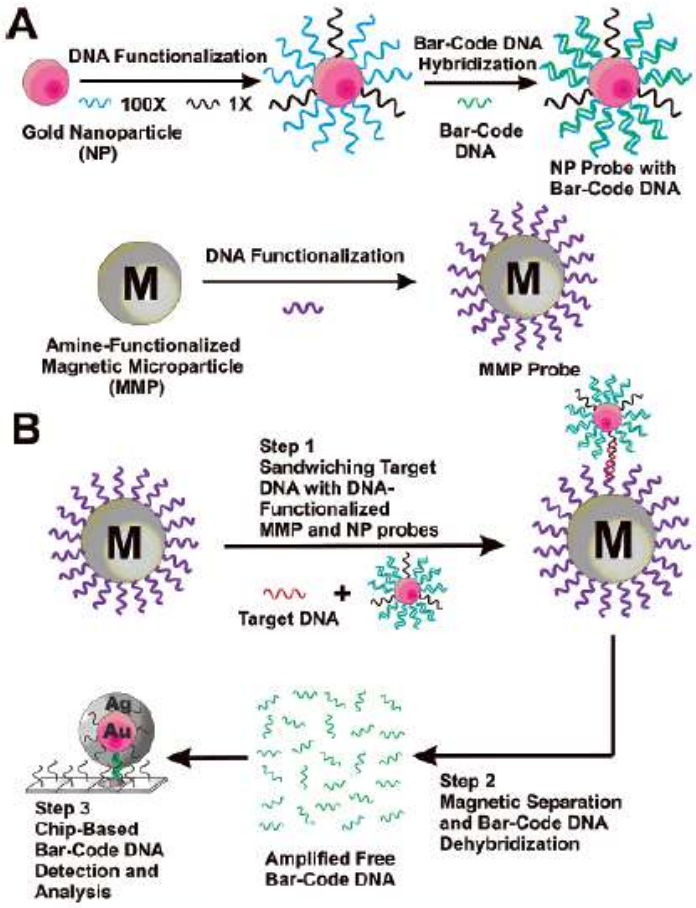


*Figure 1.* The DNA-BCA assay. (A) Nanoparticle and magnetic microparticle probe preparation. (B) Nanoparticle-based PCR-less DNA amplification scheme.

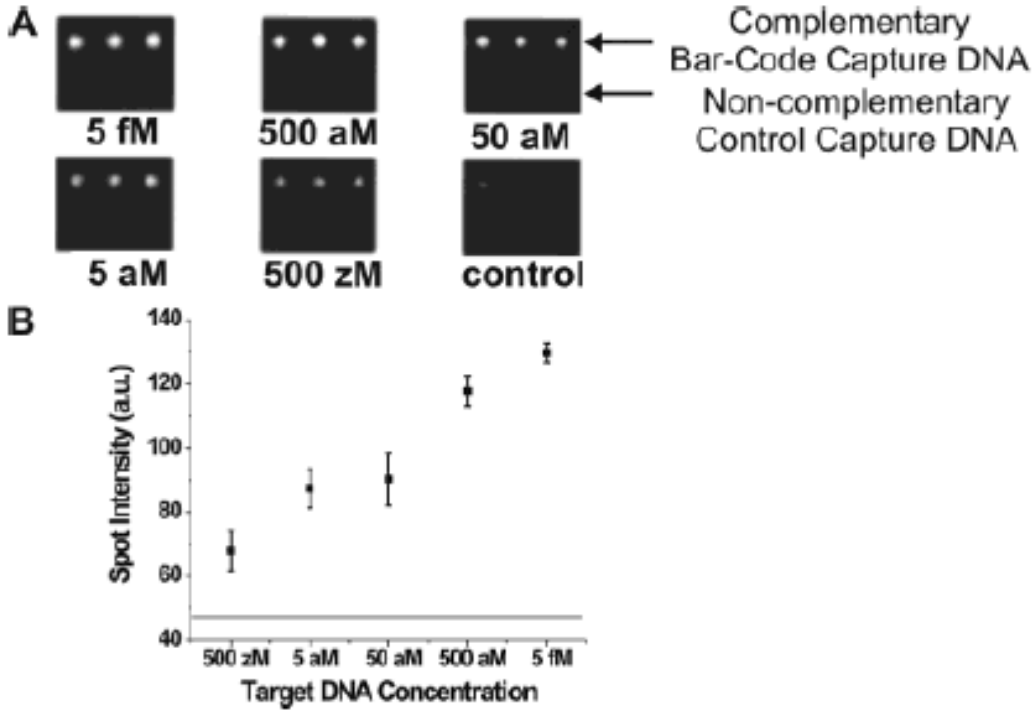


*Figure 2.* Amplified anthrax bar-code DNA detection with the Verigene ID system. (A) Anthrax bar-code DNA detection with 30 nm NP probes. (B) Quantitative data of spot intensities with 30 nm NP probes (Adobe Photoshop, Adobe Systems, Inc., San Jose, CA). The horizontal line represents control signal intensity (47 ± 2).

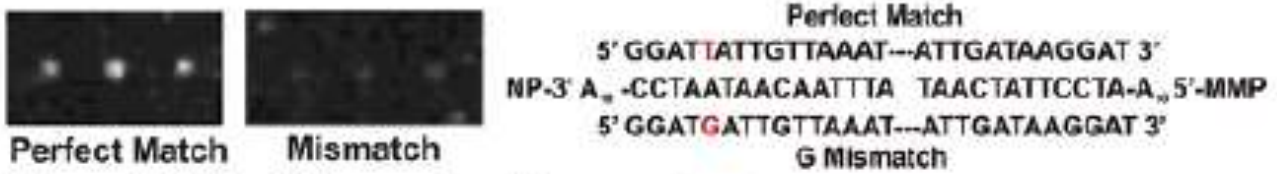


*Figure 3.* Single base mismatch experiment.

# Nanoparticle-Based Bio–Bar Codes for the Ultrasensitive Detection of Proteins

26 SEPTEMBER 2003 VOL 301 SCIENCE

Jwa-Min Nam,* C. Shad Thaxton,* Chad A. Mirkin†

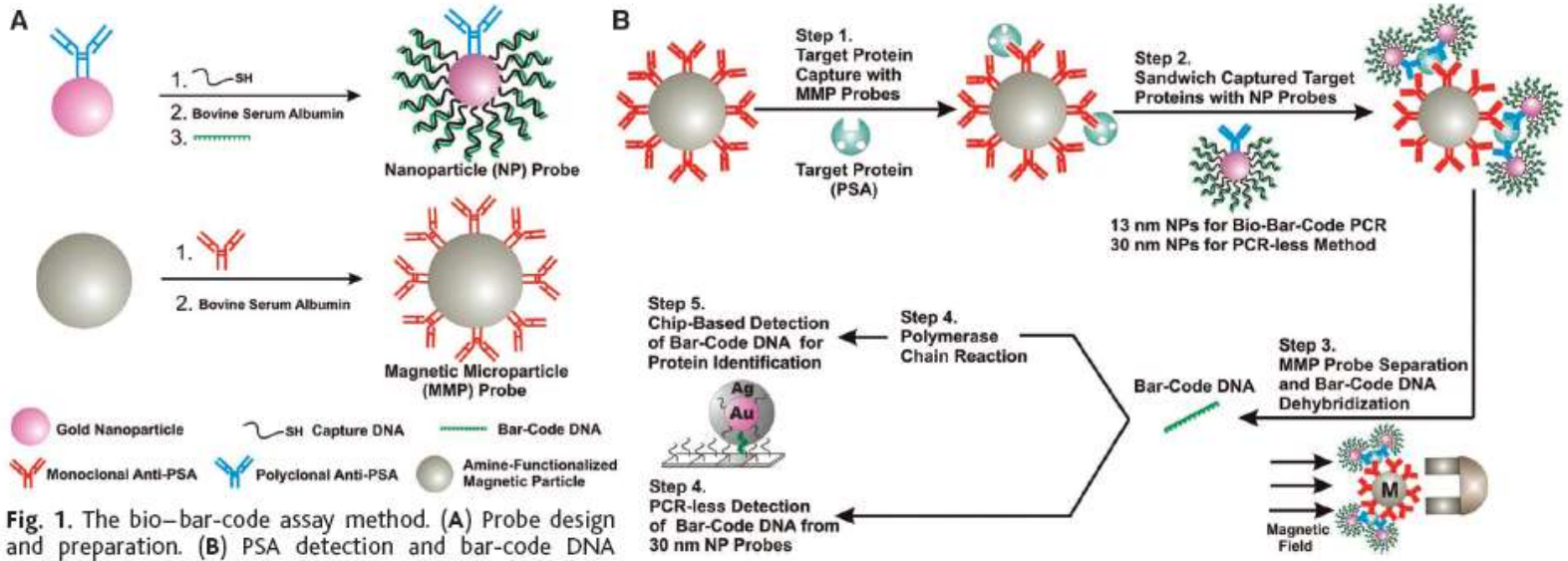


**Fig. 1.** The bio–bar-code assay method. (**A**) Probe design and preparation. (**B**) PSA detection and bar-code DNA amplification and identification. In a typical PSA-detection experiment, an aqueous dispersion of MMP probes functionalized with mAbs to PSA (50 μl of 3 mg/ml magnetic probe solution) was mixed with an aqueous solution of free PSA (10 μl of PSA) and stirred at 37°C for 30 min (Step 1). A 1.5-ml tube containing the assay solution was placed in a BioMag microcentrifuge tube separator (Polysciences, Incorporated, Warrington, PA) at room temperature. After 15 s, the MMP-PSA hybrids were concentrated on the wall of the tube. The supernatant (solution of unbound PSA molecules) was removed, and the MMPs were resuspended in 50 μl of 0.1 M phosphate-buffered saline (PBS) (repeated twice). The NP probes (for 13-nm NP probes, 50 μl at 1 nM; for 30-nm NP probes, 50 μl at 200 pM), functionalized with polyclonal Abs to PSA and hybridized bar-code DNA strands, were then added to the assay solution. The NPs reacted with the PSA immobilized on the MMPs and provided DNA strands for signal amplification and protein identification (Step 2). This solution was vigorously stirred at 37°C for 30 min. The MMPs were then washed with 0.1 M PBS with the magnetic separator to isolate the magnetic particles. This step was repeated four times, each time for 1 min, to remove everything but the MMPs (along with the PSA-bound NP probes). After the final wash step, the MMP probes were resuspended in NANOpure water (50 μl) for 2 min to dehybridize bar-code DNA strands from the nanoparticle probe surface. Dehybridized bar-code DNA was then easily separated and collected from the probes with the use of the magnetic separator (Step 3). For bar-code DNA amplification (Step 4), isolated bar-code DNA was added to a PCR reaction mixture (20-μl final volume) containing the appropriate primers, and the solution was then thermally cycled (*20*). The bar-code DNA amplicon was stained with ethidium bromide and mixed with gel-loading dye (*20*). Gel electrophoresis or scanometric DNA detection (*24*) was then performed to determine whether amplification had taken place. Primer amplification was ruled out with appropriate control experiments (*20*). Notice that the number of bound NP probes for each PSA is unknown and will depend upon target protein concentration.

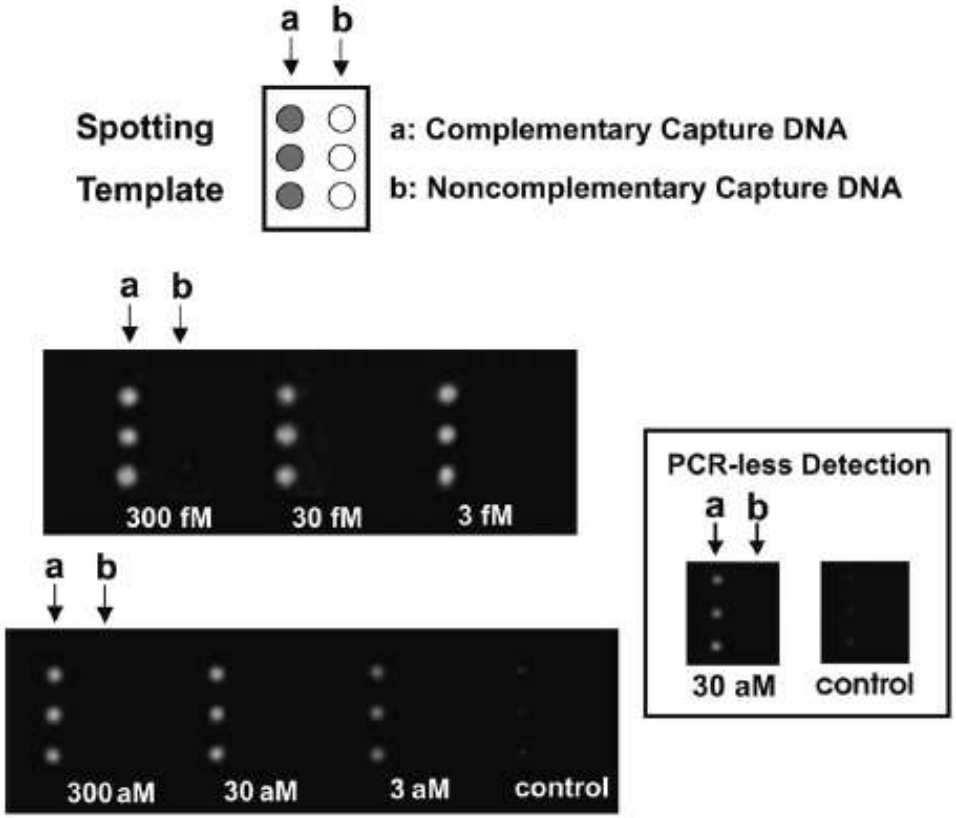


**Fig. 2.** Scanometric detection of PSA-specific bar-code DNA. PSA concentration (sample volume of 10 μl) was varied from 300 fM to 3 aM and a negative control sample where no PSA was added (control) is shown. For all seven samples, 2 μl of antidinitrophenyl (10 pM) and 2 μl of β-galactosidase (10 pM) were added as background proteins. Also shown is PCR-less detection of PSA (30 aM and control) with 30 nm NP probes (inset). Chips were imaged with the Verigene ID system (*20*).

**Table 1. Detection Limits of Nucleic Acid Assays**[a]

| | assay | ss DNA | PCR products | genomic DNA |
|---|---|---|---|---|
| nanostructure-based methods | colorimetric[29] (cross-linked Au nanoparticles) | ~10 nM | | |
| | colorimetric[36] (non-cross-linked Au nanoparticles) | 60 nM | | |
| | magnetic relaxation[97] (iron oxide nanoparticles) | 20 pM | | |
| | electrochemical[96] (nanoparticles) | 270 pM | | |
| | scanometric[35,66,67] (Au nanoparticles with Ag amplification) | 50 fM | 100 aM[b] | 200 fM |
| | Raman spectroscopy[68] (Au nanoparticles with Ag amplification) | ~1 fM | | |
| | electrical[93] (Au nanoparticles with Ag amplification) | 500 fM | | |
| | electrical[99] (Si nanowire) | 10 fM | | |
| | electrical[103] (carbon nanotube) | 54 aM | | |
| | resonant light-scattering[61–66] (metal nanoparticles) | 170 fM[b] | | 33 fM |
| | fluorescence[56] (ZnS and CdSe quantum dots) | 2 nM | | |
| | surface plasmon resonance[41] (Au nanoparticles) | 10 pM | | |
| | quartz crystal microbalance[94] (Au nanoparticles) | ~1 fM | | |
| | laser diffraction[42] (Au nanoparticles) | ~50 fM | | |
| | fluorescence[45] (fluorescent nanoparticles) | ~1 fM | | |
| | bio-bar-code amplification[71] (Au nanoparticles with Ag amplification) | 500 zM | | |
| other non-enzymatic based methods | fluorescence[35] (molecular fluorophores) | | ~600 fM[b] | |
| | fluorescence (dendrimer amplification)[134] | | 2.5 $\mu$g | |
| | electrochemical amplification[136] (electroactive reporter molecules) | 100 aM | | |

[a] Detection limits can vary based on target length and sequence; therefore, it is difficult to compare assays without testing them using identical targets and conditions. [b] Values taken from ref 34.

**Table 2. Detection Limits of Protein Assays**

| | assay | target | protein in saline | protein in serum |
|---|---|---|---|---|
| nanostructure-based methods | optical[72] (Au nanoshells) | rabbit IgG | 0.88 ng/mL (~4.4 pM)[a] | 0.88 ng/mL (~4.4 pM)[c] |
| | optical[74] (Au nanoparticles) | IgE and IgG1 | ~20 nM | |
| | magnetic relaxation[98] (iron oxide nanoparticles) | adenovirus (ADV) and herpes simplex virus (HSV) | 100 ADV/ 100$\mu$L | 50 HSV/ 100 $\mu$L |
| | scanometric[79] (Au nanoparticles with Ag amplification) | mouse IgG | 200 pM | |
| | Raman[82] (Au nanoparticles with Raman labels) | prostate-specific antigen | | 30 fM |
| | surface plasmon resonance[83,84] (triangular Ag particles on surfaces) | streptavidin(S A) and anti-biotin (AB) | ~1 pM SA and ~700 pM AB | |
| | electrical[110] (single-walled carbon nanotubes) | 10E3 antibody to U1A RNA splicing factor | ~1 nM | |
| | electrical[20] (Si nanowires) | streptavidin | 10 pM | |
| | bio-bar-code amplification[75] (Au nanoparticles with Ag amplification) | prostate-specific antigen | 30 aM (3 aM)[b] | (30 aM)[b] |
| molecular fluorophore methods | enzyme-linked immunosorbent assay | various | pM range | pM range |
| electrochemical methods | electrochemical amplification[137] (oligonucleotide reporter molecules) | IgG | 13 fM | |
| enzyme-based amplification methods | immuno-PCR[76] | bovine serum albumin | 2 fM | |
| | rolling circle amplification[77] | prostate-specific antigen | 3 fM | |

[a] Reported in ng/mL; authors converted to molar concentration for ease of comparison. [b] These values are the lower limits when PCR is used to amplify the bar-code DNA prior to scanometric detection of bar codes.

# Surface Plasmon

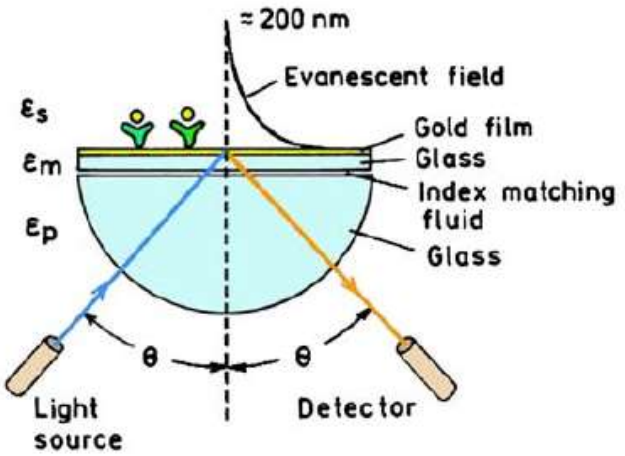


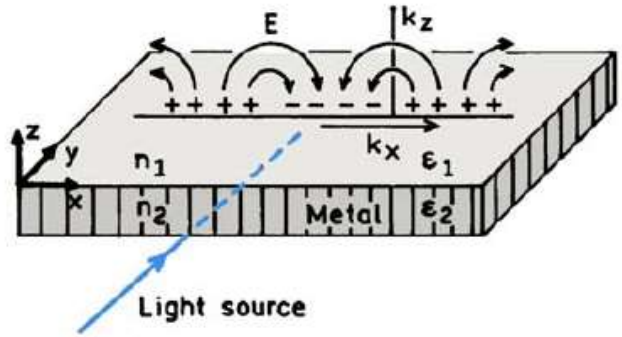


**Figure 3.** Schematics of an SPR experiment (top) and of the light-induced surface plasmons (bottom).

(b)

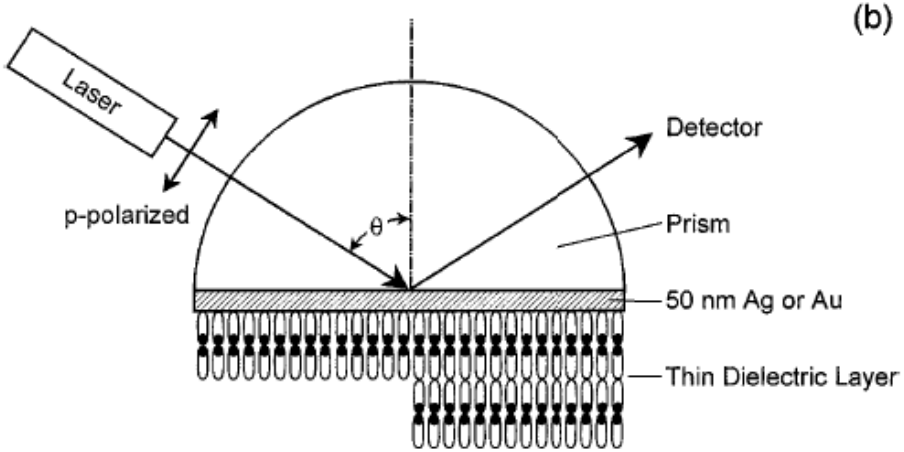


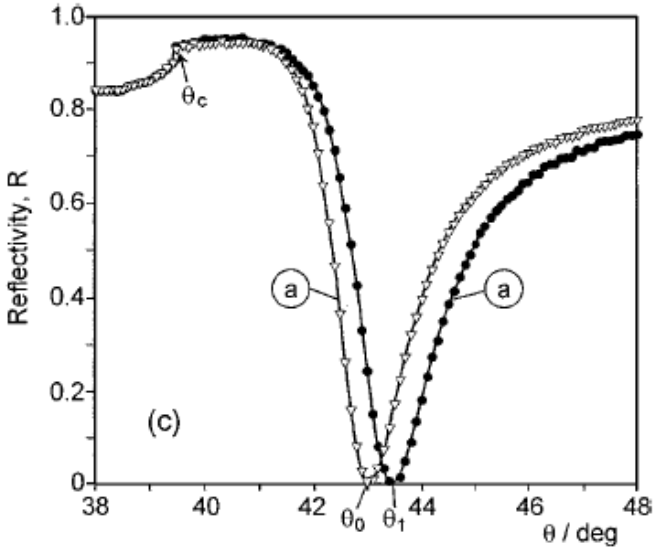

# Drift: Drude model

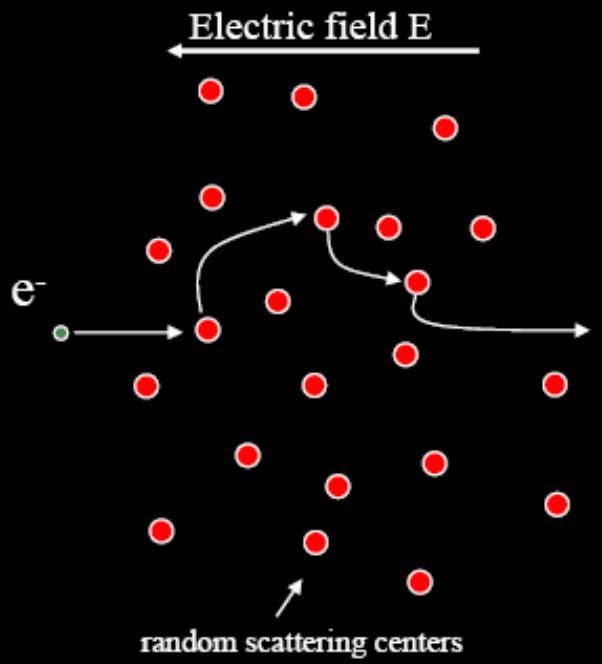


$$F = ma$$

$$eE = m\frac{\partial v}{\partial t}$$

$$v_{avg} = \underbrace{\frac{e\tau}{m}}_{\mu} E$$

$$j = nev_{avg} = \underbrace{\frac{ne^2\tau}{m}}_{\sigma} E$$



$$m\frac{\partial}{\partial t}\langle\vec{v}\rangle = q\vec{E} - \gamma\langle\vec{v}\rangle$$

$$\sigma(\omega) = \frac{\sigma_0}{1 + i\omega\tau}$$

# AC Dielectric Response

$$\varepsilon_m = 1 - \frac{\omega_p^2}{\omega^2}$$

Plasma frequency

polarizability of a small metal sphere with dielectric function $\varepsilon(\lambda)$

$$\alpha = R^3 \frac{\varepsilon - 1}{\varepsilon + 2}.$$

$$\varepsilon = \varepsilon_\mathrm{b} + 1 - \frac{\omega_\mathrm{P}^2}{\omega^2 + \mathrm{i}\omega\gamma},$$

$$\alpha = \frac{R^3(\varepsilon_\mathrm{b}\omega^2 - \omega_\mathrm{P}^2) + i\omega\gamma\varepsilon_\mathrm{b}}{[(\varepsilon_\mathrm{b} + 3)\omega^2 - \omega_\mathrm{P}^2] + i\omega\gamma(\varepsilon_\mathrm{b} + 3)}.$$

$\omega_\mathrm{R} = \frac{\omega_\mathrm{P}}{\sqrt{\varepsilon_\mathrm{b}+3}}$ $\gamma(\varepsilon_\mathrm{b} + 3)$.

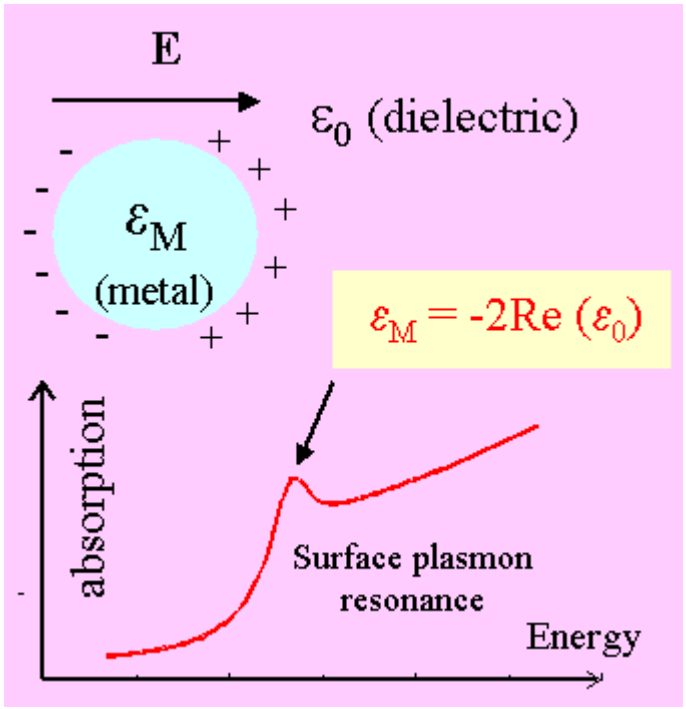


$$\varepsilon_{eff} = \varepsilon_0 + 3N\varepsilon_0 \frac{\varepsilon_M - \varepsilon_0}{\varepsilon_M + 2\varepsilon_0}$$

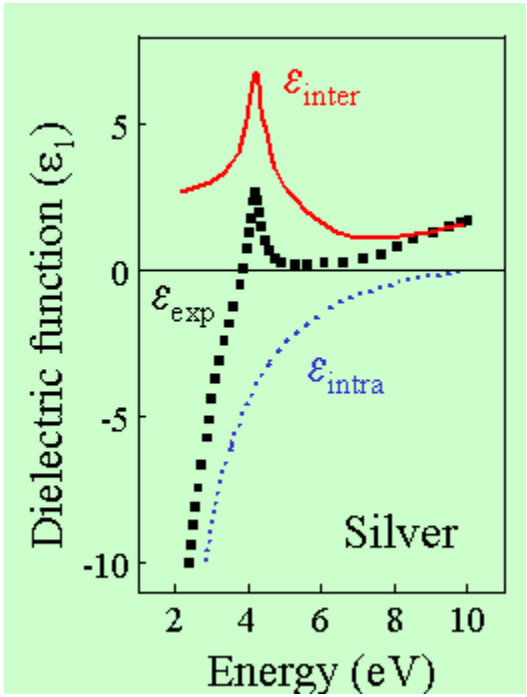

# Biomolecular Binding in Real Time

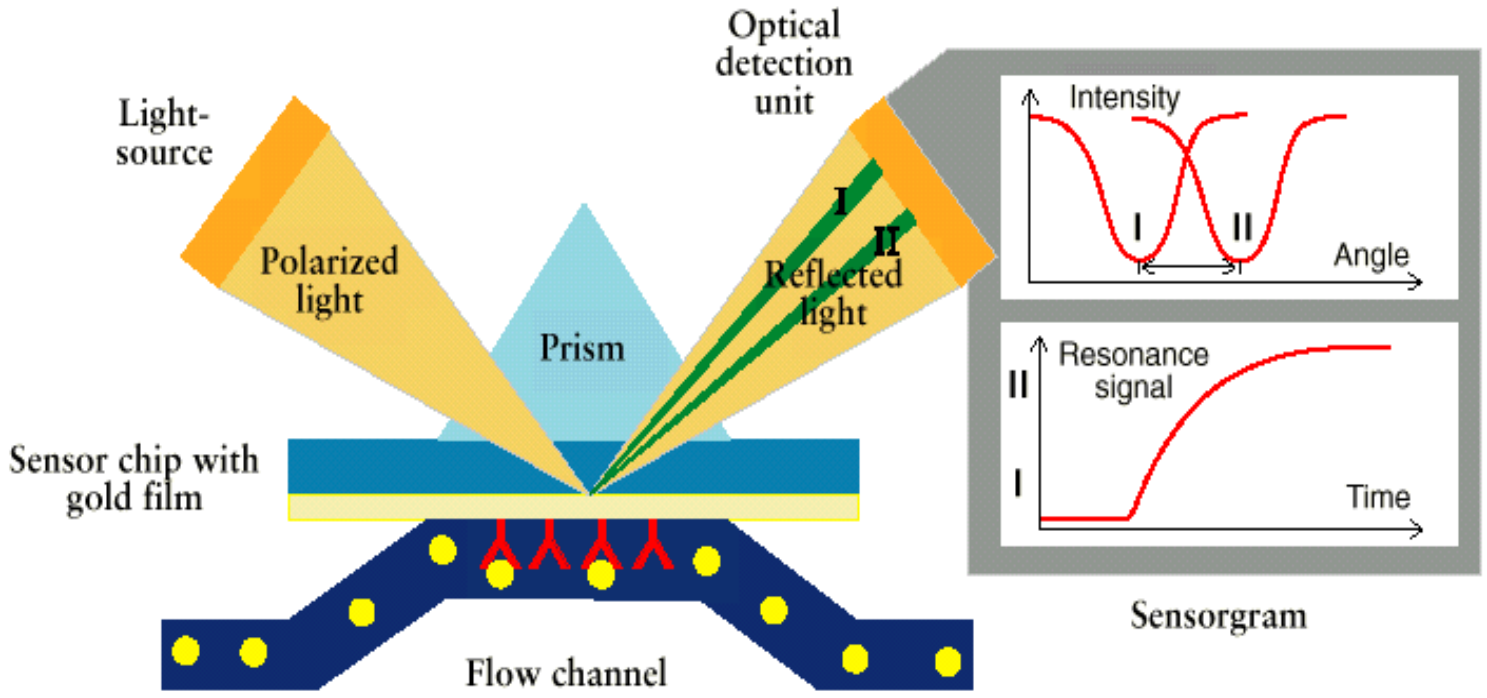

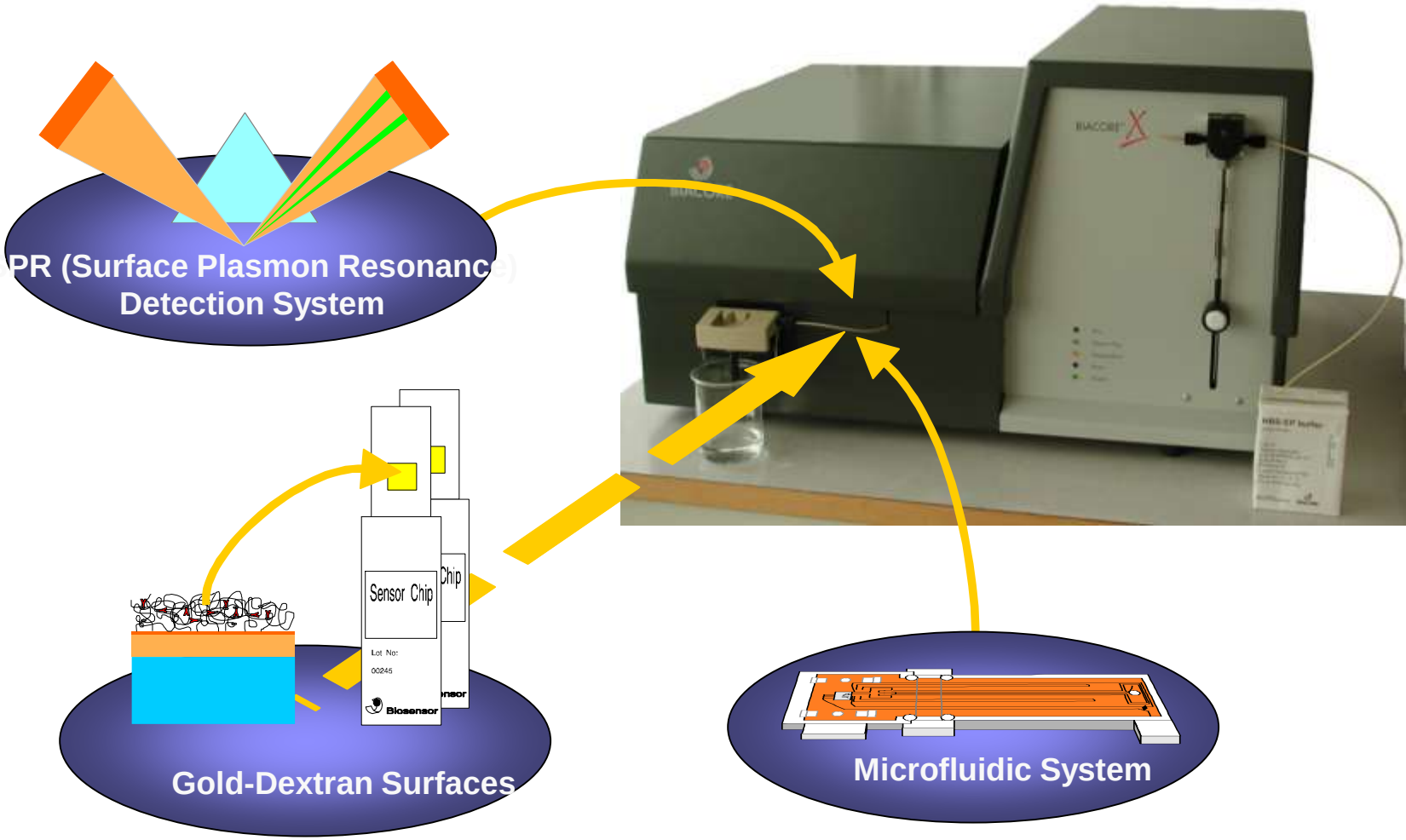
PR (Surface Plasmon Resonance)
Detection System
Sensor Chip
Lot No:
00245
Biosensor
Gold-Dextran Surfaces
Microfluidic System

# SPR Imaging Apparatus

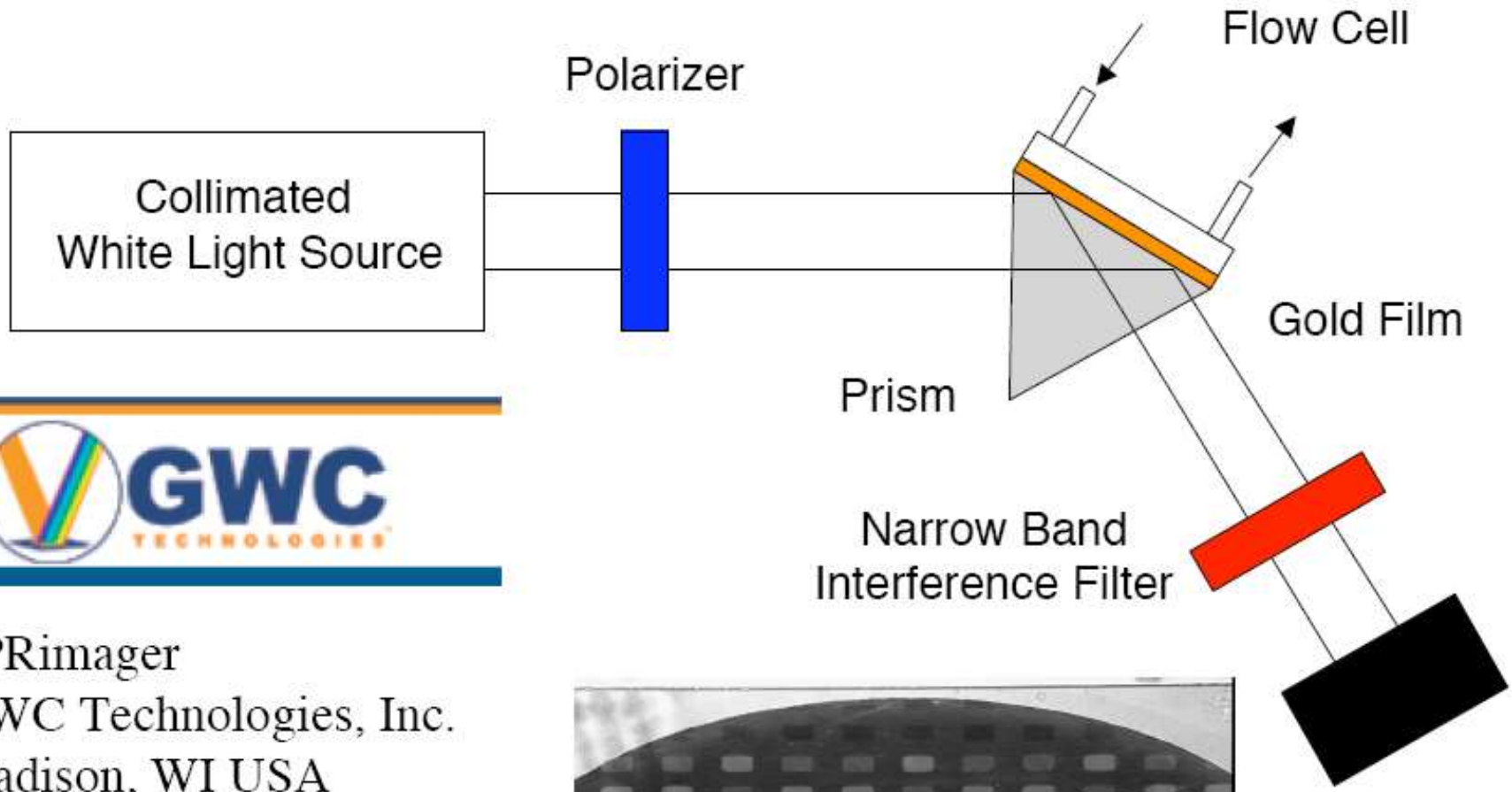


SPRimager
GWC Technologies, Inc.
Madison, WI USA

www.gwctechnologies.com

Raw Image

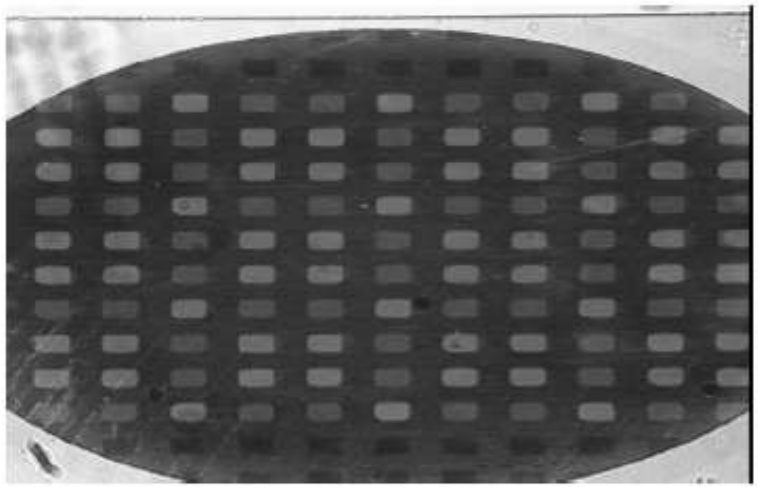

# Localized Plasmon

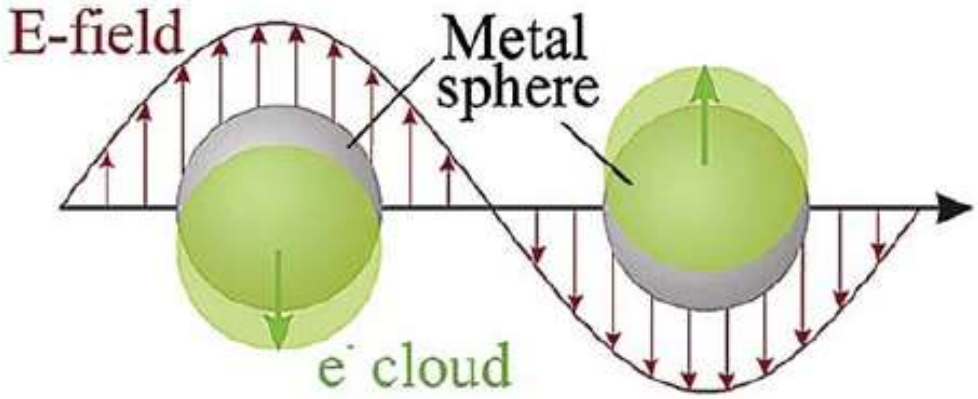


**Figure 6.** Schematic of plasmon oscillation for a sphere. From [39].

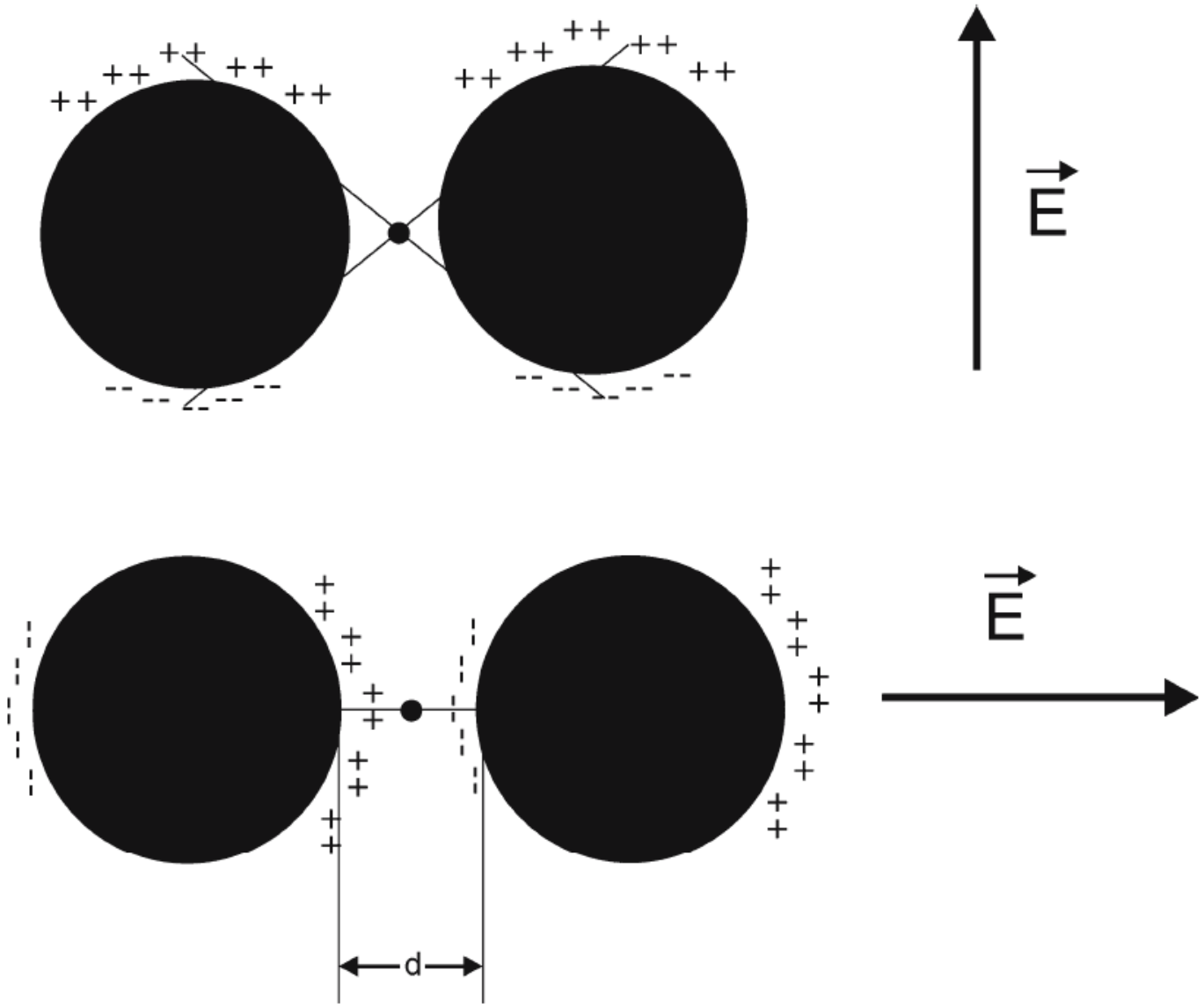
E
E
d

field enhancement

$E_s = gE_0$, where $E_0$ is the magnitude of the incident field

$$E_R \propto \alpha_R E_s \propto \alpha_R g E_0$$

$$E_{SERS} \propto \alpha_R g g' E_0$$

$$I_{SERS} \propto |\alpha_R|^2 |gg'|^2 I_0$$

$$g \cong g'$$

$$|E_L|^4 = |g|^4.$$

# Probing Single Molecules and Single Nanoparticles by Surface-Enhanced Raman Scattering

SCIENCE • VOL. 275 • 21 FEBRUARY 1997

Shuming Nie* and Steven R. Emory

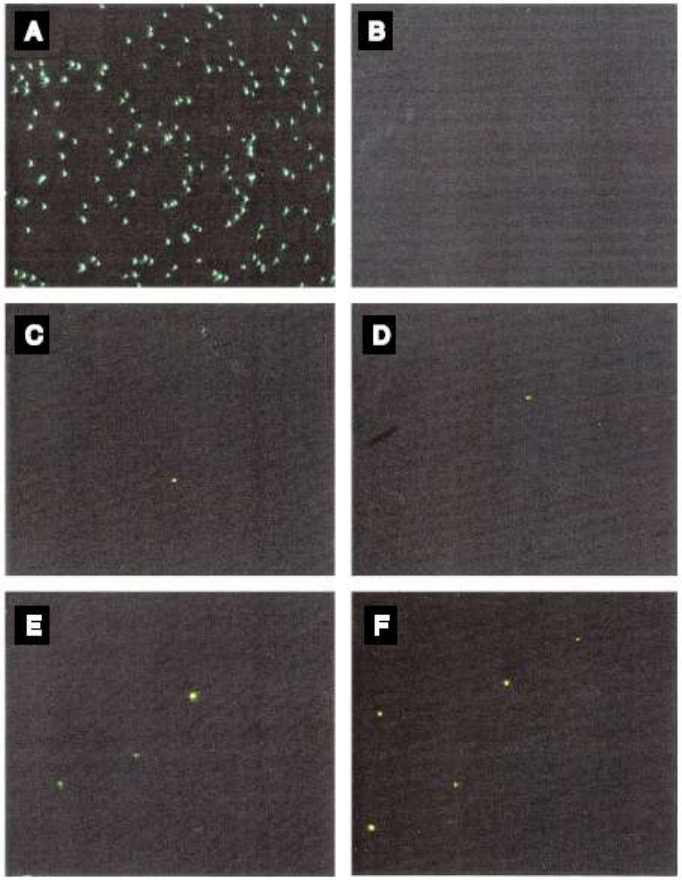


**Fig. 1.** Single Ag nanoparticles imaged with evanescent-wave excitation. Total internal reflection of the laser beam at the glass-liquid interface was used to reduce the laser scattering background. The instrument setup for evanescent-wave microscopy was adapted from Funatsu *et al.* (*11*). The images were directly recorded on color photographic film (ASA-1600) with a 30-s exposure by a Nikon 35-mm camera attached to the microscope. (**A**) Unfiltered photograph showing scattered laser light from all particles immobilized on a polylysine-coated surface. (**B**) Filtered photographs taken from a blank Ag colloid sample (incubated with 1 mM NaCl and no R6G analyte molecules). (**C**) and (**D**) Filtered photographs taken from a Ag colloid sample incubated with $2 \times 10^{-11}$ M R6G. These images were selected to show at least one Raman scattering particle. Different areas of the cover slip were rapidly screened, and most fields of view did not contain visible particles. (**E**) Filtered photograph taken from Ag colloid incubated with $2 \times 10^{-10}$ M R6G. (**F**) Filtered photograph taken from Ag colloid incubated with $2 \times 10^{-9}$ M R6G. A high-performance bandpass filter was used to remove the scattered laser light and to pass Stokes-shifted Raman signals from 540 to 580 nm (920 to 2200 $cm^{-1}$). Continuous-wave excitation at 514.5 nm was provided by an Ar ion laser. The total laser power at the sample was 10 mW. Note the color differences between the scattered laser light in (A) and the red-shifted light in (C) through (F).

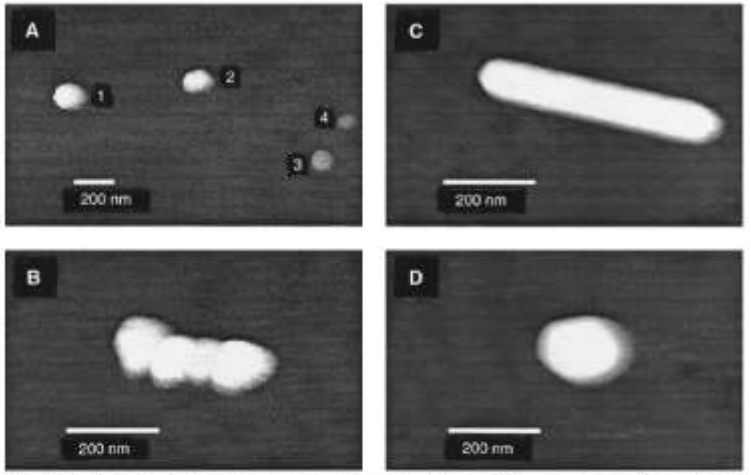


**Fig. 2.** Tapping-mode AFM images of screened Ag nanoparticles. (**A**) Large area survey image showing four single nanoparticles. Particles 1 and 2 were highly efficient for Raman enhancement, but particles 3 and 4 (smaller in size) were not. (**B**) Close-up image of a hot aggregate containing four linearly arranged particles. (**C**) Close-up image of a rod-shaped hot particle. (**D**) Close-up image of a faceted hot particle.

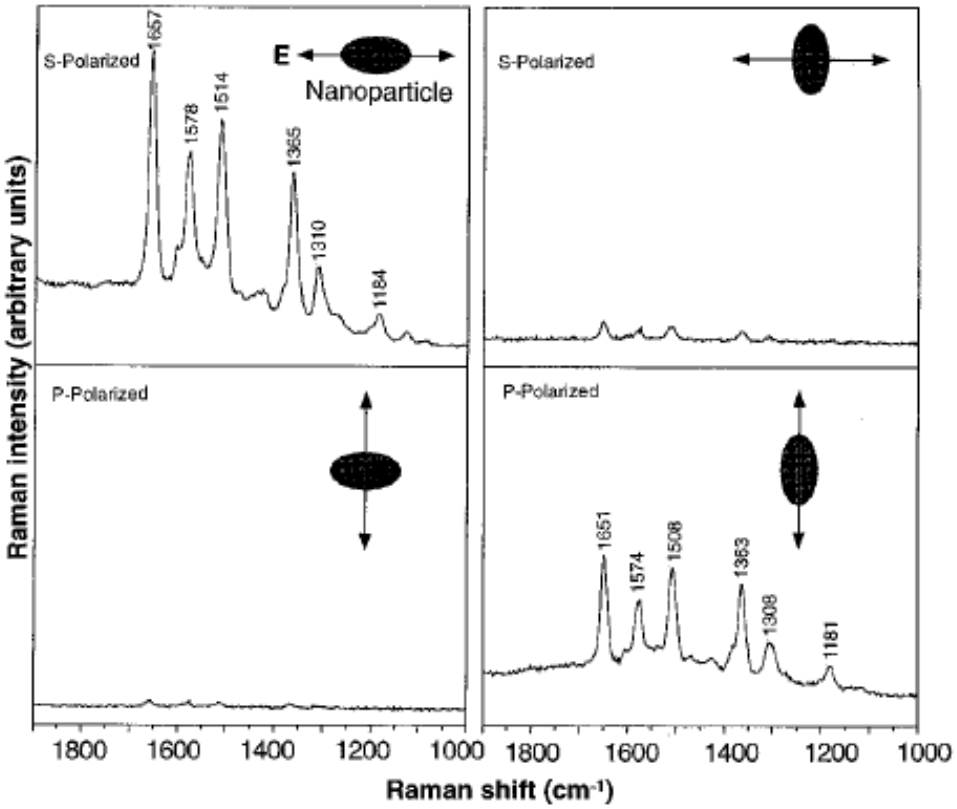


**Fig. 3.** Surface-enhanced Raman spectra of R6G obtained with a linearly polarized confocal laser beam from two Ag nanoparticles. The R6G concentration was $2 \times 10^{-11}$ M, corresponding to an average of 0.1 analyte molecule per particle. The direction of laser polarization and the expected particle orientation are shown schematically for each spectrum. Laser wavelength, 514.5 nm; laser power, 250 nW; laser focal radius, ~250 nm; integration time, 30 s. All spectra were plotted on the same intensity scale in arbitrary units of the CCD detector readout signal.

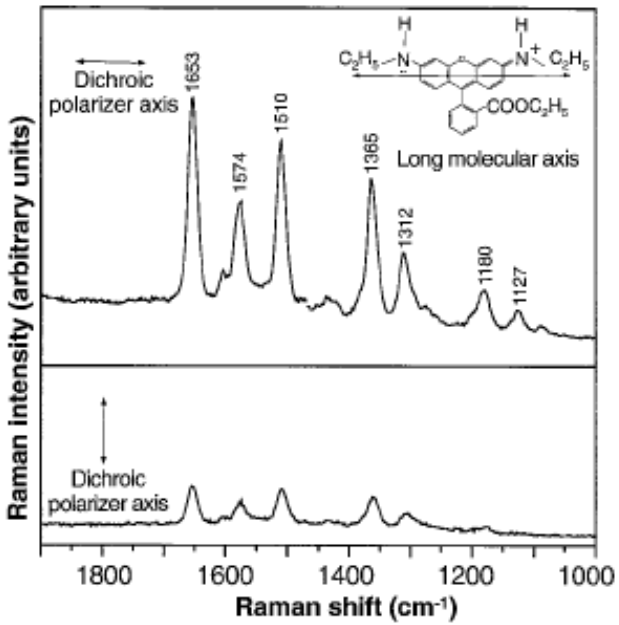


**Fig. 4.** Emission-polarized surface-enhanced Raman signals of R6G observed from a single Ag nanoparticle with a polarization-scrambled confocal laser beam. A dichroic sheet polarizer was rotated 90° to select Raman scattering signals polarized parallel (upper spectrum) or perpendicular (lower spectrum) to the long molecular axis of R6G. (**Inserts**) Structure of R6G, the electronic transition dipole (along the long axis when excited at 514.5 nm), and the dichroic polarizer orientations. Other conditions as in Fig. 3.

troscopic signatures of adsorbed molecules. For single rhodamine 6G molecules adsorbed on the selected nanoparticles, the intrinsic Raman enhancement factors were on the order of $10^{14}$ to $10^{15}$, much larger than the ensemble-averaged values derived from conventional measurements. This enormous enhancement leads to vibrational Raman signals that are more intense and more stable than single-molecule fluorescence.

# Electromagnetic contributions to single-molecule sensitivity in surface-enhanced Raman scattering

PRE 62 4318

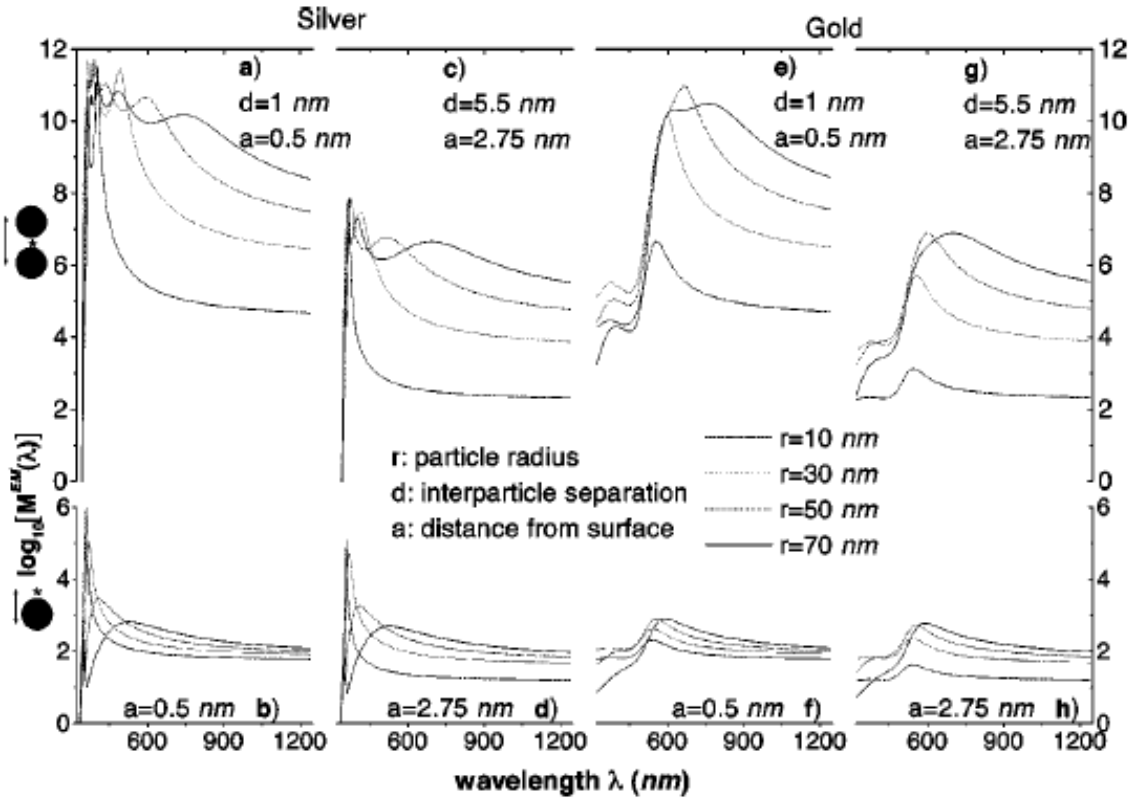

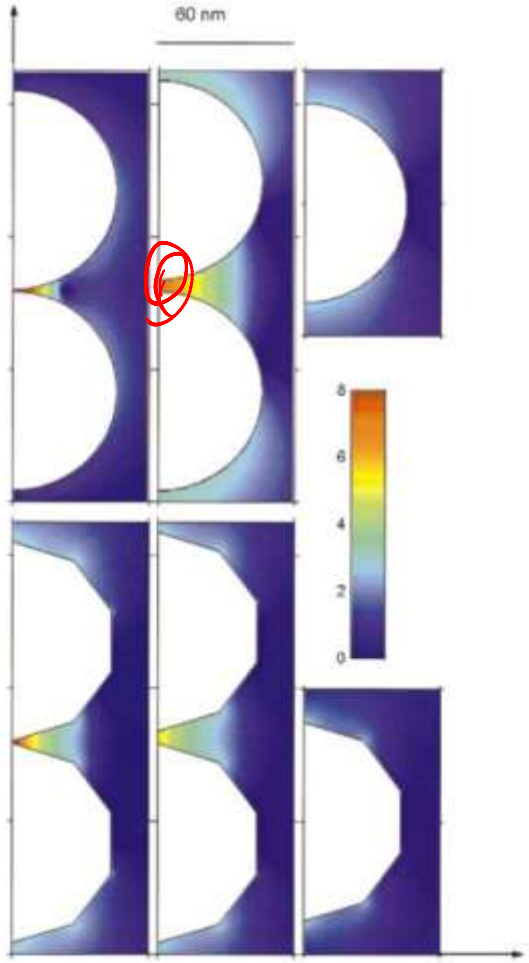


FIG. 3. (Color) EM-enhancement factor $M^{EM}$ at a cross section through six different silver particle configurations. The wavelength of the incident field is $\lambda = 514.5$ nm with vertical polarization. The left-hand column illustrates the EM enhancement for dimer configurations of two spheres (top) and two polygons (bottom) with a separation of 1 nm. The middle column shows the same situation, but with a separation distance of 5.5 nm. The right-hand column shows the case of an isolated single particle. All particles share a common largest dimension of 90 nm. Note that the color scale from dark blue to dark red is logarithmic, covering the interval $10^0 < M^{EM} < 10^8$. Regions with enhancement outside this interval are shown in dark blue and dark red, respectively.

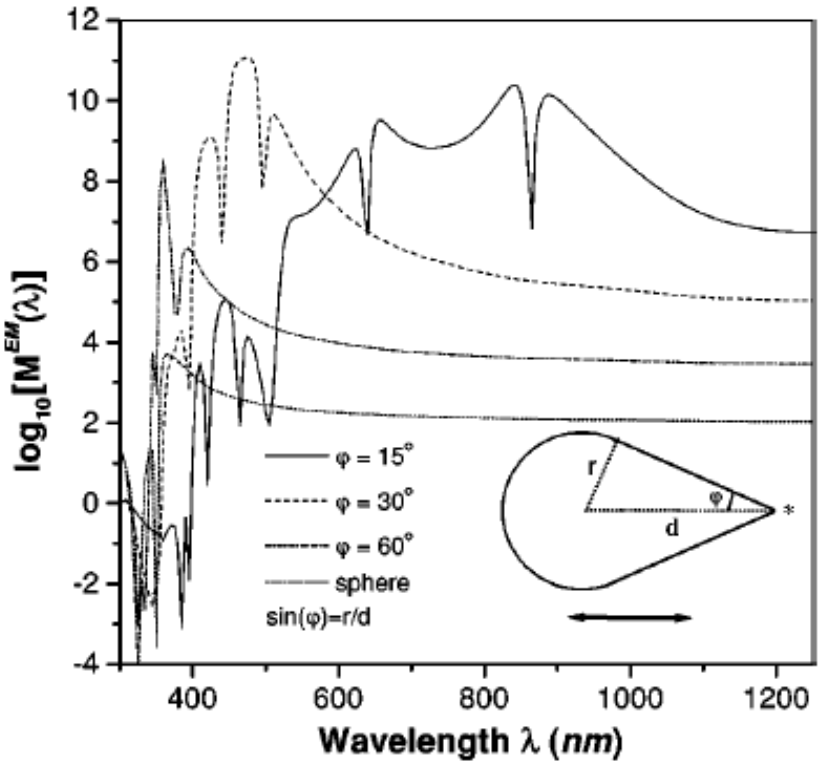


FIG. 5. EM-enhancement factor for a rotationally symmetric silver droplet as a function of the angle defining the opening edge $\phi$. The field is polarized parallel to the axis of the droplet and the evaluation position (star) is located 0.5 nm outside the tip. As the droplet becomes sharper the enhancement increases several orders of magnitude.

# Nanosphere Arrays with Controlled Sub-10-nm Gaps as Surface-Enhanced Raman Spectroscopy Substrates

J. AM. CHEM. SOC. 2005, *127*, 14992−14993

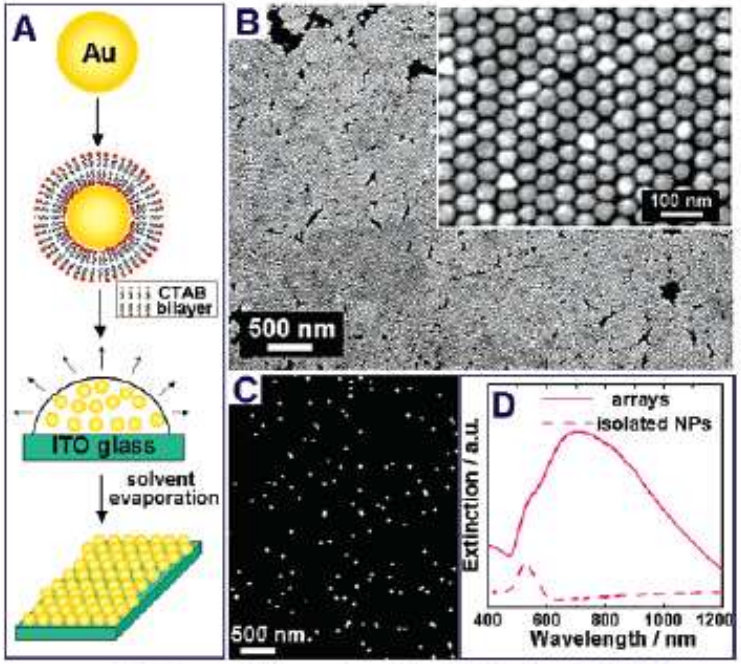


*Figure 1.* (A) Schematic illustration of the fabrication of sub-10-nm gap Au NP arrays. (B) SEM image of the arrays. (C) SEM image of monolayer of isolated Au NPs on ITO glass. (D) Vis−NIR extinction spectrum of the monolayer of isolated Au NPs and arrays.

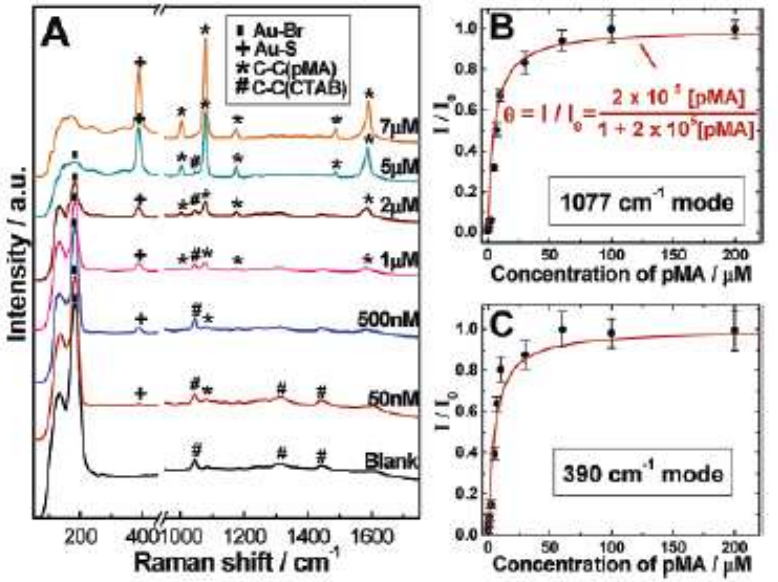


*Figure 2.* (A) SERS spectra of 5 $\mu$L of pMA with different concentrations deposited on the NP arrays. The excitation laser wavelength is 785 nm. Adsorption isotherm of pMA on the NP arrays obtained according to (B) 1077 and (C) 390 $cm^{-1}$ modes in the SERS spectra. $I_0$ is the peak intensity of a saturated pMA monolayer.

band arises from a coalescence of the dimer plasmon resonances

# Profiling the Near Field of a Plasmonic Nanoparticle with Raman-Based Molecular Rulers

NANO LETTERS

2006
Vol. 6, No. 10
2338−2343

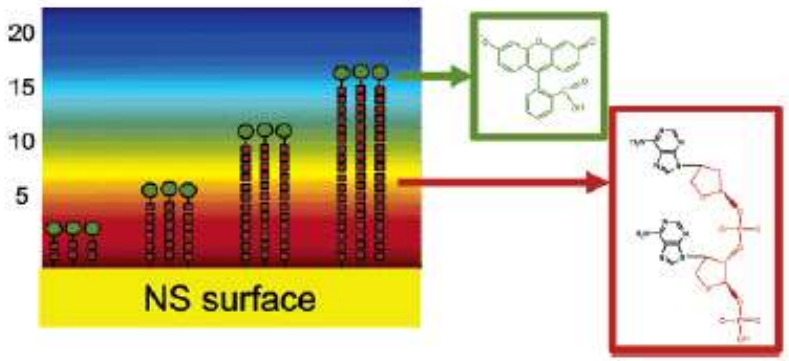


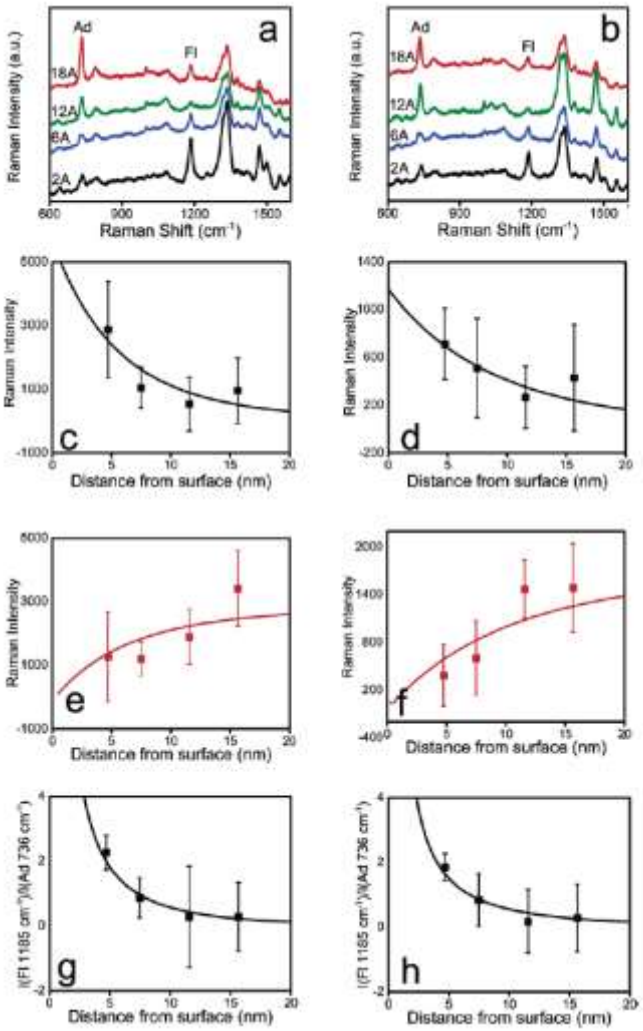


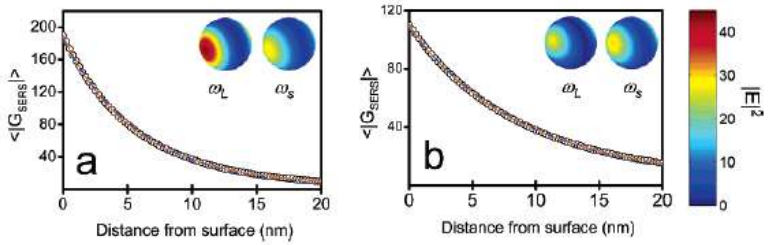

*Anal. Chem.* 2003, *75*, 6171−6176

# Spectroscopic Tags Using Dye-Embedded Nanoparticles and Surface-Enhanced Raman Scattering

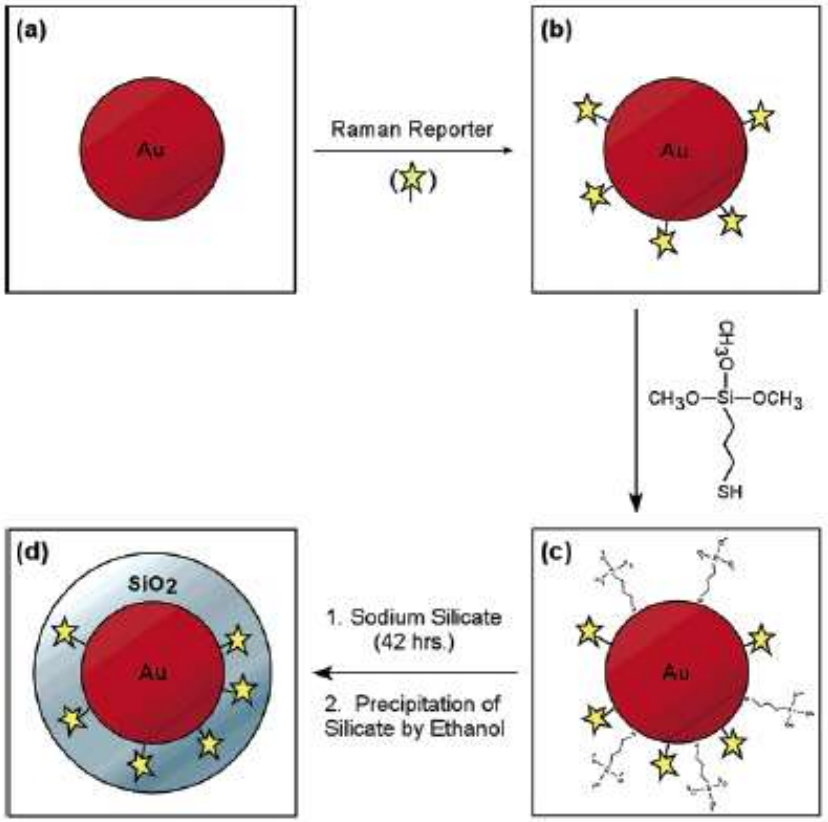


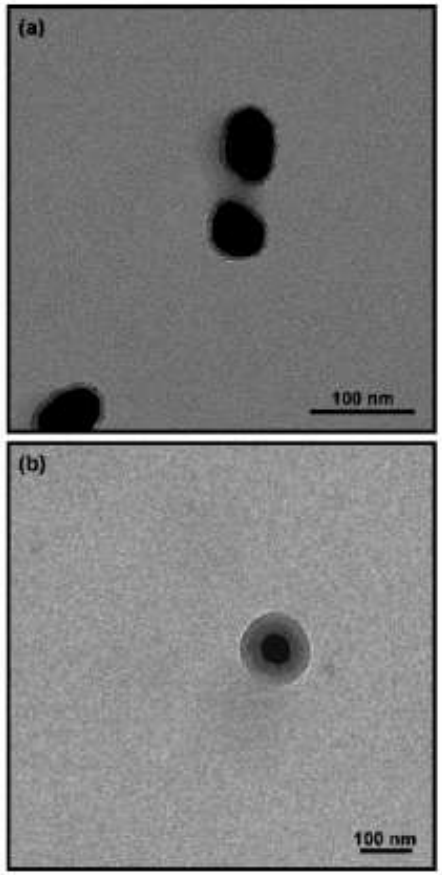

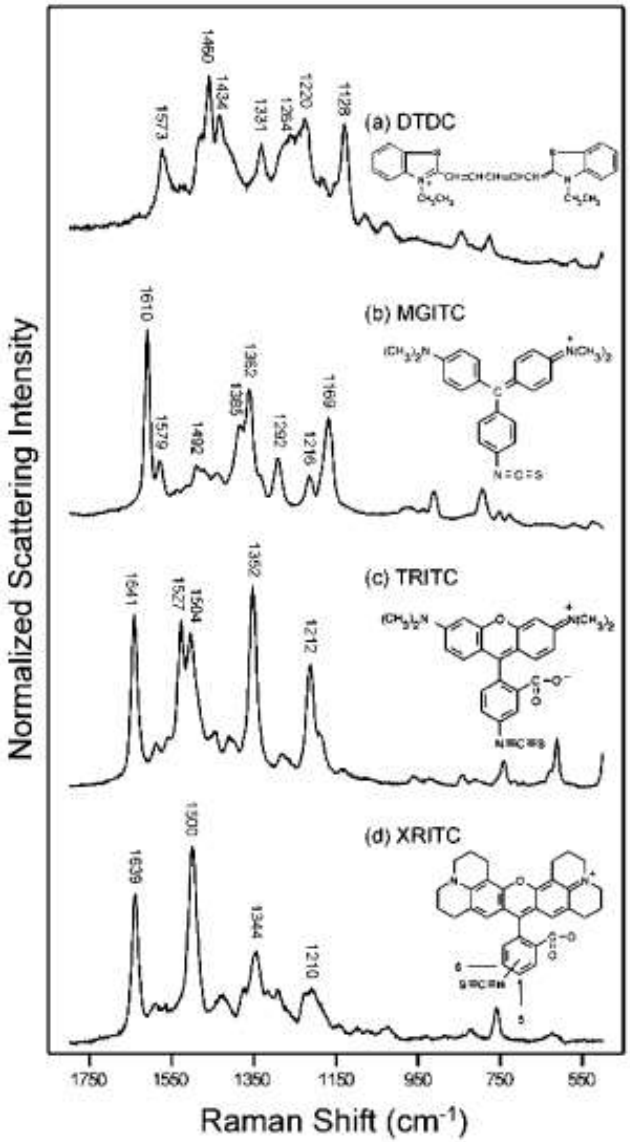


**Figure 4.** Chemical structures of four Raman reporters and their surface-enhanced resonance Raman spectra: (a) 3,3′-Diethylthiadicarbocyanine iodide (DTDC); (b) malachite green isothiocyanate (MGITC); (c) tetramethylrhodamine-5-isothiocyanate (TRITC); and (e) rhodamine-5-(and-6)-isothiocyanate (XRITC).

*Anal. Chem.* 2006, *78*, 6967−6973

# Nanoparticle Probes with Surface Enhanced Raman Spectroscopic Tags for Cellular Cancer Targeting

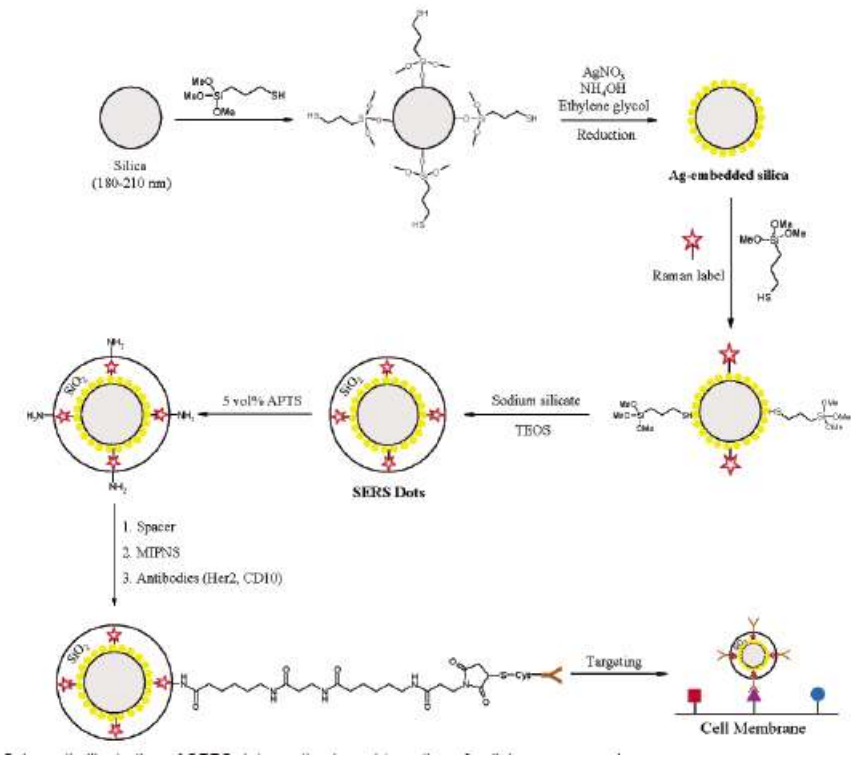


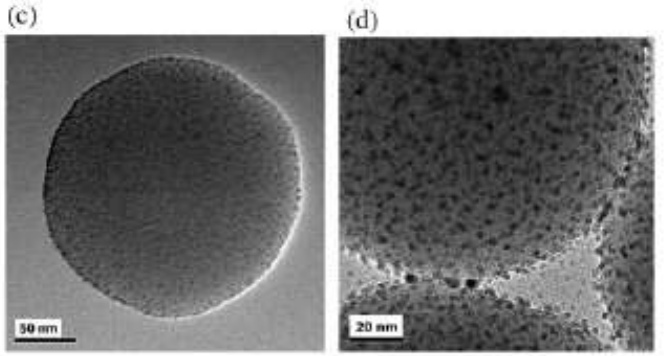


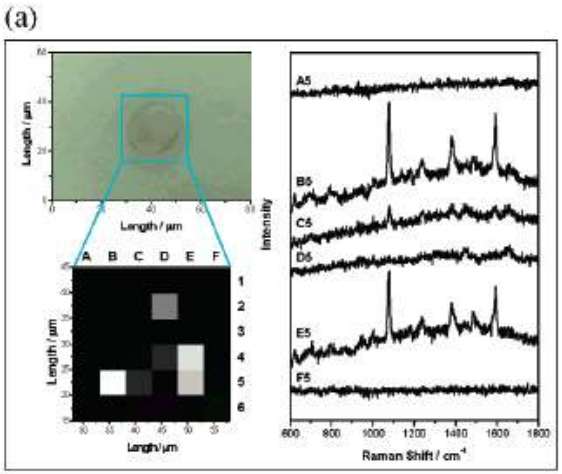

*Anal. Chem.* 2007, *79*, 916−922

# Biological Imaging of HEK293 Cells Expressing PLC$\gamma$1 Using Surface-Enhanced Raman Microscopy

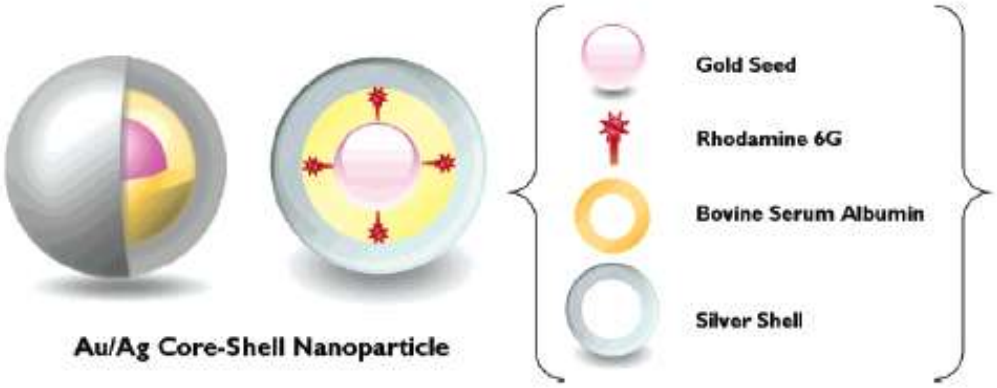


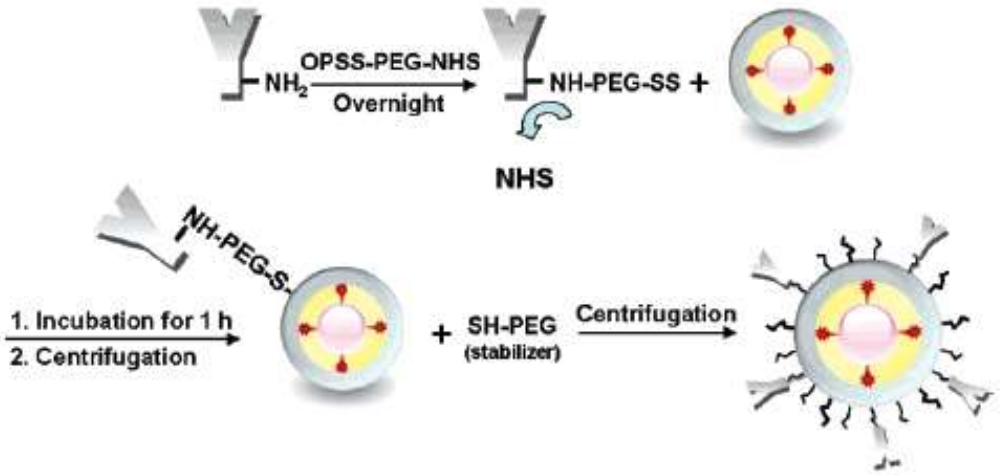

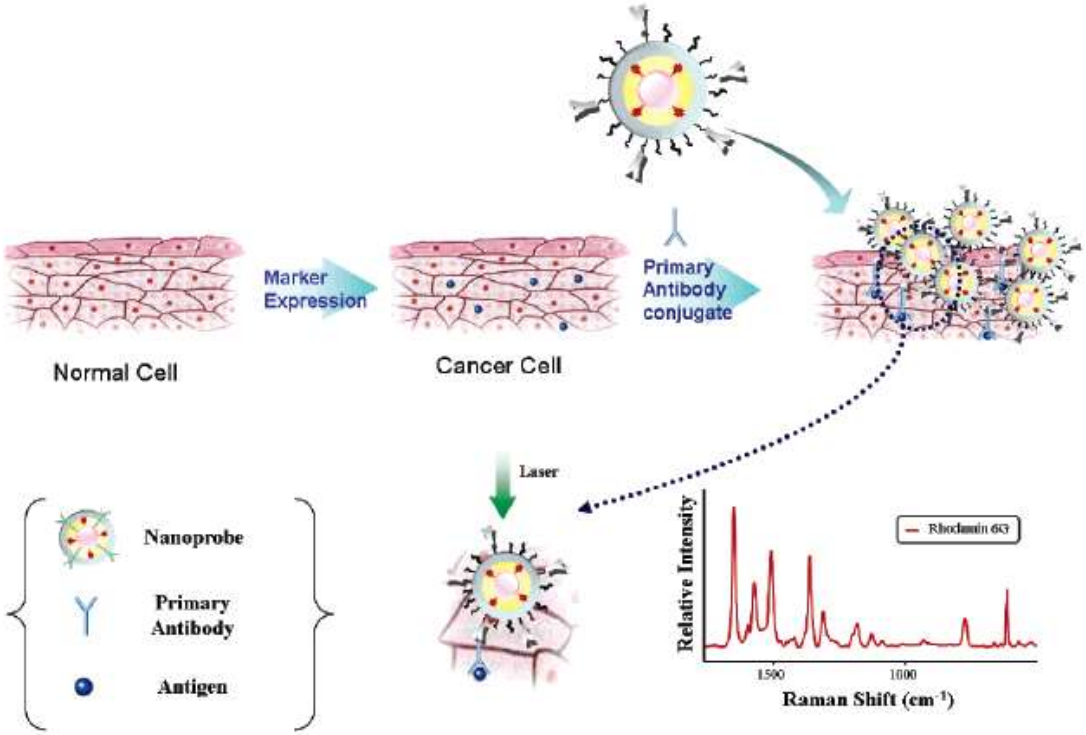


**Figure 4.** Schematic diagram depicting immobilization of Au/Ag core−shell nanoprobes on PLC$\gamma$1-expressing HEK293 cells and their SERS detection.

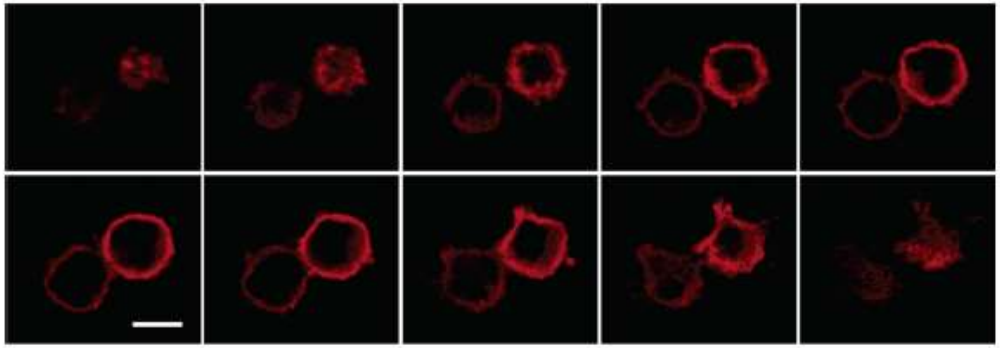

**Figure 5.** Serial fluorescence optical sections of PLC$\gamma$1-expressing HEK293 cells using red QDs. The *z*-axis interval of optical slices is 1.3 $\mu$m. Cells were incubated for 30 min in red QDs, after which the free QDs were washed away. These fluorescence images indicate that PLC$\gamma$1 markers are only expressed on the surface membranes. Scale bar, 10 $\mu$m.

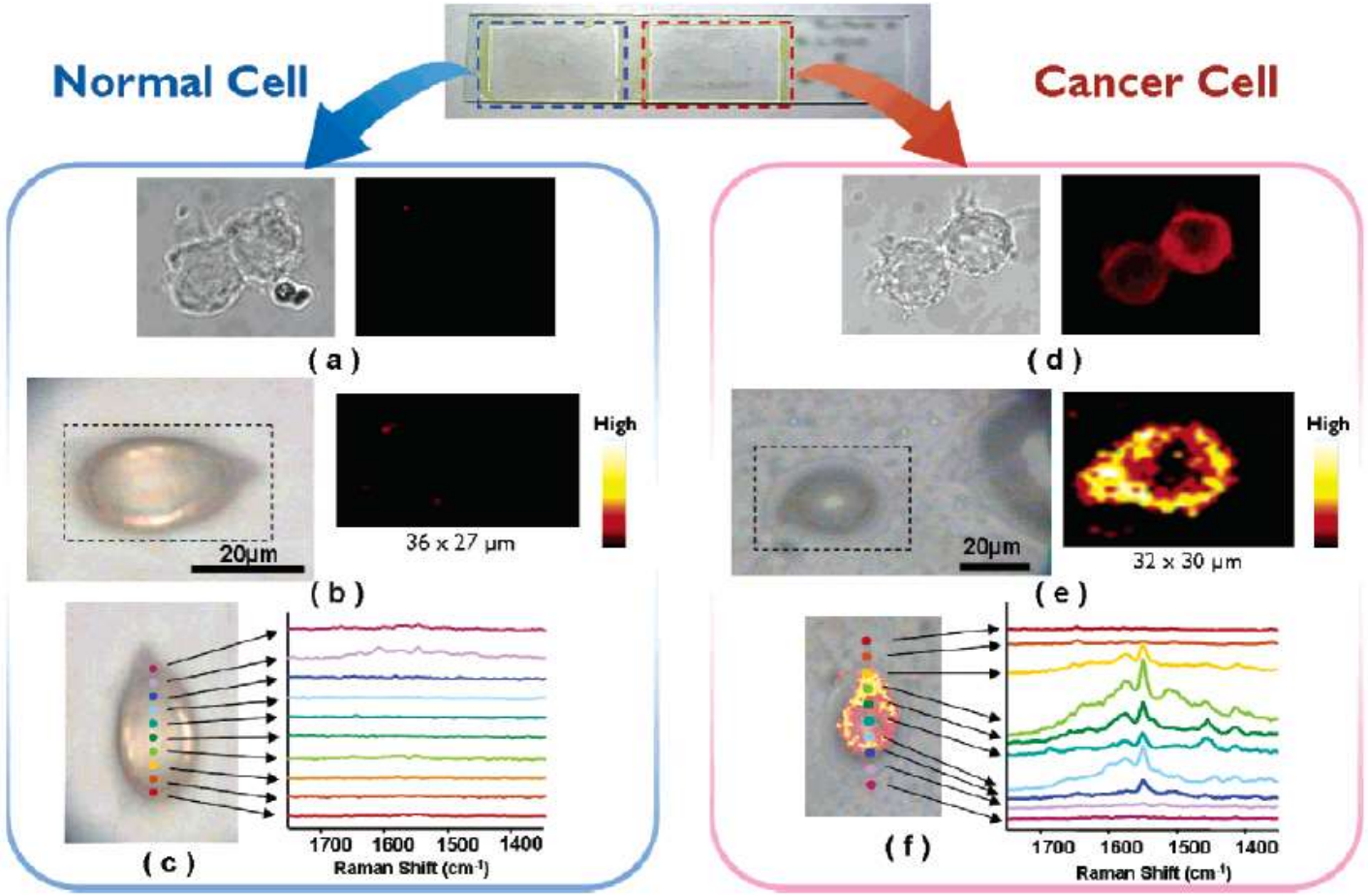


**Figure 6.** Fluorescence and SERS images of normal HEK293 cells and PLC$\gamma$1-expressing HEK293 cells. (a) QD-labeled fluorescence images of normal cells: (left) brightfield image, (right) fluorescence image. (b) SERS images of single normal cell: (left) brightfield image, (right) Raman mapping image of single normal cell based on the 1650-cm$^{-1}$ R6G peak. The cell area was scanned with an interval of 1 $\mu$m. Intensities are scaled to the highest value in each area. (c) Overlay image of brightfield and Raman mapping for single normal cell. Colorful spots indicate the laser spots across the middle of the cell along the *y* axis. (d) QD-labeled fluorescence images of cancer cells: (left) brightfield image, (right) fluorescence image. (e) SERS images of single cancer cell: (left) brightfield image, (right) Raman mapping image of single cancer cell based on the 1650-cm$^{-1}$ R6G peak. The cell area was scanned with an interval of 1 $\mu$m. Intensities are scaled to the highest value in each area. (f) Overlay image of brightfield and Raman mapping for single cancer cell. Colorful spots indicate the laser spots across the middle of the cell along the *y* axis.

J|A|C|S
COMMUNICATIONS

Published on Web 12/15/2006

# Mammalian Cell Surface Imaging with Nitrile-Functionalized Nanoprobes: Biophysical Characterization of Aggregation and Polarization Anisotropy in SERS Imaging

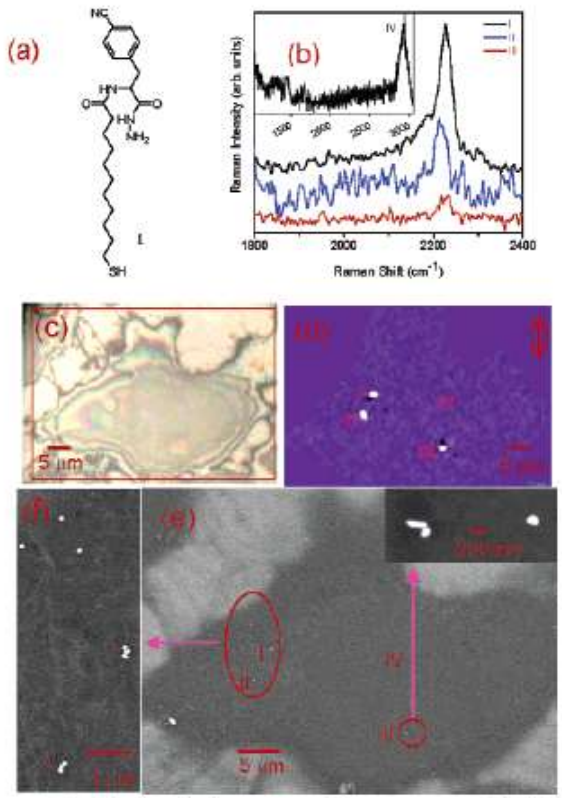


***Figure 1.*** (a) The chemical structure of Raman reporter **1**; (b) Raman spectra of the CN vibration mode extracted from positions I, II, and III of the cell shown in the optical image (c). Inset of (b) is a cellular Raman spectrum taken from spot IV of the same cell. (d) Raman intensity map of the C≡N band of the same cell, and (e) the corresponding SEM image. Inset in (e) showed the NPs in the lower right circle. (f) The group of NPs as shown in the large oval of (e).

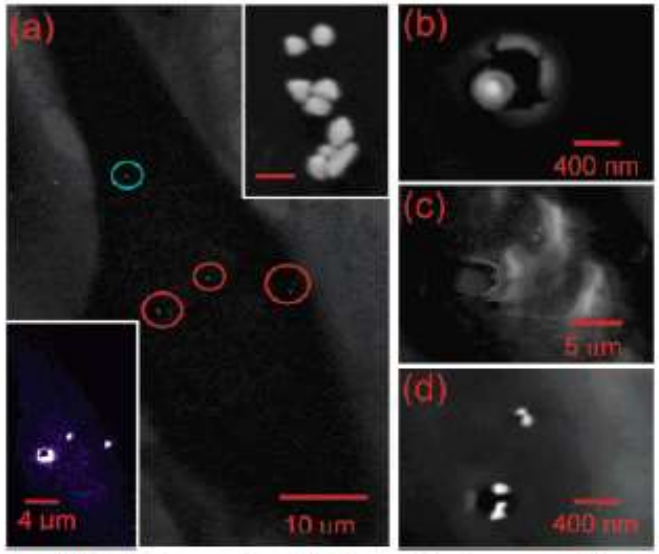


***Figure 2.*** (a) SEM image of a cell. Upper right inset: magnification of a group of aggregated NPs. The scale bar is 200 nm. Lower left inset: the corresponding Raman intensity image of the same cell obtained with a power density of $10^5$ W/cm$^2$. Laser-induced damage to the cell is shown in (b) the monomer (blue circle in a), (c) the aggregates, and (d) a pair of dimers.

# Molecular imaging of live cells by Raman microscopy

Almar F Palonpon[1,2], Mikiko Sodeoka[2,3] and Katsumasa Fujita[1,2]

**Current Opinion in Chemical Biology** 2013, **17**:708–715

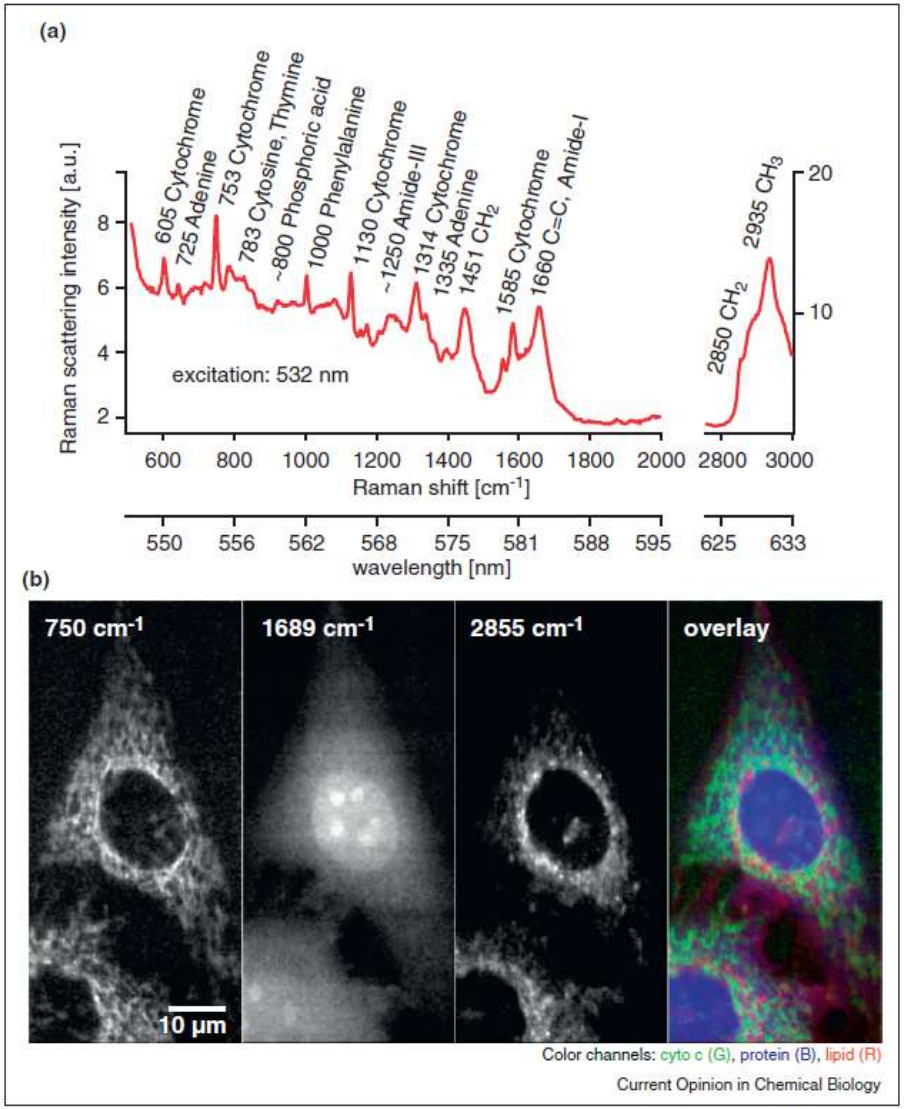

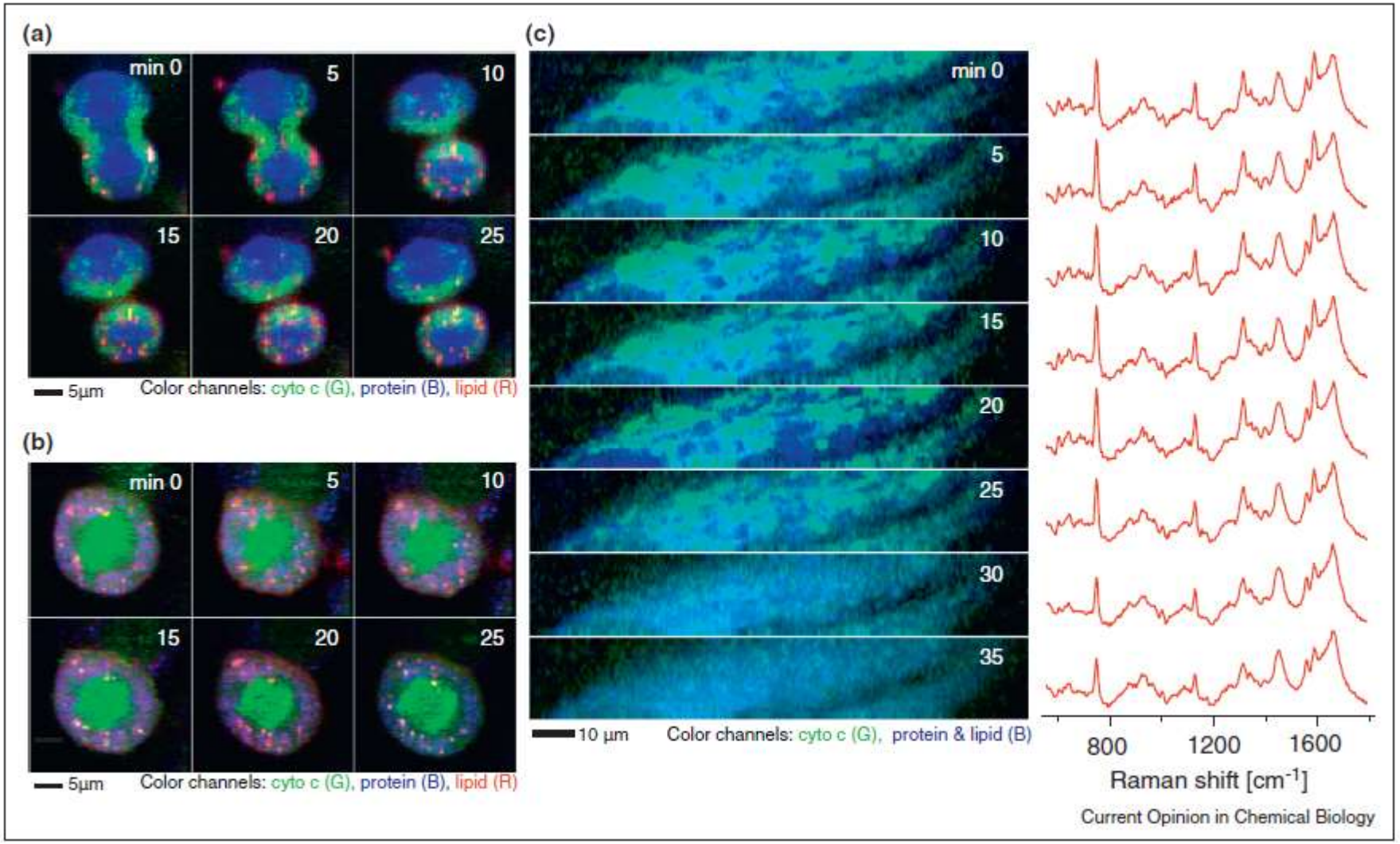
(a)
min 0
5
10
15
20
25
5µm
Color channels: cyto c (G), protein (B), lipid (R)
(b)
min 0
5
10
15
20
25
5µm
Color channels: cyto c (G), protein (B), lipid (R)
(c)
min 0
5
10
15
20
25
30
35
10 µm
Color channels: cyto c (G), protein & lipid (B)
800
1200
1600
Raman shift [cm-1]
Current Opinion in Chemical Biology

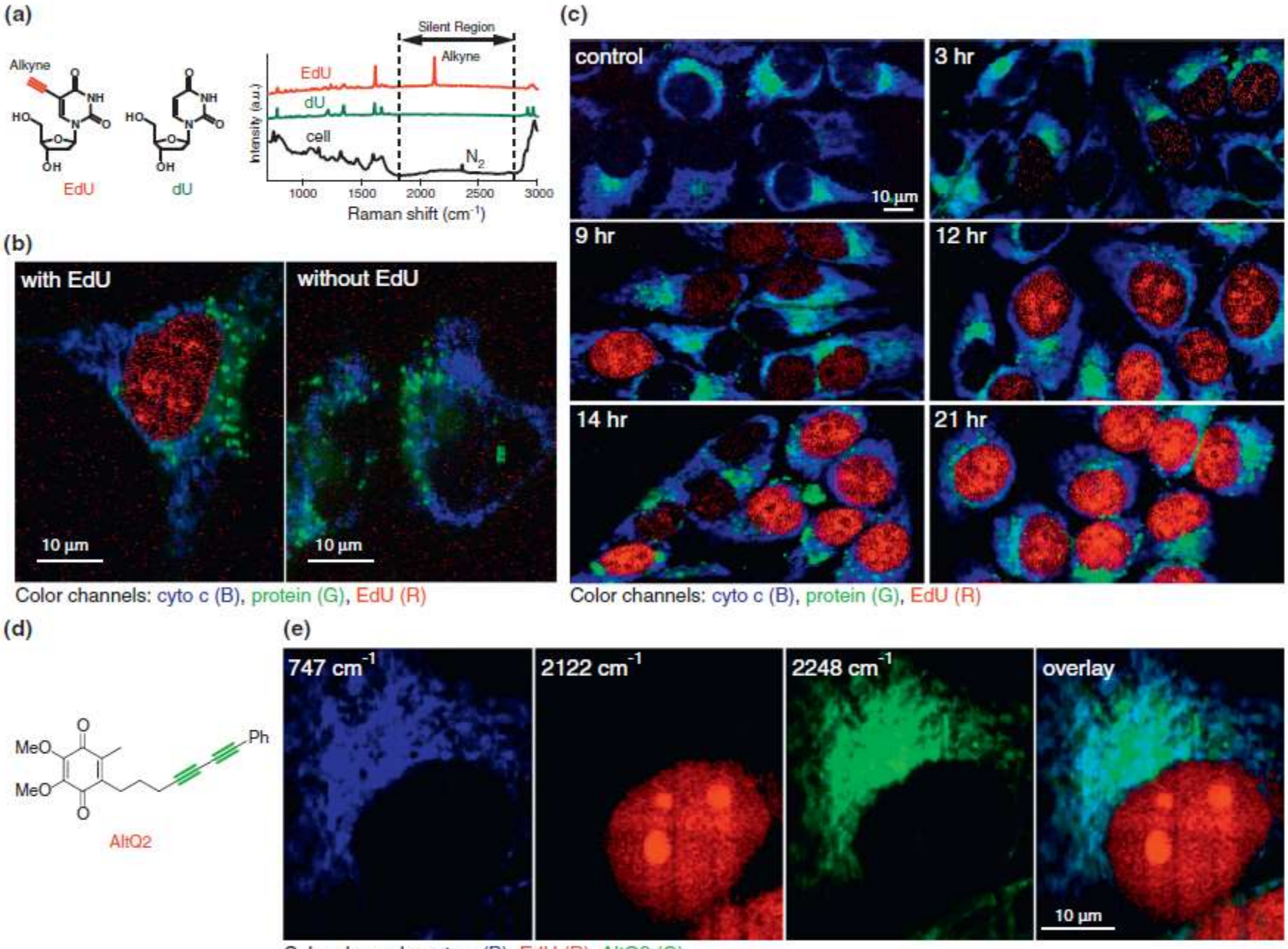
(a)
Alkyne
EdU
dU
Silent Region
Alkyne
EdU
dU
cell
$N_2$
Intensity (a.u.)
1000
1500
2000
2500
3000
Raman shift ($cm^{-1}$)
(b)
with EdU
without EdU
10 μm
10 μm
Color channels: cyto c (B), protein (G), EdU (R)
(c)
control
3 hr
9 hr
12 hr
14 hr
21 hr
10 μm
Color channels: cyto c (B), protein (G), EdU (R)
(d)
MeO
MeO
Ph
AltQ2
(e)
747 $cm^{-1}$
2122 $cm^{-1}$
2248 $cm^{-1}$
overlay
10 μm
Color channels: cyto c (B), EdU (R), AltQ2 (G)

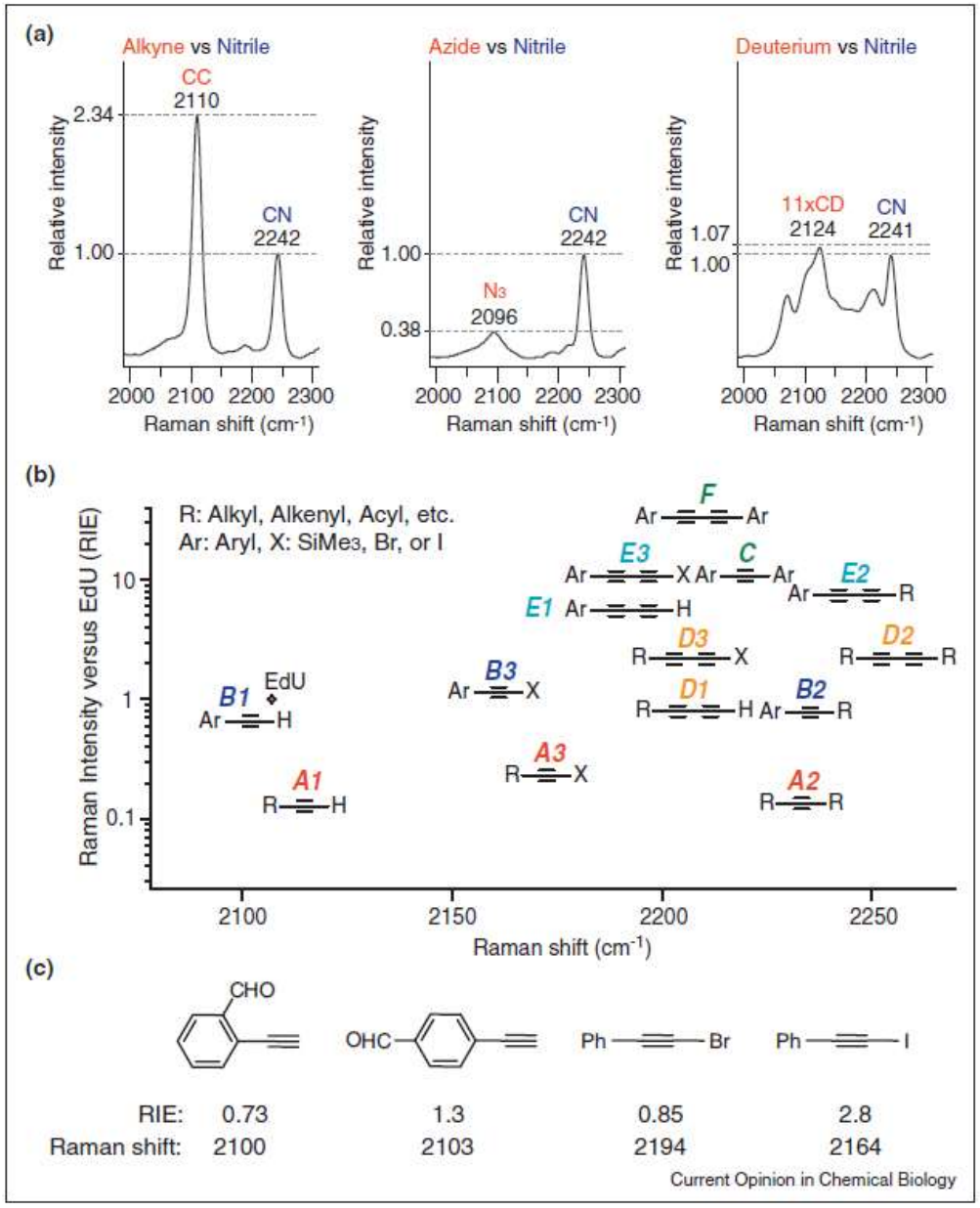
(a)
Alkyne vs Nitrile
CC
2110
CN
2242
2.34
1.00
Relative intensity
2000 2100 2200 2300
Raman shift (cm-1)
Azide vs Nitrile
CN
2242
N3
2096
1.00
0.38
Relative intensity
2000 2100 2200 2300
Raman shift (cm-1)
Deuterium vs Nitrile
11xCD
2124
CN
2241
1.07
1.00
Relative intensity
2000 2100 2200 2300
Raman shift (cm-1)
(b)
R: Alkyl, Alkenyl, Acyl, etc.
Ar: Aryl, X: SiMe3, Br, or I
Raman Intensity versus EdU (RIE)
10
1
0.1
F
E3
C
E2
E1
D3
D2
B3
EdU
B1
D1
B2
A3
A1
A2
2100
2150
2200
2250
Raman shift (cm-1)
(c)
CHO
OHC
Ph
Br
Ph
I
RIE: 0.73 1.3 0.85 2.8
Raman shift: 2100 2103 2194 2164
Current Opinion in Chemical Biology

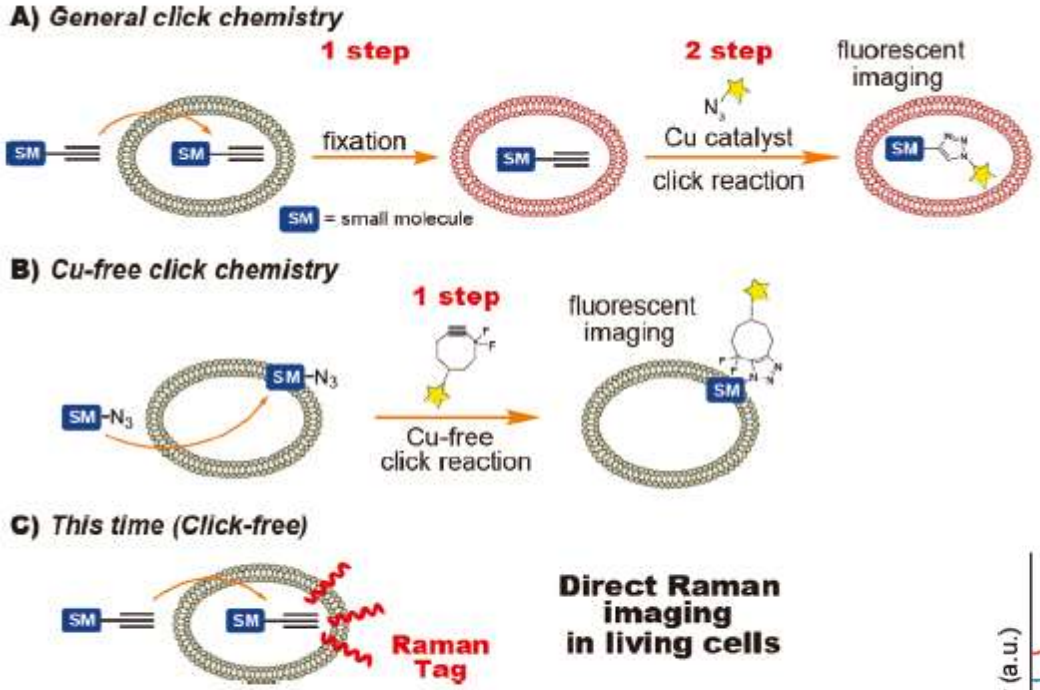


Figure 1. Concept of click-free imaging.

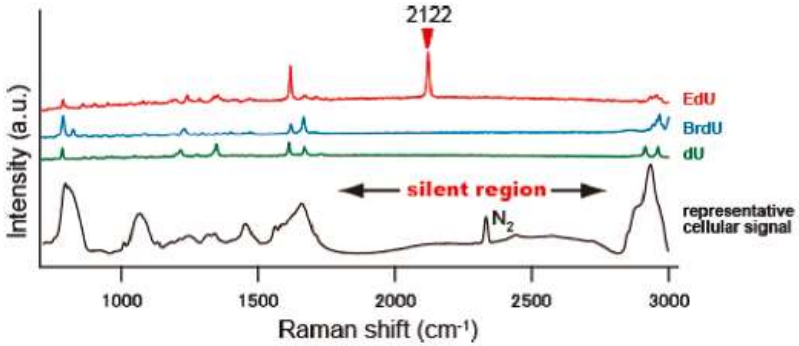


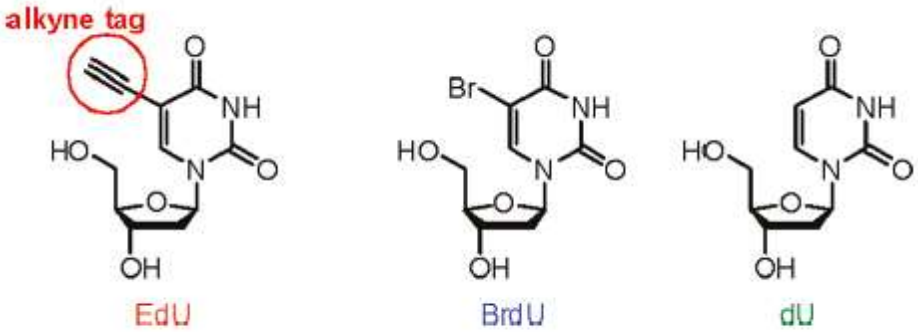


Figure 2. Structures of thymidine analogues.

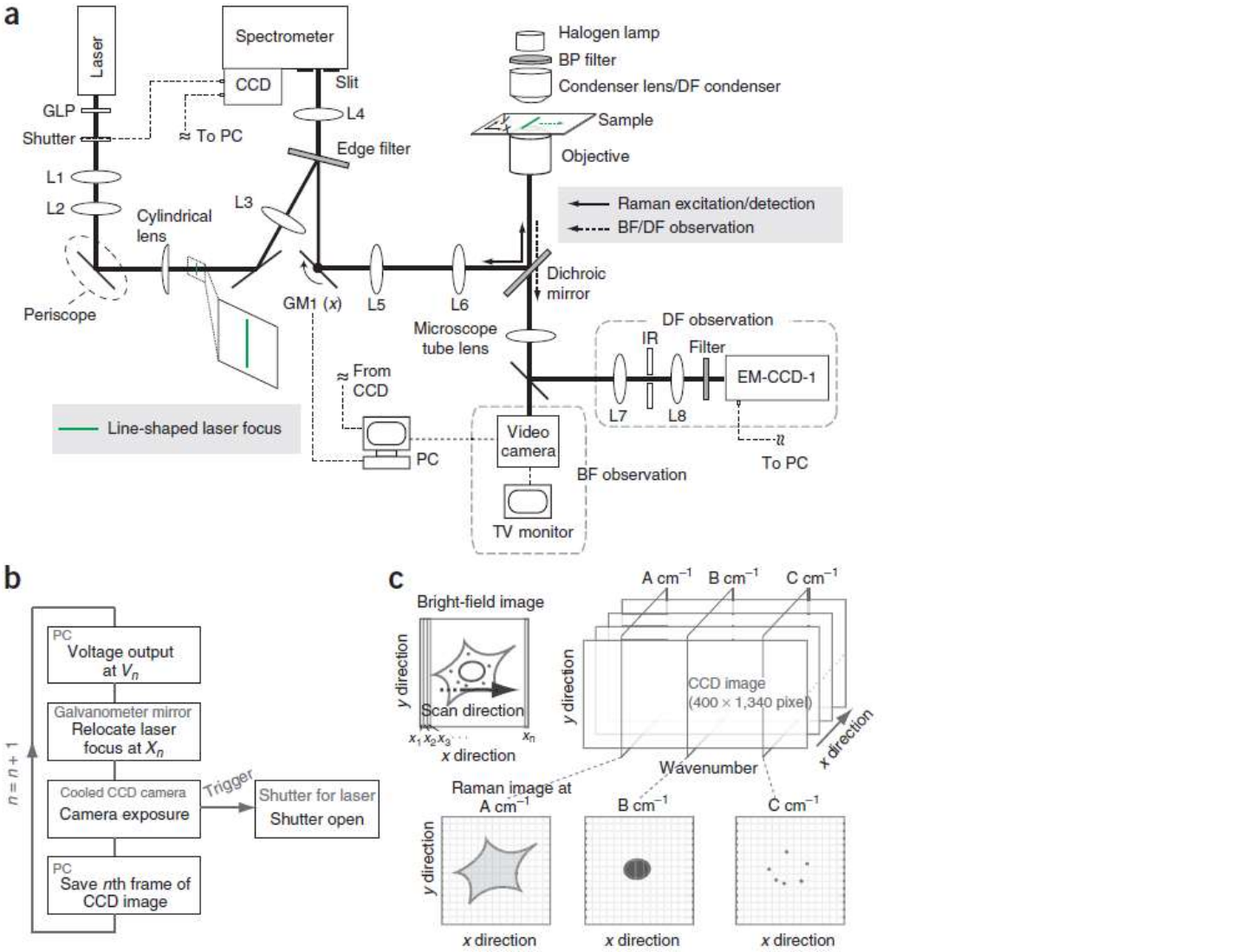
a
Laser
Spectrometer
CCD
Slit
GLP
Shutter
To PC
L4
Edge filter
L1
L2
L3
Cylindrical lens
Periscope
GM1 (x)
L5
L6
Halogen lamp
BP filter
Condenser lens/DF condenser
Sample
Objective
Raman excitation/detection
BF/DF observation
Dichroic mirror
Microscope tube lens
DF observation
IR
Filter
EM-CCD-1
L7
L8
To PC
From CCD
PC
Video camera
BF observation
TV monitor
Line-shaped laser focus
b
PC
Voltage output at $V_n$
Galvanometer mirror
Relocate laser focus at $X_n$
Cooled CCD camera
Camera exposure
Trigger
Shutter for laser
Shutter open
PC
Save nth frame of CCD image
n = n + 1
c
Bright-field image
y direction
Scan direction
x direction
A cm$^{-1}$
B cm$^{-1}$
C cm$^{-1}$
CCD image (400 × 1,340 pixel)
Wavenumber
Raman image at A cm$^{-1}$
B cm$^{-1}$
C cm$^{-1}$

# Alkynyl sugar analogs for the labeling and visualization of glycoconjugates in cells

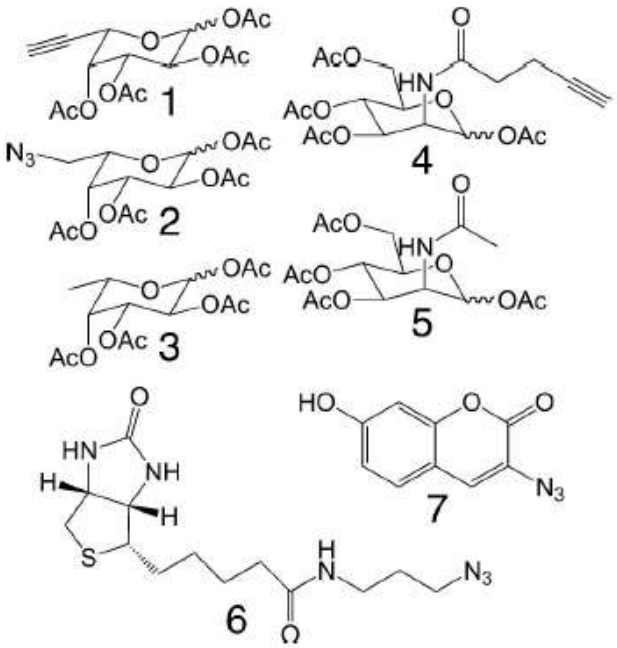


Scheme 1. Modified sugar analogs and probes used in this study.

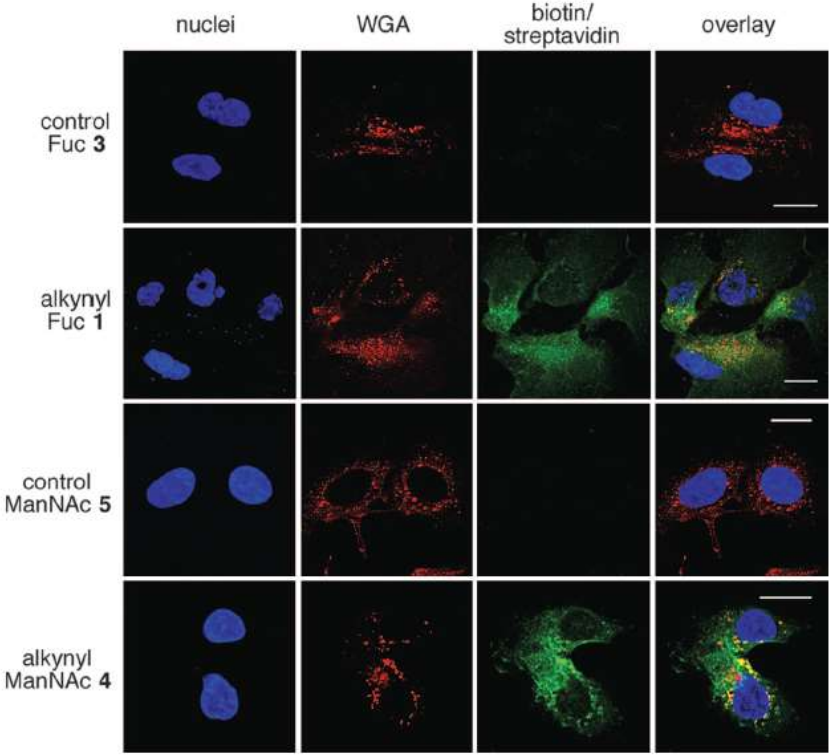

# Cell-permeable probe for identification and imaging of sialidases

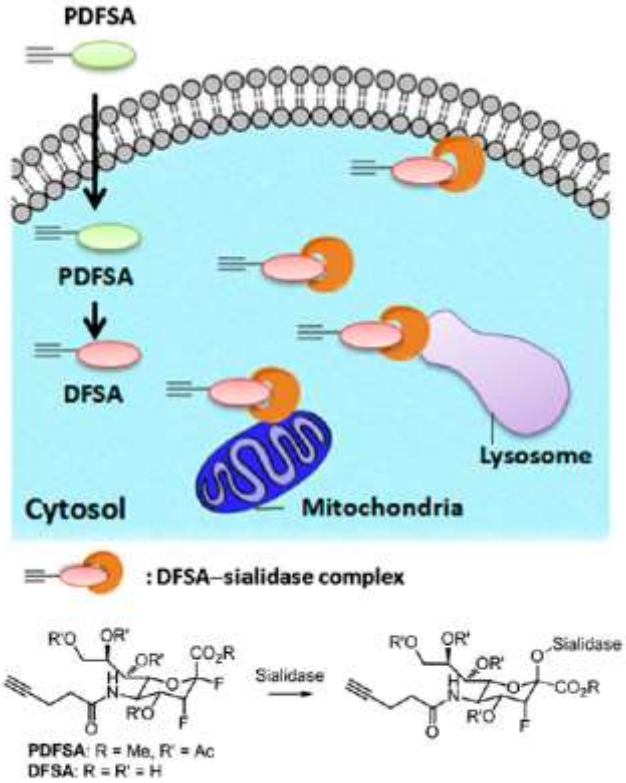


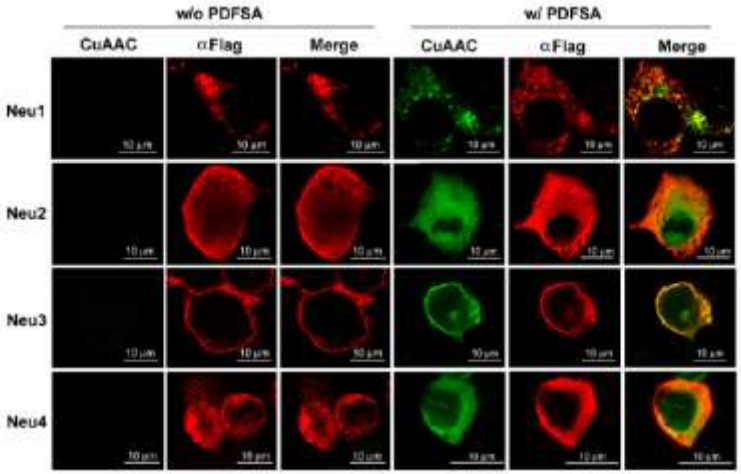


Fig. 1. Identification and imaging of sialidase with activity changes using these activity-based sialidase probes.